

INFORMATION TO USERS

This manuscript has been reproduced from the microfilm master. UMI films the text directly from the original or copy submitted. Thus, some thesis and dissertation copies are in typewriter face, while others may be from any type of computer printer.

The quality of this reproduction is dependent upon the quality of the copy submitted. Broken or indistinct print, colored or poor quality illustrations and photographs, print bleedthrough, substandard margins, and improper alignment can adversely affect reproduction.

In the unlikely event that the author did not send UMI a complete manuscript and there are missing pages, these will be noted. Also, if unauthorized copyright material had to be removed, a note will indicate the deletion.

Oversize materials (e.g., maps, drawings, charts) are reproduced by sectioning the original, beginning at the upper left-hand corner and continuing from left to right in equal sections with small overlaps.

ProQuest Information and Learning
300 North Zeeb Road, Ann Arbor, MI 48106-1346 USA
800-521-0600

UMI[®]

NOTE TO USERS

This reproduction is the best copy available.

UMI[®]

University of Alberta

Influence of Oil Contamination on Geotechnical Properties of Silty Sand
by

Rafael Rodríguez Ochoa



A thesis submitted to the Faculty of Graduate Studies and Research in partial
fulfillment of the
requirements for the degree of Master of Science

in

Geotechnical Engineering

Department of Civil and Environmental Engineering

Edmonton, Alberta

Spring, 2005



Library and
Archives Canada

Bibliothèque et
Archives Canada

Published Heritage
Branch

Direction du
Patrimoine de l'édition

395 Wellington Street
Ottawa ON K1A 0N4
Canada

395, rue Wellington
Ottawa ON K1A 0N4
Canada

Your file *Votre référence*

ISBN:

Our file *Notre référence*

ISBN:

NOTICE:

The author has granted a non-exclusive license allowing Library and Archives Canada to reproduce, publish, archive, preserve, conserve, communicate to the public by telecommunication or on the Internet, loan, distribute and sell theses worldwide, for commercial or non-commercial purposes, in microform, paper, electronic and/or any other formats.

The author retains copyright ownership and moral rights in this thesis. Neither the thesis nor substantial extracts from it may be printed or otherwise reproduced without the author's permission.

AVIS:

L'auteur a accordé une licence non exclusive permettant à la Bibliothèque et Archives Canada de reproduire, publier, archiver, sauvegarder, conserver, transmettre au public par télécommunication ou par l'Internet, prêter, distribuer et vendre des thèses partout dans le monde, à des fins commerciales ou autres, sur support microforme, papier, électronique et/ou autres formats.

L'auteur conserve la propriété du droit d'auteur et des droits moraux qui protègent cette thèse. Ni la thèse ni des extraits substantiels de celle-ci ne doivent être imprimés ou autrement reproduits sans son autorisation.

In compliance with the Canadian Privacy Act some supporting forms may have been removed from this thesis.

Conformément à la loi canadienne sur la protection de la vie privée, quelques formulaires secondaires ont été enlevés de cette thèse.

While these forms may be included in the document page count, their removal does not represent any loss of content from the thesis.

Bien que ces formulaires aient inclus dans la pagination, il n'y aura aucun contenu manquant.


Canada

To my father, Rafael Rodríguez Lozano, for his encouragement and support in all the stages of my life.

To my mother, Teresa Ochoa Vazquez, for her caring and cooking, which makes me happy at all times.

To the Geotechnical Centre at the U of A, specially to my friends Soe Moe, Yetimgeta, Yang and Francisco, for having shared with me their expertise and advice.

To Carmen, for her invaluable help and guidance through my studies in Canada.

ABSTRACT

Mexico is a major supplier of crude oil worldwide, and most of its oil production comes from offshore reservoirs mainly located in the Bay of Campeche, Gulf of Mexico, Mexico. Because oil exploitation is carried out offshore, a number of offshore structures have been developed in order to access the oil reservoirs. Among these structures, offshore platforms are considered the key elements of the entire exploration and production system. Recent in situ investigations have discovered crude oil migration from the oil reservoir in the Cantarell field, considered the most important oil field in the Bay of Campeche, into the upper soil strata and sea water. Given the critical role for offshore platforms, there is concern that oil contamination may negatively impact the mechanical properties of the foundation soils and present a risk to the stability of the offshore platforms.

The objectives of this research are to assess the impact of oil contamination on the mechanical properties of reconstituted, analog sand having the same grain size distribution as an important sand layer found near a major oil migration area within the Bay of Campeche. The mechanical properties studied included shear strength and stress-strain behaviour. The interface friction and the stress-displacement behaviour between the analog sand and mild steel were also addressed to aid in pile-sand interaction investigations.

It was found that the undrained, triaxial compression stress-strain behaviour of the oil contaminated analog sand was improved due to oil contamination. Direct shear test results also corroborated the improvement in the strength of the oil contaminated sand found from the triaxial testing. The interface direct shear test results showed that the interfacial friction angle decreases as a result of oil contamination and, depending on the design calculations for the offshore piles, may present a risk to offshore platform stability.

ACKNOWLEDGMENTS

This project was carried out under the kind supervision of Dr. Rick Chalaturnyk, whose guidance and support were the corner stones for its completion.

I want to thank Steve Gamble for his expertise and support during the laboratory work. Appreciation is also extended to Gilbert Wong and to Kent Leung.

I want to express my especial thanks to the Mexican Petroleum Institute (IMP) for providing the necessary information for the research work.

I am very grateful to the National Polytechnic Institute (IPN) for the opportunity provided and for encouraging the pursuit of my graduate studies, special thanks are extended to Professor Carlos Magdaleno and to Professor Jesús Reyes García.

I wish to express my appreciation for the economic support provided for the National Association of Universities and Institutes of Superior Education, A.C. (ANUIES) through the National Program for Betterment of the Academic Lectures (SUPERA).

TABLE OF CONTENTS

1.	Introduction.....	1
1.1	Statement of the Problem.....	1
1.2	Objectives of Research.....	2
1.3	Scope of Thesis.....	3
1.4	Organization of Thesis.....	4
2.	Literature Review.....	5
2.1	Overview of the Mexican Petroleum Industry.....	5
2.2	Overview of Offshore Platforms.....	8
2.3	Problems Related to Emanations of Gas.....	11
2.4	Previous Studies in the Cantarell Field related to the Hydrocarbon macro-seep.....	12
2.4.1	Introduction.....	12
2.4.2	Cantarell Field Overview.....	14
2.4.2.1	General Subsurface Stratigraphy.....	16
2.4.2.2	Buried Fault.....	17
2.4.2.3	Distribution of Gas and the “Chimney” Feature.....	18
2.4.2.4	Characteristics of the Chimney Hydrocarbons.....	19
2.4.2.5	Lateral Migration of Hydrocarbons.....	21
2.4.3	Effects of Liquid Deposits on Mechanical Properties.....	23
2.4.4	Summary.....	25
2.5	Influence of Oil Contamination on the Mechanical Properties of Sand....	27
2.5.1	Shear Strength.....	27
2.5.1.1	Triaxial Tests.....	27
2.5.1.2	Direct Shear Tests.....	35

2.5.2	Interface Steel-Sand Shear Strength.....	39
2.5.2.1	Direct Shear Test Apparatus.....	39
2.5.2.2	Interface Testing Apparatus.....	43
3.	Testing Program.....	49
3.1	Introduction.....	49
3.2	Materials used in Laboratory Program.....	49
3.2.1	Analog Sand.....	49
3.2.2	Oil.....	52
3.2.3	Steel.....	55
3.2.4	Water.....	56
3.3	Triaxial Tests.....	56
3.3.1	Sample Preparation.....	57
3.3.1.1	Samples with Water as Permeating Liquid.....	59
3.3.1.2	Samples with Oil-Water mix as Permeating Liquid.....	60
3.3.2	Testing Procedure.....	60
3.3.2.1	Saturation Phase.....	60
3.3.2.2	Consolidation Phase.....	61
3.3.2.3	Compression Phase.....	61
3.3.3	Problems Observed during the Test Program.....	62
3.4	Direct Shear Test.....	63
3.4.1	Sample Preparation.....	64
3.4.1.1	Samples with Water as Permeating Liquid.....	65
3.4.1.2	Samples with Oil-Water mix as Permeating Liquid.....	65
3.4.2	Testing Procedure.....	67

5.	Conclusions and Recommendations.....	105
5.1	Conclusions.....	105
5.2	Recommendations for Further Research.....	108
	BIBLIOGRAPHY.....	110
	APPENDIX A Sand Samples.....	116

LIST OF TABLES

Table 2.1	Soil Parameters.....	32
Table 2.2	Summary of the Shear Strength Parameters Obtained from Triaxial Testing.....	34
Table 2.3	Test Parameters Used for Direct Shear Tests.....	35
Table 2.4	Summary Results on Interfaces.....	41
Table 3.1	Description of Soil Layer IV.....	50
Table 3.2	Soil Properties for Analog Sand.....	52
Table 4.1	Test Conditions for Water Samples.....	74
Table 4.2	Test Conditions for Oil Samples.....	75
Table 4.3	Summary of Soil Parameters - Triaxial Test -.....	84
Table 4.4	Initial Soil Conditions - Direct Shear Test -.....	88
Table 4.5	Soil Conditions after Inundation and Consolidation - Direct Shear Test -.....	88
Table 4.6	Failure Conditions - Direct Shear Test -.....	89
Table 4.7	Water Content after Shearing - Direct Shear Test -.....	89
Table 4.8	Summary of Soil Parameters - Direct Shear Test -.....	94
Table 4.9	Initial Soil Conditions - Interface Direct Shear Test -.....	95
Table 4.10	Soil Conditions after Inundation and Consolidation - Interface Direct Shear Test -.....	95
Table 4.11	Failure Conditions - Interface Direct Shear Test -.....	96
Table 4.12	Water Content after Shearing - Interface Direct Shear Test -.....	96
Table 4.13	Summary of Soil Parameters - Interface Direct Shear Test -.....	103
Table 4.14	Summary of Soil Parameters close to Critical State - Interface Direct Shear Test -.....	103

Table 4.15	Initial Tangent Modulus – Based on Triaxial Test -.....	103
Table 4.16	Summary of Soil Parameters.....	103
Table 4.17	Interface Steel-Soil Direct Shear Test Results.....	104

LIST OF FIGURES

Figure 2.1	Bay of Campeche.....	7
Figure 2.2	Jacket-type Platform with Skirt Piles.....	10
Figure 2.3	Borehole Localization.....	15
Figure 2.4	Localization of Sand Layers.....	17
Figure 2.5	Results of Drained Tests and Simulations for Clean Loose Sand...29	
Figure 2.6	Results of Drained Tests and Simulations for Oil Contaminated Loose Sand.....	29
Figure 2.7	Results of Drained Tests and Simulations for Clean Dense Sand...30	
Figure 2.8	Results of Drained Tests and Simulations for Oil Contaminated Dense Sand.....	30
Figure 2.9	Pore Pressure vs. Axial Strains in Undrained Tests for Loose Sand.....	31
Figure 2.10	Deviator Stress vs. Mean Stress in Undrained Tests for Loose Sand.....	31
Figure 2.11	Results of Undrained Tests for Dense Sand.....	32
Figure 2.12	Typical Plots of Shear Stress versus Horizontal Displacement ($D_r=65\%$).....	36
Figure 2.13	Variation of Angle of Friction versus Degree of Saturation.....	36
Figure 2.14	Relationship between Relative Density and Friction Angle for Heavy Crude Oil and Light Gas Oil.....	38
Figure 2.15	Results of Tests on Steel Interface and Clean Loose Crushed Quartz Sand.....	41
Figure 2.16	Results of Steel Interface and Oil Contaminated Loose Crushed Quartz Sand.....	41
Figure 2.17	Constant Normal Stress Tests on Clean Loose Sand.....	44
Figure 2.18	Constant Normal Stress Tests on Oil Contaminated Loose Sand..	44

Figure 2.19	Constant Normal Stress Tests on Clean Medium Dense Sand.....	45
Figure 2.20	Constant Normal Stress Tests on Oil Contaminated Medium Dense Sand.....	45
Figure 2.21	Constant Volume Tests on Clean Medium Dense Sand.....	47
Figure 2.22	Constant Volume Tests on Oil Contaminated Medium Dense Sand.....	47
Figure 3.1	Grain Size Distribution Curves.....	51
Figure 3.2	Oils Tested at Different Rates using the Brookfield Viscometer....	54
Figure 3.3	Triaxial Test Equipment Configuration.....	57
Figure 3.4	Direct Shear Test Equipment Configuration.....	64
Figure 3.5	Oil Contaminated Sand Specimen Prepared in the Triaxial Cell....	66
Figure 3.6	Oil Contaminated Specimen Preparation.....	67
Figure 3.7	Oil Contaminated Specimen Preparation in the Shearbox.....	67
Figure 3.8	Shearbox Assembly for Interface Shear Test.....	71
Figure 3.9	Steel Plate Placed into the Lower Half of the Shearbox.....	71
Figure 4.1	Pore Pressure Dissipation for Water and Oil Samples #1 ($\sigma'_3=250$ kPa).....	77
Figure 4.2	Pore Pressure Dissipation for Water and Oil Samples #2 ($\sigma'_3=500$ kPa).....	78
Figure 4.3	Undrained Stress-Strain Behaviour for Water and Oil Specimens #1 ($\sigma'_3 = 250$ kPa).....	81
Figure 4.4	Undrained Stress-Strain Behaviour for Water and Oil Specimens #2 ($\sigma'_3 = 500$ kPa).....	82
Figure 4.5	Undrained Stress-Strain Behaviour for Water and Oil Specimens #3 ($\sigma'_3 = 670$ kPa).....	83
Figure 4.6	Stress Ratio Plot for All Triaxial Tests	84
Figure 4.7	p' - q Diagram ($\sigma_3=650$ kPa, $\sigma'_3=250$ kPa).....	85

Figure 4.8	p'-q Diagram ($\sigma_3=900$ kPa, $\sigma_3'=500$ kPa).....	85
Figure 4.9	p'-q Diagram for Water ($\sigma_3=1,070$ kPa, $\sigma_3'=670$ kPa); for Oil ($\sigma_3=1,055$ kPa and $\sigma_3'=655$ kPa).....	86
Figure 4.10	Direct Shear Behaviour of Water and Oil Specimen #1 ($\sigma_n = 62.5$ kPa).....	91
Figure 4.11	Direct Shear Behaviour of Water and Oil Specimen #2 ($\sigma_n = 125$ kPa).....	92
Figure 4.12	Direct Shear Behaviour of Water and Oil specimen #3 ($\sigma_n = 250$ kPa).....	93
Figure 4.13	Shear Stress vs Horizontal Displacement ($\sigma_n = 62.5$ kPa) Interface Direct Shear Test	100
Figure 4.14	Shear Stress vs Horizontal Displacement ($\sigma_n = 125$ kPa) Interface Direct Shear Test	101
Figure 4.15	Shear Stress vs Horizontal Displacement ($\sigma_n = 250$ kPa) Interface Direct Shear Test.....	102
Figure A.1	Sand Sample (Water #3) used in the Triaxial Test Program having Water as Permeating Liquid.....	117
Figure A.2	Sand Sample (Oil #3) used in the Triaxial Test Program having Oil-Water Mix as Permeating Liquid.....	118
Figure A.3	Sand Sample (Soil-Soil Oil # 3) used in the Direct Shear Test Program, having Oil-Water Mix as Permeating Liquid.....	119
Figure A.4	Sand Sample (Steel-Soil Oil # 2) used in the Interface Direct Shear Test Program, having Oil-Water Mix as the Permeating Liquid.....	120

1. INTRODUCTION

1.1 Statement of the Problem

In 1978, geophysical studies carried out to find the best location for the construction of a new offshore platform in the Cantarell petroleum field in the Bay of Campeche, Gulf of Mexico, Mexico, discovered gas accumulations beneath the foundation soils. As a consequence, the location of the AKAL-H platform was changed 800 meters from its original location in order to avoid any further problem related to foundation stability.

Subsequent surveys conducted in 1978, 1997 and 2002 have indicated that the quantity of vertical hydrocarbon migration has increased over time. Geophysical surveys have also indicated that lateral migration is very likely and may increase in size. It was also estimated that sites currently with minimal liquid and solid hydrocarbon contents could become more heavily permeated with hydrocarbons, particularly within the more porous granular strata.

Taking into account the current extent and potential expansion of hydrocarbons within the foundation zone of some existing structures as AKAL-H platform and AKAL-C complex, and probably future platforms, it is critical to assess the impact this contamination could have on the mechanical properties of those foundation soils.

1.2 Objectives of Research

The main objective of this research is to assess the impact of oil contamination on the mechanical properties of a reconstituted, analog sand, which matches the grain size distribution of an important sand layer found near the AKAL-H platform.

The mechanical properties studied include shear strength and the stress-strain behaviour. Furthermore, the interface friction and the stress-displacement behaviour between the artificial sand and mild steel are addressed to aid in the pile-sand interaction investigation.

This research will primarily focus on the following important soil parameters: initial tangent modulus (E_i); effective and total friction angles (ϕ' , ϕ); cohesion (c); interface friction angle (δ). An additional goal in this study is the development of laboratory procedures to achieve these objectives, especially for the preparation of the oil contaminated sand specimens.

1.3 Scope of Thesis

Triaxial undrained tests are used to obtain the stress-strain behaviour of the artificial sand, and the shear strength soil parameters. These triaxial tests were conducted using a reconstituted, analog silty sand specimen fully saturated with fresh water or with a mix of fresh water and oil.

The analog sand is silty sand obtained from a sieve analysis of Saskatchewan sand and adding 19.32 % of rock flour (silt size grains) based on dry weight. This matches the grain size distribution curves of the soil layer #4 found in the foundation soils in the Cantarell field. The oil is a commercial one used for car engines, which matches the kinematic viscosity of the “Maya” Mexican crude oil. Direct shear tests were used to compare the shear strength parameters between reconstituted water sand specimens and reconstituted oil-water sand specimens.

Interface direct shear tests were used to compare the interface frictional resistance between sand and mild steel for reconstituted sand specimens saturated with fresh water and reconstituted sand specimens saturated with oil-water mix.

1.4 Organization of Thesis

Chapter 2 presents a review of the significant literature for this work. An overview of the Mexican petroleum industry is first reviewed followed by the problem in the Offshore Cantarell Oil Field and previous investigations in this area. A summary of papers related to the impact of oil contamination on the mechanical properties of sand, in particular shear strength and interface steel-sand shear strength, is presented.

Chapter 3 describes the testing program carried out in this research, including materials, equipments, and procedures used for the triaxial tests, direct shear tests and interface direct shear tests.

Chapter 4 presents the laboratory results and discuss the findings obtained from the triaxial tests, direct shear tests and interface direct shear tests.

Chapter 5 summarizes the conclusions and provides some recommendations for future work.

2. LITERATURE REVIEW

2.1 Overview of the Mexican Petroleum Industry

In 1938, when President Lázaro Cárdenas nationalized American and British oil operations in Mexico, there were almost 400 foreign companies and more than 200 wells on production in the country. Thenceforth, the Mexican government has been in charge of the management of all national hydrocarbons resources through the public institution called Petroleos Mexicanos (PEMEX) (Sandoval, 1998).

Based on energy production statistics in 2002, Mexico ranks 7th place in the world for the volume of crude oil production with 3.3 millions of barrels daily. As of January 2004, the proven crude oil reserves were estimated to be 16,040 millions of barrels, placing Mexico 13th in world for proven reserves (SE, 2004).

Currently, Mexico produces three different types of oil:

- a heavy oil, termed Maya, with an American Petroleum Institute (API) gravity¹ of 22° and represents 72% of the total production;
- a light oil, termed Itsmo, with an API gravity of 32° and represents 15% of the total production;
- a super light oil, termed Olmeca, with an API gravity of 39° and represents 13% of the total production (SE, 2004).

¹ API gravity is used to classify crude oil according to their densities.

Regarding the crude oil production PEMEX, Exploracion y Produccion (PEP) has delineated several oil production regions, each region having a variety of oil fields and wells, sorted as follow: 1) Northeast Region, containing Ku-Maloob-Zap and Cantarell fields; 2) Southwest Region, containing the Abkatun-Pol-Chuc and Litoral de Tabasco fields; 3) North Region, containing Burgos, Poza Rica-Altamira and Veracruz fields; and 4) South Region, containing the Cinco Presidentes, Bellota-Jujo, Samaria-Luna, Muspac and Macuspana fields.

At the moment, the Northeast Region is the most productive region, achieving around 2,416 thousands barrels per day in 2003. This amount represents about 72% of Mexico's total crude oil production (SE, 2004).

The main reason for this high productivity is based on the important activity underway in the Cantarell field, which alone accounts for about 61 % of the national crude oil production, and is one of the largest offshore development projects in the world (SE, 2004).

The Cantarell complex is located about 80 kilometers offshore in the Bay of Campeche, Gulf of Mexico, Mexico. It is composed of four major fields: Akal, Nohock, Chack and Kutz. Figure 2.1 shows the Bay of Campeche.

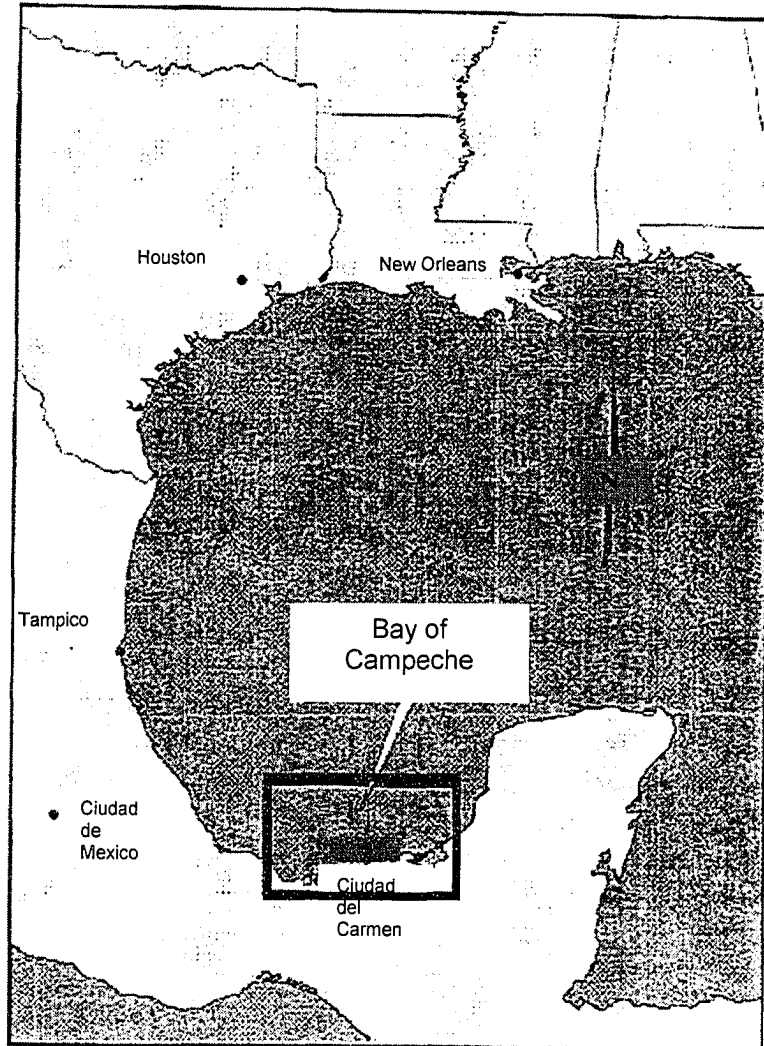


Figure 2.1 Bay of Campeche
(modified from FUGRO report 2002)

PEP has intensified its exploration and production activities in the Bay of Campeche, recently constructing 27 new wells in the first semester of 2004, alone with the associated construction of new offshore platforms and 61 active drill rings (PEMEX, 2004).

Of the 27 new wells, 16 were used to increase oil production in the Bay of Campeche and 11 were used to explore for new oil reservoirs (PEMEX, 2004).

The Cantarell field currently contains active 217 oil wells from a total of 360 that were drilled in that zone (PEMEX, 2004).

2.2 Overview of Offshore Platforms

Evolution in the design of offshore platforms, which were first introduced in the early 20th century, has resulted in a number of innovative structures constructed from various materials over a wide range of depths. These have included timber platforms structures, concrete gravity structures tethered/floating structures, guyed towers, and other 'exotic' designs, as well as the now 'conventional' fixed-bottom pile-supported steel platforms structures, that were first introduced after World War II (Drawe and Reifel, 1986).

The most detailed treatment related to the "conventional" offshore platforms previously published has been the American Petroleum Institute's (API) Recommended Practice for Planning, Designing, and Constructing Fixed Offshore Platforms (RP2A), first issued in October 1969 and continuously expanded and updated since then by practitioners from the offshore petroleum industry (Drawe and Reifel, 1986).

The offshore platforms can be categorized according to their function, as follows: drilling platforms, production platforms, self-contained drilling and production platforms, quarters platforms, riser and manifold platforms, bridges

and flare platforms. The drilling platforms are the most common type in the Bay of Campeche (anonymous, 2001a). The platforms can also be categorized based on their supporting structure. The most popular in Mexico the called “Jacket” platform steel platforms anchored to the seafloor by steel piles. These types of platforms were developed in United States, with the first installation of this type carried out in 1946 (anonymous, 2001b). Figure 2.2 shows a jacket platform.

In general, Jacket-type platforms consist of three main components, these are according to the construction process as follows: the substructure, which is the structure located from the sea level to the seafloor and is designed to serve as a template for pile driving, and as lateral bracing for the piles; the foundation, compose of open tubular steel pipes (steel piles) located from the sea level to the required depth based on the structural and geotechnical analysis, carrying both lateral and vertical loads; and the superstructure, which is the structure located above sea level and comprised of the necessary trusses and deck space for supporting operational and other loads (anonymous, 2001a).

The most common pile diameter sizes used for the foundation of the platforms in the Bay of Campeche are: 36, 42, 45, 54 and 60 inches. These are installed using the pile driving technique usually at depths between 60 and 120 meters. For pile driving, a steam hammer is one the most common tool (anonymous, 2001a).

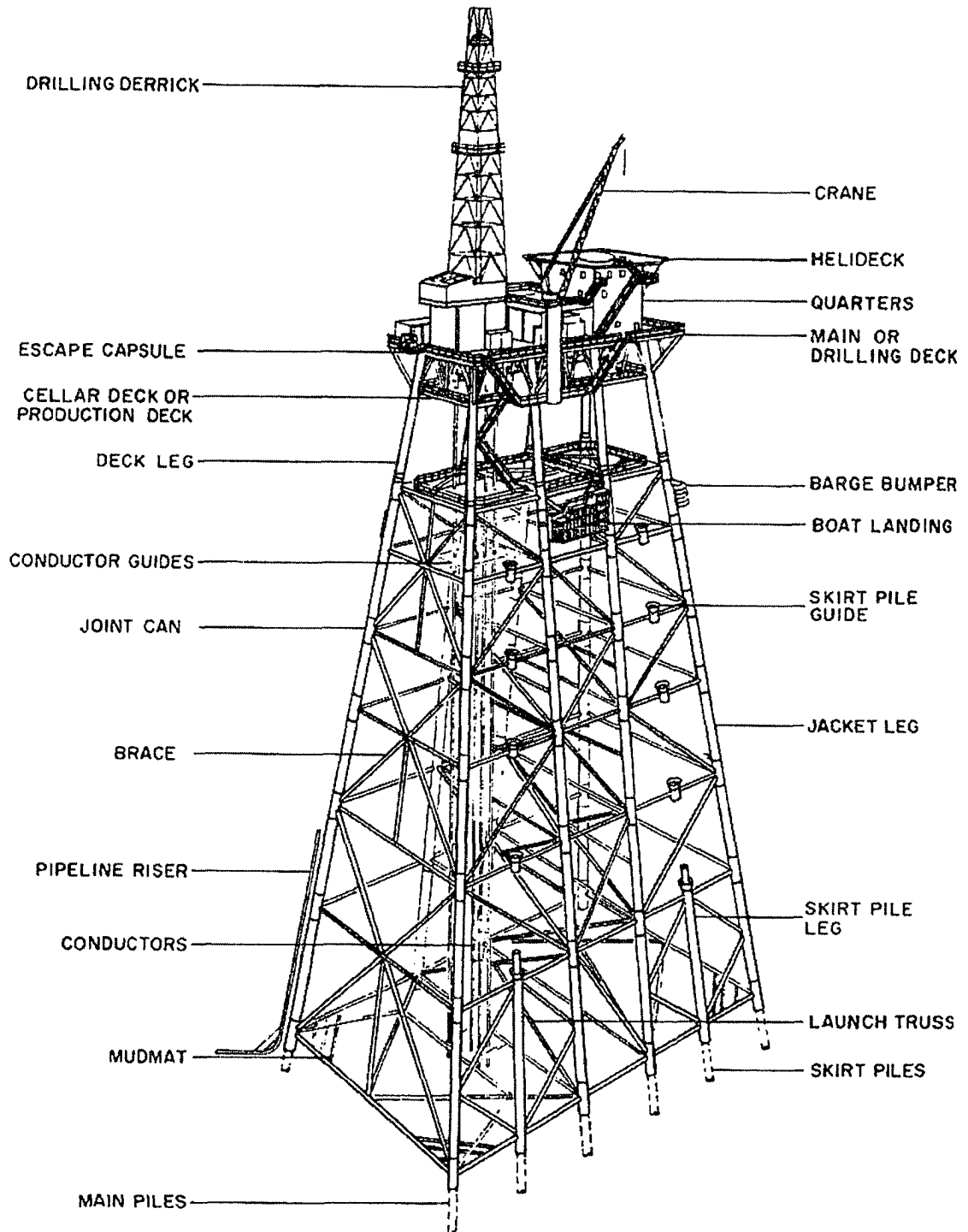


Figure 2.2 Jacket-type Platform with Skirt Piles
(from Drawe and Reifel, 1986)

Of the more than 250 platforms in the Bay of Campeche, about half of these are four-leg and tripod platforms and the rest are eight-leg systems (Bea, et al., 1999).

For platforms in the Bay of Campeche, the primary design load arises from hurricanes waves; with secondary design loads due to earthquakes (Bea et al., 1999).

2.3 Problems Related to Emanations of Gas

The accumulation of gas in the shallow subsurface soils of the Cantarell heavy oil field was first detected in 1978, during pre-construction geophysical studies for the AKAL-H platform. Consequently, the platform location was shifted from its original location about 800 meters in order to avoid any stability issues associated with the gas.

During explorations studies of the Cantarell field in 1997, shallow subsurface gas was discovered but this time the gassy zone had expanded beneath the AKAL-H platform, the same platform that 19 years ago was re-located in order to avoid these gassy accumulations.

Since then, the researches from the Instituto Mexicano del Petroleo (IMP), with the help of a group from the Norway Geotechnical Institute (NGI), have been in charge to perform geophysical and geotechnical investigations to assess and monitor this natural phenomena.

Until 2001, offshore platforms POOL-D, AKAL-H, and AKAL-GR had registered problems related to shallow subsurface gas. For the POOL-D platform in particular, these gas accumulations are believed to have resulted in an explosion near the platform. Creating a crater 30 meters deep and 76 meters in diameter, and subsequently downgrading of the lateral support capacity of six piles (IMP, 2000).

2.4 Previous Studies in the Cantarell Field related to the Hydrocarbon macro-seep

2.4.1 Introduction

The major concern about hydrocarbon migration in the Cantarell field is related to the possible negative impact on the mechanical properties of the subsurface soils that could affect the existing and future structures constructed in this zone.

This thesis will be focus mainly in the impact of liquid hydrocarbon permeating the pore fluids in the granular mass.

Among the various projects related to the hydrocarbon migration in the Cantarell field, the most intense investigation related to this problem was carried out by Fugro-Chance de Mexico S.A. de C.V. and Constructora Subacuatica Diavaz S.A. de C.V. (FUGRO, 2002).

Offshore geotechnical and geochemical investigations were conducted at the proposed AKAL-H (Gas 1) platform location in the Cantarell Field, Bay of Campeche, Gulf of Mexico, Mexico. The main objective of the geotechnical and geochemical investigation was to obtain information on soil and foundation conditions, and to evaluate the potential effects of gas and hydrocarbon deposits within the platform foundation areas.

FUGRO (2002) noted the following three observations: 1) The presence of both hydrocarbon and inorganic gases, either in solution or existing as free gas within the soil pore fluids, at anomalous and very anomalous concentrations; 2) The excess pore pressure that may arise episodically in response to events within the deeper reservoir; and 3) The presence of liquid and solid hydrocarbon deposits and inclusions within the soil profile.

2.4.2 Cantarell Field Overview

The water depths in the AKAL-H (Gas 1) area vary from about 41.5 m in the southeast to about 42.5 m in the northwest. The seafloor is smooth through the area and the regional slope of the study area is towards the northwest at about 0.18 percent (0.10°). A water depth of 42.1 m is representative for the AKAL-H (Gas 1) location (referenced to Mean Sea Level).

Field investigations conducted by FUGRO (2002) utilized four different in situ tools: in situ vane, standard piezocone penetrometer, piezoprobe and the deepwater gas probe in four different boreholes localized from South to North as follow: AKAL-H (Gas 2), AKAL-H (Gas 1), AKAL-H (Gas 3) and AKAL-C TRIPODE (Gas). A high resolution geophysical survey was also conducted in the vicinity of the AKAL-H (Gas 1) borehole. Figure 2.3 shows the boreholes localization.

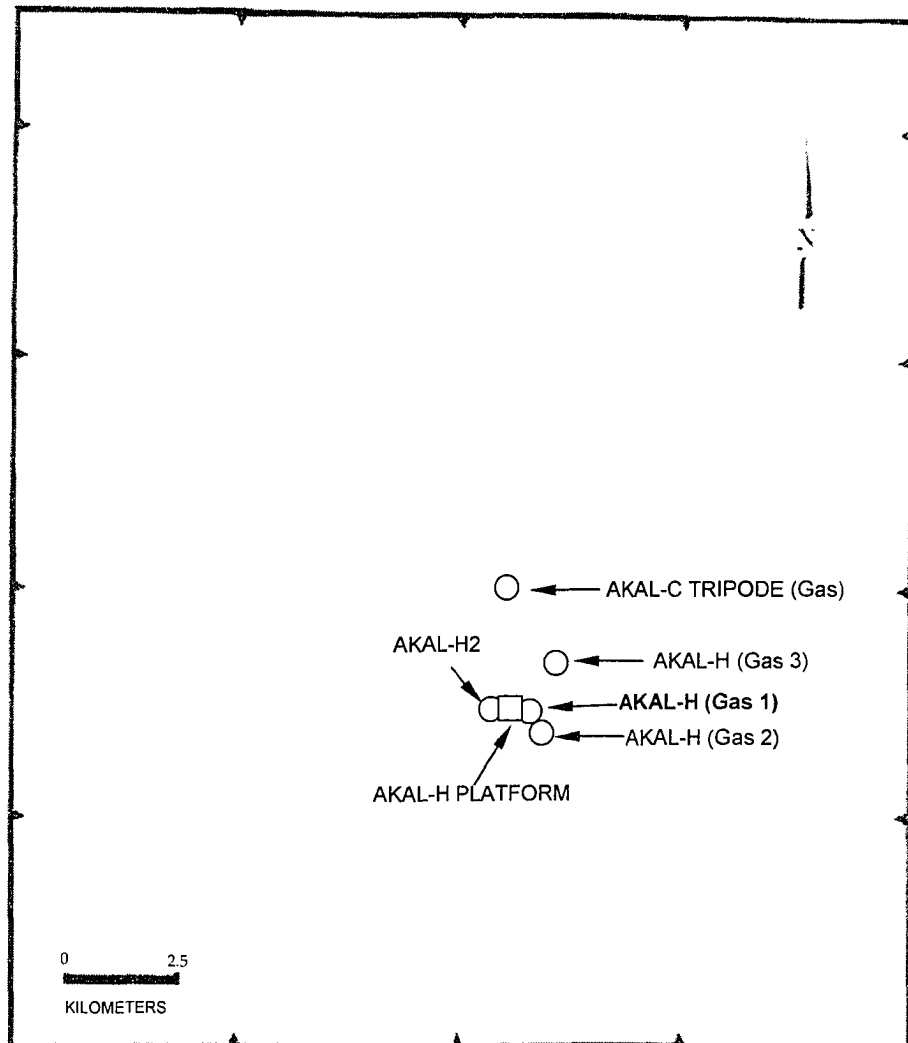


Figure 2.3 Borehole Localization
(modified from FUGRO 2002)

2.4.2.1 General Subsurface Stratigraphy

The survey area is approximately 3.5 km wide and 4.0 km long. The long axis of the area is oriented north-northwest. The seafloor itself is a very soft to firm clay. Beneath this superficial layer of geologically recent deposits lies what has been interpreted by FUGRO (2002) as a buried reef feature. Geotechnical samples from this feature are predominately calcareous sands and silts with occasional shell and coral fragments, generally in a layer less than 4 m thick. Below this feature is a very stiff clay layer; highly overconsolidated through desiccation. Immediately below this layer, generally at about 23 m depth, the stratigraphy comprises four major sand units, designated as Sands A, B, C and D, separated by overconsolidated clay strata. These alternating layers of carbonate to calcareous sand and less thick layer of overconsolidated clay extend to a depth of about 120 meters. Below these strata hard clay interlayered with claystone and occasional limestone are encountered. FUGRO (2002) concluded that the four sand units appeared to be continuous across the survey area, although some variability in thickness and gradation. Figure 2.4 shows the four sand layers.

indicating that it is ancient and has been inactive. Geophysical data indicate that the fault extends into the deep strata and probably to the reservoir level. Channels along the face of this fault are suspected of being the major vertical migration route for deep thermogenetic hydrocarbons moving into the foundation zone soils (FUGRO, 2002).

2.4.2.3 Distribution of Gas and the “Chimney” Feature

The geophysical survey also revealed evidence of gas in the superficial and semi-deep soils in a majority of the study area. The gas generally occurred within a corridor centered on the buried fault. The gas found within this corridor extends up to about 900 m to the west and about 1,350 m to the east of the fault. Outside of the corridor, the concentrations of gas in the shallow and semi-deep soils decreases significantly. A large zone of chaotic seismic data was also used to identify a “chimney” feature where gassy shallow soils obscure the underlying stratigraphy. The chimney feature indicates proximity to major vertical migration routes of thermogenic gas and oil from deep below the surface to less competent, and more porous, foundation-level strata that allow the gas and oil to disperse into a large area as the vertical migration continues. Within the chimney, migration of gas and oil is not limited to the zone directly adjacent to the fault plane; because of the large volume of hydrocarbons escaping upward

along the fault, the gas and oil is filtering vertically through the overlying soils, forming a high-saturation zone. The soils within this zone are permeated with gas and oil.

The majority of the gas pockets in the superficial clay and “buried reef” carbonate sands are located in the southern half of the area and are associated with the chimney feature. Several seafloor mounds were identified in the area and it is inferred that these were formed through the expulsion of shallow gas through the seafloor (FUGRO 2002). There are many gas plumes in the water column associated with gas in the superficial soils. A comparison of the distributions of gas in the superficial soils and gas expulsion into the water column identified during studies in the area in 1978, 1997 and 2002 indicate that the quantity and extend of the gas in the superficial soils has increased over time (FUGRO, 2002).

2.4.2.4 Characteristics of the Chimney Hydrocarbons

The AKAL-H (Gas 3) borehole location lies within the chimney feature. The majority of samples recovered from this borehole below the superficial clay were visibly permeated with hydrocarbons (FUGRO, 2002). Geochemical analyses indicate that the hydrocarbons are of thermogenetic and not biogenetic origin and in concentrations that are associated with a major seep. In the upper clay, the absence of the more highly volatile (gasoline-range) and more

biodegradable (n-alkane) components of the hydrocarbon, coupled with the high concentration of carbon dioxide, indicates that biodegradation is active within the soil. A sharp increase in the concentration of these components corresponds to the appearance of a layer of solidified hydrocarbons, or bitumen, at about 13.4 m penetration. The bitumen layer is a naturally formed, high concentration of the hydrocarbons, which has possibly intruded into a previously existing channel feature, displacing the soil. The presence of the more volatile components of naturally occurring oil within the bitumen indicates that the layer is relatively fresh and not a relic feature (FUGRO, 2002).

Below the bitumen layer, the soils are permeated with hydrocarbons but the concentration of the high molecular weight components generally decrease with depth. This reduction may be an indication that the borehole is not centered over and within a direct vertical migration path, but instead lies some distance away. The absence of excess pore pressure in the dissipation tests performed at the site (FUGRO, 2002) may be also be due to the borehole being offset from a nearby and more direct migration route. The headspace gas in the samples does increase with depth, slightly, which may be associated with a reduction in biogenetic degradation. This is consistent with the increasing concentrations of the lighter n-alkane components with depth below the bitumen layer (FUGRO, 2002).

2.4.2.5 Lateral Migration of Hydrocarbons

Gas and oil in the deeper strata is generally concentrated within the corridor where the shallow gas is located. It is inferred that the gas is migrating upward along the fault and dispersing within the chimney into the shallower strata. Under certain conditions, when the hydrocarbons encounter highly porous sand zones, lateral migration away from the fault and chimney feature has occurred. Accumulations of gas were detected in the geophysical survey at elevations within proximity of the AKAL-H (Gas 1) and AKAL-C TRIPODE (Gas) borehole sites, generally near the top of sand units or just below thin clay sub-layers within the sand units (as later identified in the geotechnical borings). The hydrocarbons at these sites, outside the chimney feature, appear to be thin lateral stringers of hydrocarbon that have migrated away from the chimney. Geochemical analyses of samples from the borehole sites outside the chimney confirm that the hydrocarbons are of the same origin as the hydrocarbons within the major seep zone and appear to have migrated relatively recently from thermogenic sources at depth.

The mechanism for hydrocarbon migration are not well established. Many theories have been advanced but few seem to be able to account for the large accumulations of hydrocarbons in the typical reservoir. One theory proposed

that is consistent with the absence of excess pressure measured during the field surveys (FUGRO, 2002) is migration through microfracturing, where migration occurs in a series of pulses which lead to hydraulic microfracturing of the porous medium and lateral movement of the hydrocarbon fluids and gases. The accumulation in the upper regions of the sand layers could also be an indication of lateral flow in response to pressure gradients but soil pore fluids are not easily displaced. Although the buoyancy of hydrocarbon liquids and gases, and other inorganic gases will result in an upward component of force, buoyancy alone would likely require a large amount of time to displace pore fluid and accumulate beneath the clay layers.

It is important to note that the concentration of hydrocarbons in the stringers within the sand strata below AKAL-C TRIPODE (Gas) and AKAL-H (Gas 1) are sometimes as high as those encountered in the samples from the chimney feature borehole, AKALH (Gas 3). This demonstrates that migration within a complex subsurface lithology, such as that at Cantarell field, is not likely to lead to uniform spherical diffusion and dispersion of the fluid and gas. Instead, preferential migration routes may become established and lead to a highly variable and unpredictable distribution of hydrocarbon (FUGRO, 2002).

2.4.3 Effects of Liquid Deposits on Mechanical Properties

The nature of the hydrocarbon deposits encountered in the geotechnical and geochemical investigation (FUGRO, 2002) at the four gas-study boreholes include the following:

- sands, silts and clays with liquid hydrocarbon inclusions (pockets);
- sands, silts and clays with liquid hydrocarbon permeating the pore fluids;
- solid tar-like pitch (bitumen); and
- conglomerate materials of degenerated tar-like hydrocarbon and clay, sand or silt.

Small pockets of liquid hydrocarbon inclusions had little measurable influence on the response of the soils based on in situ or standard laboratory strength tests. Where the soil was permeated with liquid hydrocarbons, no direct effects could be discerned; but as the hydrocarbon, content increased, it is almost certain that free gas will exist in the pore spaces which could affect the soil response (FUGRO, 2002).

Solid hydrocarbons (bitumen), of sufficient quantity, will affect soil properties adversely in foundation design. Where soil hydrocarbons are most problematic is where they exist either as an independent subsurface unit or

where they exist at a sufficiently high concentration within a conglomerate soil-hydrocarbon material to dominate the soil response (FUGRO, 2002).

At the AKAL-H (Gas 1) borehole site, pockets of what appeared to be hydrocarbon were encountered at 22.9 m penetration in Stratum III, a very stiff clay. Additional hydrocarbons were found permeating the pore fluids between about 94.2 and 107 m penetration in Stratum X, a calcareous fine sand stratum, which is part of the Sand D geologic unit as defined in the geophysical survey (FUGRO, 2002).

Geochemical tests on the shallow soil strata above 27.7 m revealed a hydrocarbon content slightly above background level (100 to 5,000 ppm). These hydrocarbons, as well as those in the deeper strata, are not expected to have a discernable effect on the cohesive soil shear strength. No discernable effect on the shear strength of cohesive samples with these inclusions was noted in either laboratory testing or in the in situ (PCPT) record. This conclusion was established through a comparison of the strength data presented on the boring logs for all four gas borings as well as inspection of the shear strength data from unconsolidated-undrained triaxial tests (FUGRO, 2002).

Hydrocarbons present in the granular stratum X, part of the geologic unit Sand D, showed very high methane content in the head-space gas test and the fluorescence test results indicate a significant hydrocarbon content of higher

molecular weight compounds. As the hydrocarbon was observed to be liquid permeating the pore fluids of the matrix of dense to very dense siliceous fine sand, the effect on the material properties with regard to foundation design was evaluated using creep tests performed on similar samples from AKAL-H (Gas 3). These tests demonstrated that creep effects were minimal after 24 hours of sustained load in triaxial compression. At stress ratios (the ratio of the deviator stress to the consolidation stress) ranging up to 0.25, the creep “n”, representing the decrease in Young’s modulus over time, was essentially zero (FUGRO, 2002).

2.4.4 Summary

Based on field and laboratory studies carried out in the Cantarell field as well as intense analysis regarding the impact of liquid hydrocarbons on the mechanical properties of the foundation soils, the following conclusions were reached (FUGRO, 2002):

- Elevated concentrations of thermogenic hydrocarbons (gases and liquids) and inorganic gas, as well other supporting data (pore water sampling and geophysical data), support an interpretation of active fluid migration from depth;
- Anomalous (significant above background level) light hydrocarbons present in foundation level strata at the AKAL-H (Gas 1) borehole site and at selected

depths within the AKAL-H (Gas 2) and AKAL-C TRIPODE (Gas) sites are not at present expected to adversely impact the mechanical properties of the soils;

- Anomalous high molecular weight hydrocarbons present as liquid and gassy inclusions in the pore fluids at selected depths within AKAL-H (Gas 1) and (Gas 2); and AKAL-C TRIPODE (Gas) boreholes are also not expected alone to adversely impact foundations. Tests indicate granular soils with liquid hydrocarbons in the pore fluid do not display creep behaviour;
- The geochemical profile from borehole AKAL-H (Gas 3) displays fresh oils with minimal bacterial alteration in the samples from deeper than about 13.4 m. Visual examination of samples from between about 13.4 and 32.3 m penetration reveals that the layer is composed of relatively fresh bitumen. Such material will display pronounced creep behaviour and cannot be relied upon for either pile frictional resistance or end bearing, although it may provide limited resistance during short-term loading. No similar layers of bitumen were encountered at the borehole sites outside the chimney feature; and
- The presence of high volumes of gas and liquids in the superficial clay soils at the AKAL-H (Gas 3) site is altering the strength and modulus of the soil. These effects can best be directly accounted for through in situ vane shear testing.

The report concludes that the lithology and geologic processes ongoing in the Cantarell Field survey area are very complex and difficult to predict. There

are concerns with not only naturally occurring phenomena but also reservoir development effects on the stability of existing and proposed structures. The data available at present is insufficient to fully and quantitatively define the gas-related impacts on existing and future structures within the survey area.

2.5 Influence of Oil Contamination on the Mechanical Properties of Sand

2.5.1 Shear Strength

2.5.1.1 Triaxial Tests

Based on the triaxial test, it is possible to obtain the strength parameters (cohesion c and angle of internal friction ϕ) and also deformation characteristics of the soils (initial tangent modulus E_i), and is the most common test technique used to investigate the mechanical properties of oil contaminated sands.

The investigations carried out by Evgin et al., (1989), Amor (1990), Evgin and Das (1992), Hasan et al., (1995) considered two states of initial relative density for the sand: (loose and dense) and two liquids for saturation: (water and oil). All samples were consolidated and sheared under triaxial compression conditions up to about 20% axial strain.

Hasan et al., (1995) also conducted triaxial compression tests but used a constant relative density of 60% in all the tests and the oil saturation in the specimens was equivalent to soil contaminated with 6% of heavy crude oil.

The results obtained by Evgin and Das (1992) provide the best representation of the mechanical behaviour of samples under the triaxial test, saturated with water and oil and are discussed below.

Drained Tests

The results of experiments on loose, clean sand under drained test conditions are provided in Figure 2.5 and the results of similar tests, where loose samples were saturated with oil, are shown in figure 2.6 for the same range of confining pressures. Comparisons between these two Figures indicate that the effect of oil contamination is to decrease the strength and increase the contractive volumetric strains.

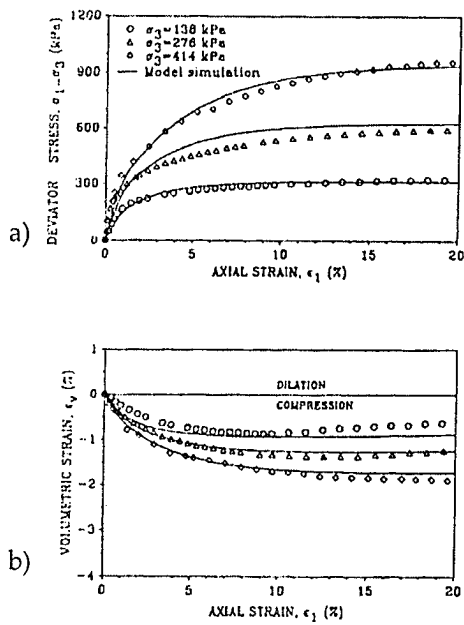


Figure 2.5 Results of Drained Tests and Simulations for Clean Loose Sand
 a) deviator stress vs. axial strain,
 b) volumetric strain vs. axial strain

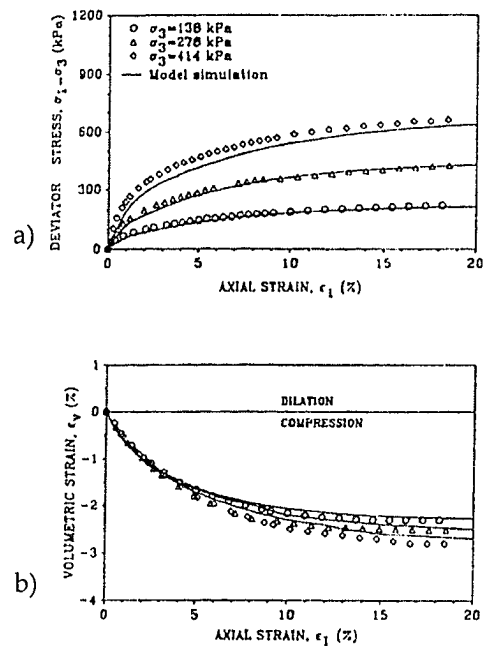


Figure 2.6 Results of Drained Tests and Simulations for Oil Contaminated Loose Sand
 a) deviator stress vs. axial strain,
 b) volumetric strain vs. axial strain

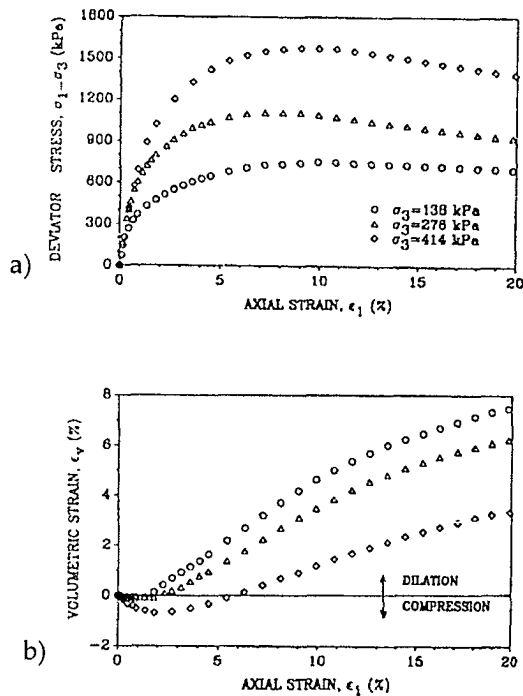


Figure 2.7 Results of Drained Tests and Simulations for Clean Dense Sand
 a) deviator stress vs. axial strain
 b) volumetric strain vs. axial strain

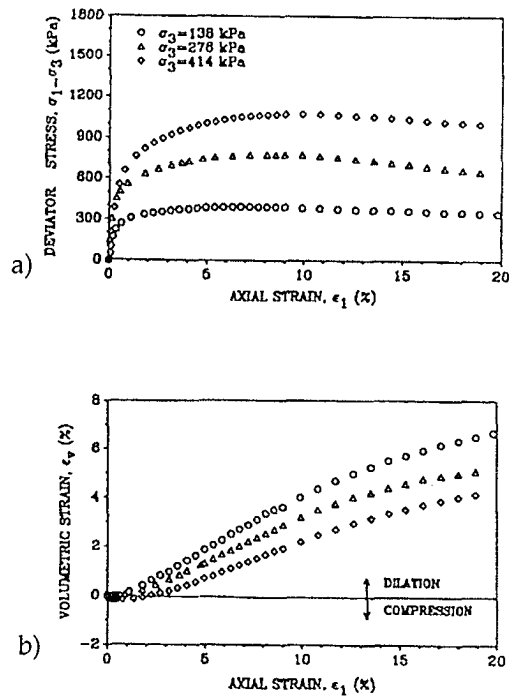


Figure 2.8 Results of Drained Tests and Simulations for Oil Contaminated Dense Sand
 a) deviator stress vs. axial strain
 b) volumetric strain vs. axial strain

Figure 2.7 shows the stress strain response of the clean, dense sand in drained triaxial tests. The confining pressures used in these tests are 138, 276, and 414 kPa. Test data related to the oil contaminated sand are presented in Figure 2.8. Figures 2.7 and 2.8 indicate that the strength of the dense sand decreases

when the soil is saturated with oil. There is little difference in the volumetric strains developed in clean and contaminated dense sands during shearing.

Undrained Tests

The undrained behaviour of loose sand for both clean and oil contaminated states is presented in Figures 2.9 and 2.10 at a confining pressure of 138 kPa. During shear, oil contaminated loose sand generates higher pore pressures than clean sand, as shown in Figure 2.9. Their respective effective stress paths are illustrated in Figure 2.10.

Figure 2.11 shows the results of undrained tests on dense sand. These tests were conducted using a confining pressure of 276 kPa. No significant change is caused by oil contamination on the pore pressure response of dense sand.

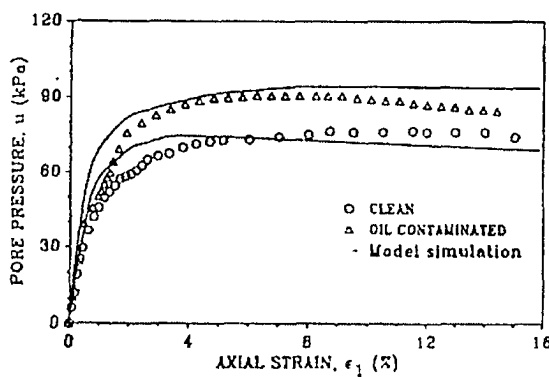


Figure 2.9 Pore Pressure vs. Axial Strains in Undrained Tests for Loose Sand

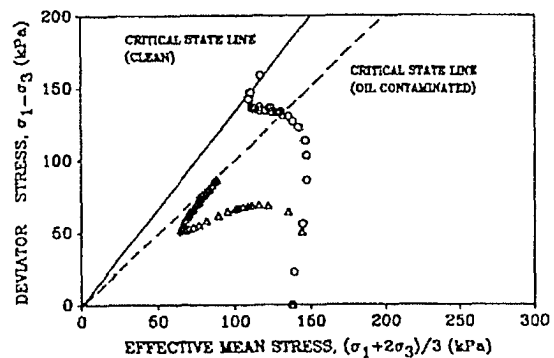


Figure 2.10 Deviator Stress vs. Mean Stress in Undrained Tests for Loose Sand

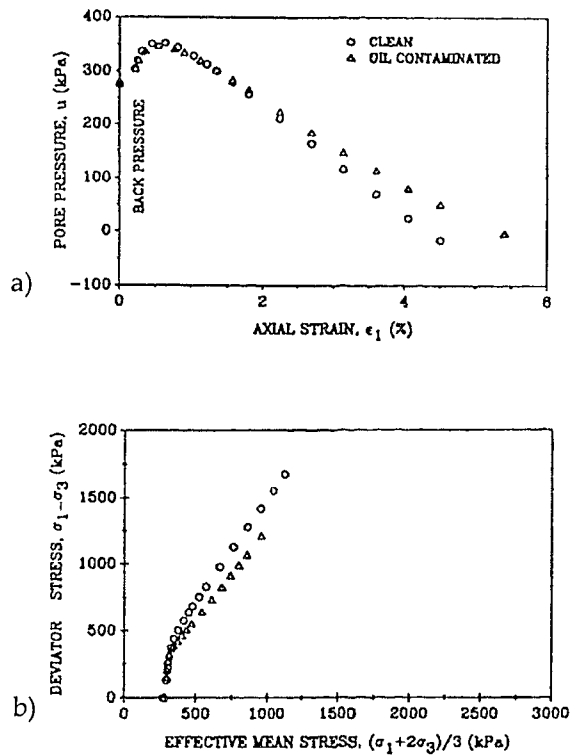


Figure 2.11 Results of Undrained Tests for Dense Sand
a) pore pressure vs. axial strain;
b) deviator stress vs. mean stress

Table 2.1 summarizes the Mohr-Coulomb strength parameters and the initial tangent modulus determined from the experimental results by Amor (1990).

Table 2.1 Soil Parameters

Type of Sand		Loose		Dense	
		Clean	Contaminated	Clean	Contaminated
Internal Friction Angle (degrees)		32.2	26.2	41.5	35.3
Initial Tangent Modulus (MPa) for	$\sigma_3=138\text{kPa}$	19	6	62	100
	$\sigma_3=276\text{kPa}$	28	14	93	167
	$\sigma_3=414\text{kPa}$	38	23	116	250

Oil contamination clearly causes a decrease in the angle of friction as well as the initial tangent modulus. Except for the initial tangent modulus of dense sand which is increased because of oil contamination.

Similar results were found by Hasan et al., (1995) who determined strength parameters for clean and contaminated sands were ($c=0, \phi=32^\circ$) and ($c=0, \phi=30^\circ$), respectively, showing a decrease in the friction angle due to oil contamination. The amount of decrease is less than that found by Evgin and Das (1992) because a lower degree of oil saturation was used by Hasan et al., (1995). Moreover, the stress-strain curves obtained by Hasan et al., (1995) showed a softer response for the contaminated sand, with values of the initial tangent modulus, E_i , of nearly half the corresponding values for clean sand, matching the trend obtained by Evgin and Das (1992).

Saad (1998) carried out some isotropically consolidated undrained triaxial tests on quartzite sand contaminated with 60 g/kg heavy crude oil at different temperatures and on clean sand at room temperature using a modified triaxial cell to enable testing at controlled temperatures. The specimens were prepared on the base of the triaxial cell, in a rubber membrane stretched in a thin mold and were compacted to the maximum dry density using vibration under a surcharge.

Table 2.2 presents a summary of the strength parameters for different temperatures. It is clear from the results that the angle of internal friction (ϕ) for the oil contaminated sand is not sensitive to the testing temperature. However, the oil contamination resulted in a reduction of more than 2° in the ϕ value. This reduction is attributed to the lubrication provided by the oil at the grain contacts.

Table 2.2 Summary of the Shear Strength Parameters Obtained from Triaxial Testing

Temperature (°C)	Oil Content (g/kg)	Cohesion, c (kPa)	Friction angle, ϕ (degrees)
10	60	11.1	41.7
15	60	9.2	41.5
23	60	7.1	43.1
35	60	7.3	42.7
50	60	11.9	42.2
23	0	0	45.5

According to Saad (1998), the observations with regard to the shear strength parameters and effect of temperature on such properties are expected to change if samples are tested using drained triaxial testing or if the samples are prepared at lower densities. The effect of temperature will be more pronounced at these two situations or their combination.

Based on the experimental results presented above, it can be concluded that the shear strength parameters base on as-molded triaxial tests are not

sensitive to the testing temperature when samples are compacted to their maximum dry densities.

2.5.1.2 Direct Shear Tests

Cook et al., (1992) carried out direct shear tests on dry and oil contaminated Mississippi River sand where crude oil was used as the soil contaminant. These tests were conducted using different degrees of oil contamination, S_o , initial relative densities, D_r , and total normal pressures with the main objective to investigate the possible negative effects of the presence of oil in the pore spaces on the strength-deformation behaviour, and the angle of internal friction.

The test parameters for the direct shear tests are given in Table 2.3. All tests were performed in an undrained condition at a constant rate of horizontal displacement of 0.25 mm/minute.

Table 2.3 Test Parameters Used for Direct Shear Tests

Initial relative density, D_r (%)	40,60,85
Degree of oil contamination, S_o (%)	0-28.5
Total normal pressure (kPa)	34.5-172.5

The data from the direct shear tests conducted in the laboratory were used to obtain shear stress versus horizontal displacement plots for the specimens of clean dry sand, and also for crude oil contaminated sand specimens.

As shown in Figure 2.12, the peak shear stress decreases as the degree of oil saturation increases. Other interesting fact that can be observed from Figure 2.12 is that the magnitude of horizontal displacement required to mobilize peak shear stress increases sharply with an increase in the degree of oil saturation.

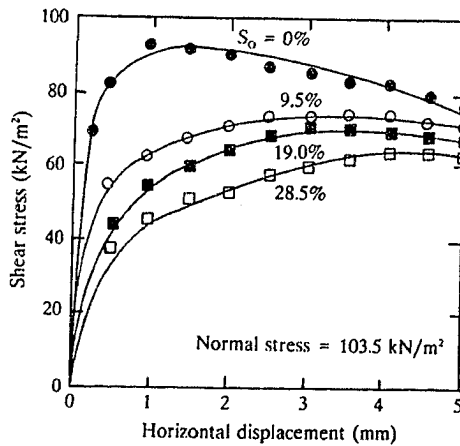


Figure 2.12 Typical Plots of Shear Stress versus Horizontal Displacement ($D=65\%$)

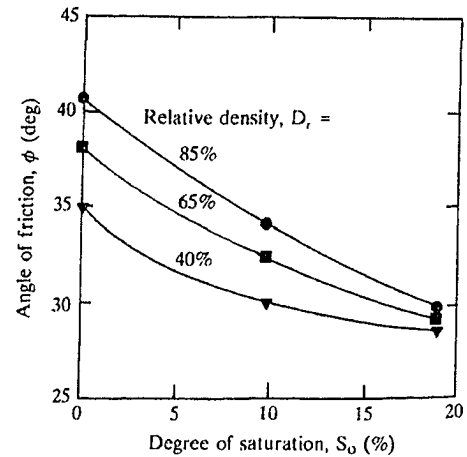


Figure 2.13 Variation of Angle of Friction versus Degree of Saturation

Figure 2.13 shows that the decrease in the angle of friction is a function of both the initial relative density of sand and the degree of crude oil saturation. For the range of parameters studied by Cook et al., (1992) the percentage decrease in the values of angle of friction ranged from 17.6% to 25% as compared to its value at the same relative density in the dry state. Additionally, for a given degree of oil saturation, the decrease in angle of friction is larger for sand at a higher relative density. Clearly, the results of Cook et al., (1992) show that shear strength parameters of sand are adversely affected by oil contamination.

Hasan et al., (1995) also carried direct shear tests on Jahra sand to examine the influence of relative density, type of oil, and percent contamination on the effective strength parameters. Tests were conducted at relative densities of 30%, 60%, and 90%. For four types of oil, the percent oil contamination varied between 2% and 6% by weight. The tests were performed in a shear box 100mm x 100mm x 20mm with a rate of shear equal to 0.75 mm/min used for all the tests.

Figure 2.14 shows the relationship between the angle of friction and relative density for clean sand, sand mixed with heavy crude oil, and sand mixed with light gas oil at different oil contents. These results show that the maximum reduction of the friction angle, ϕ , of 5-7° occurs with heavy crude oil. This reduction was evident for all relative densities from loose to very dense conditions. Moreover, for the range of oil saturation employed in this study, the influence of oil saturation on ϕ is negligible.

No cohesion was found for any specimen tested in this program.

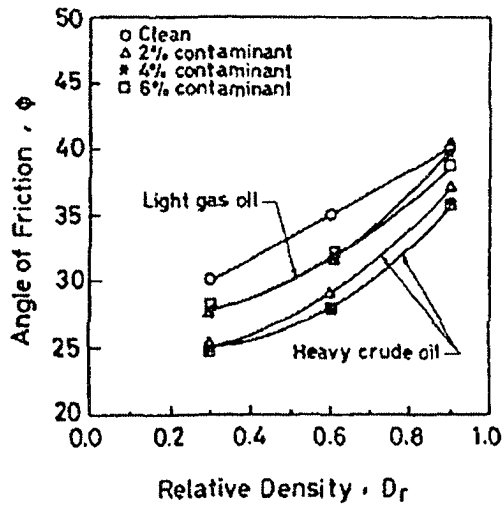


Figure 2.14 Relationship between Relative Density and Friction Angle for Heavy Crude Oil and Light Gas Oil

From this investigation it can be concluded that oil contamination leads to decrease strength. However, the changes are not significant in relation to the percentage of oil. The reduction in the angle of friction was 2° for specimens prepared at a relative density of 60% and mixed with 6% of heavy crude oil.

Heavy crude oils affect the strength parameters of sand more than light gas oil and benzene at all relative densities.

2.5.2 Interface Steel-Sand Shear Strength

2.5.2.1 Direct Shear Test Apparatus

One of the first reported works about the behaviour of interfaces between oil contaminated sand and steel was done by Amor (1990) in his master's thesis research at the University of Ottawa. During his investigation the following materials were used:

- a factory crushed fine to medium quartz sand, designed Silica-24; and
- a Motomaster grade 50 heavy duty motor oil.

All tests were conducted in a Wykeham-Farrance strain-controlled direct shear machine using a 38mm depth, 50mm² shear box. For test program, the sand was prepared at a loose state obtained by pluvial deposition. The density of the sand specimens ranged from 1.35 g/cm³ to 1.40 g/cm³. Two different types of interfaces were tested. The first interface was between the sand and a block of mortar prepared by mixing sand and Portland cement. The finished surface was polished to obtain a clean level interface. The second interface had a steel block with a surface intentionally made smooth.

The test procedures were similar to conventional direct shear testing, with the major difference being in the set up of the samples. The shear box was

assembled in the testing machine with the concrete or the steel block in the bottom half. Sand was placed in the top half of the box by pluvial deposition.

Since the testing program was aimed at establishing the effect of oil contamination on the behaviour on the interfaces, the test procedure was the same for both, clean and oil contaminated sand. Oil contamination was achieved by submerging the shear box in oil. Three normal stresses were applied for each particular case and the shear displacement rate used was 0.30 mm per minute. This deformation rate was used in testing the interfaces in order to have no pore pressure generation in drained tests.

Experimental results

The primary purpose of the experiments in Amor's study was to investigate the effect of oil contamination on the frictional behaviour of the interfaces. The experimental data are plotted in the form of shear stress-horizontal displacement curves in Figures 2.15, 2.16 for steel-sand interfaces. The maximum shear resistance versus normal stress plots provide the interface friction angle, δ . Table 2.4 summarizes the results for interface angles.

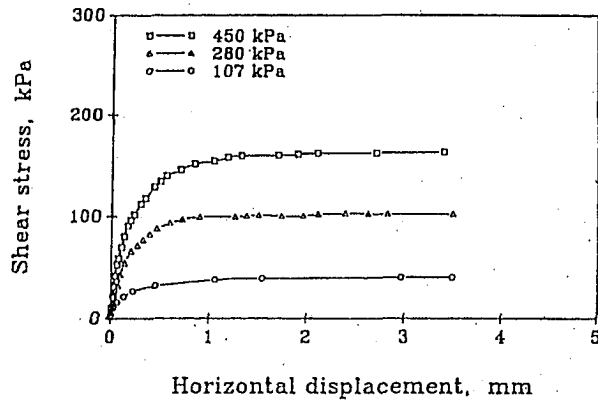


Figure 2.15 Results of Tests on Steel Interface and Clean Loose Crushed Quartz Sand

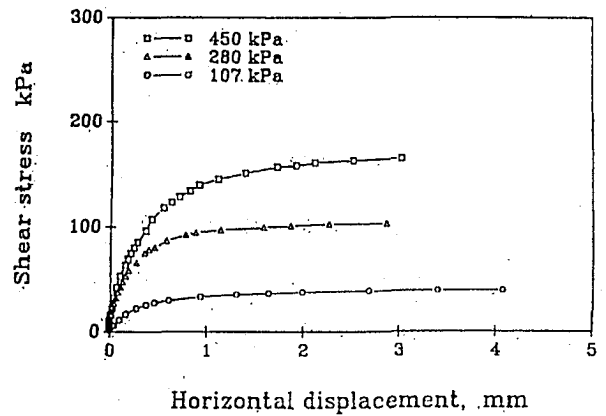


Figure 2.16 Results of Steel Interface and Oil Contaminated Loose Crushed Quartz Sand

The interface friction angle, δ , varied by about 1.5° as a result of oil contamination for the sand-concrete interface, while almost no change in the interface friction angle was obtained for the case of steel-sand interface.

Table 2.4 Summary Results on Interfaces

Type of test	Friction angle
Direct Shear test on sand	30.0
Interface concrete and clean sand	27.3
Interface concrete and oil contaminated sand	25.9
Interface steel and clean sand	20.0
Interface steel and oil contaminated sand	20.3

Clearly, Amor's (1990) conclusion was that oil contamination has little effect on the interface behaviour for a smooth surface, and only a modest influence for a rough surface.

In contrast, Hasan and Mostafa (1996) found that for smooth surfaces, oil is more efficient in reducing the interface angle of friction (δ), than bentonite. Moreover, for rough lubricated surfaces the viscosity of the lubricant has less significant effect on reducing the interface angle of friction. Also Hasan and Mostafa (1996) found that for rough surfaces both oil and bentonite have nearly the same effect on reducing the interface angle of friction, while for smooth surfaces the reduction in the interface angle of friction depends on the lubricant type. Their results also show that not only the stress-displacement relationship is affected by the existence of the lubricant in the interface, but the volume change as well. In the case of rough surfaces, lubricants tend to decrease the amount of dilation during the shear tests, while in the case of smooth surfaces, sand tends to compress (decrease in volume) during shear tests for different lubricants. The results also showed that there is no well-defined peak in the case of smooth surfaces with or without lubricant.

It is important to mention that the sand specimens made by Hasan and Mostafa (1996) were reconstituted and tested dry in all tests, and when a lubricant was used, a thin film of the lubricant was applied on the upper surface of the construction materials utilizing a small brush.

2.5.2.2 Interface Testing Apparatus

Evgin et al., (1996) present a valuable contribution in his paper called "Effect of Oil Contamination on the Behaviour of an Interface".

The experimental program included (1) constant normal stress tests and (2) constant volume tests.

The soil container was a direct shear type with a cylindrical shape having base diameter of 60 mm. The interface was between a smooth steel plate and Hostun RF Sand. The average surface roughness of the steel plate was 3 μm . At this value of roughness, the surface of the steel plate was considered smooth. Motor oil (SAE 15 W-40) was used as the contaminant.

For the experiments with oil contaminated samples, oil was placed on the surface of the steel plate before the sand was pluviated into the soil container. This procedure resulted in the contamination of 3~4 mm thick layer of soil next to the surface of the steel plate. In each experiment, after the application of the normal stress, the sample was sheared in one direction up to about 7 mm.

Constant Normal Stress Tests

The different values of constant normal stress, 100, 150, and 200 kPa, were used in the experiments. The test results for both clean and oil contaminated loose sands are shown in Figures 2.17 and 2.18 respectively. The shear strength developed at the interface for oil contaminated loose sand was less than that of

the interface between the clean loose sand and steel plate. The coefficient of friction of the interface was 0.48 for the clean loose sand and 0.43 for the oil contaminated loose sand. The amount of tangential displacement required for the peak strength to develop was between 1 to 2 mm.

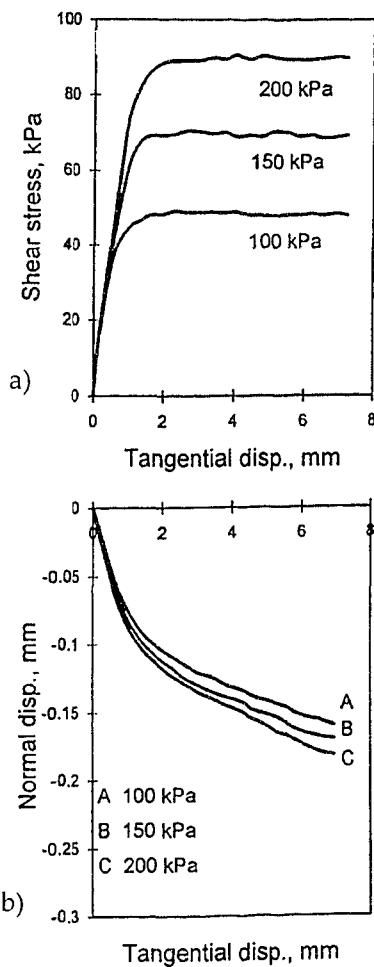


Figure 2.17 Constant Normal Stress Tests on Clean Loose Sand
a) variation of shear stress
b) variation of normal displacement with tangential displacement

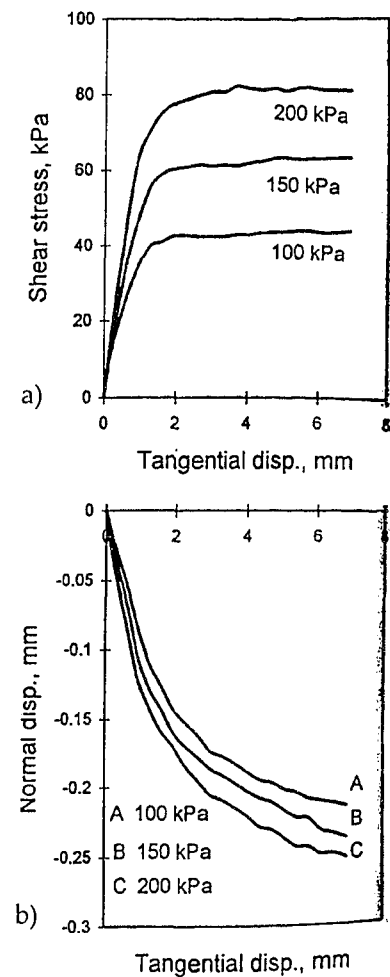


Figure 2.18 Constant Normal Stress Tests on Oil Contaminated Loose Sand
a) variation of shear stress
b) variation of normal displacement with tangential displacement

The deformations of the sample in the direction normal to the interface are shown in Figures 2.17b and 2.18b. For all test conditions, the loose specimens contracted or compressed throughout shearing but oil contaminated specimens contracted almost 50% more than the clean sand specimens.

For medium dense sand, Figures 2.19 and 2.20 illustrate the interfacial behaviour for clean and oil contaminated sands. Clean medium dense sand shows slight strain softening and a dilation response during shear.

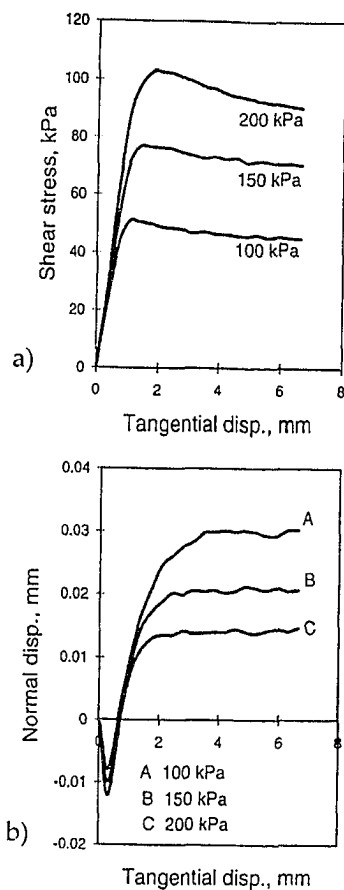


Figure 2.19 Constant Normal Stress Tests on Clean Medium Dense Sand
 a) variation of shear stress
 b) variation of normal displacement with tangential displacement

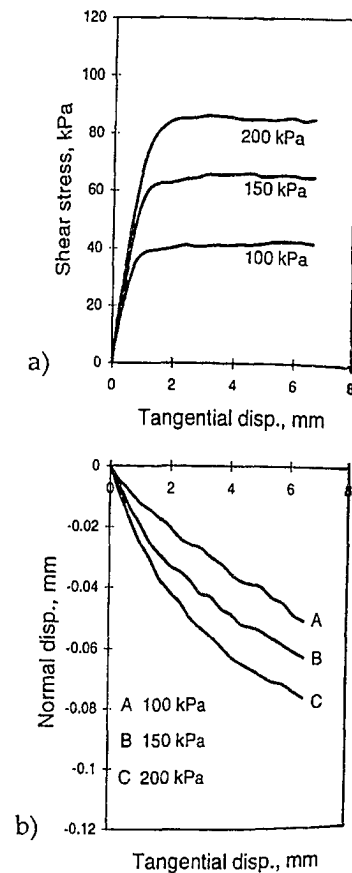


Figure 2.20 Constant Normal Stress Tests on Oil Contaminated Medium Dense Sand
 a) variation of shear stress
 b) variation of normal displacement with tangential displacement

For oil contaminated medium dense sand specimens, however, both strain softening and dilatational volume behaviour disappeared and the interface friction angle became smaller. The coefficient of friction of the interface was 0.51 for the clean sand and only 0.43 for oil contaminated medium dense sand.

These test results also show that the influence of density on the coefficient of interface friction is significant. Whether the sample dilates or contracts during shearing depends on the initial density, as expected, but also depends on whether the interface is contaminated with oil.

Constant Volume Tests

In these tests, an automated control system continuously adjusted the normal stress in order to maintain the volume constant during shear. As a result, the normal stress, which changed during the test, influenced the development of shear resistance of the interface. Each test continued as long as the normal stress remained positive. In all constant volume tests with loose, sand for example, the normal stress reduced to zero during shearing.

The variations of shear stress and normal stress during constant volume tests are shown in Figures 2.21a and 2.21b for the clean medium dense sand samples. There was a reduction in normal stress up to 0.8 mm of tangential displacement followed by increasing the normal stress up to a constant value slightly larger than the original normal stress.

Figure 2.22 illustrates the results for oil contaminated medium dense sand samples. As shown in Figure 2.22, oil contamination leads to significant changes in the sand-steel interface. The normal stress drops continuously during shear and the shear strength of the interface becomes as low as 50% of the strength value obtained from interface tests on clean medium dense sand samples.

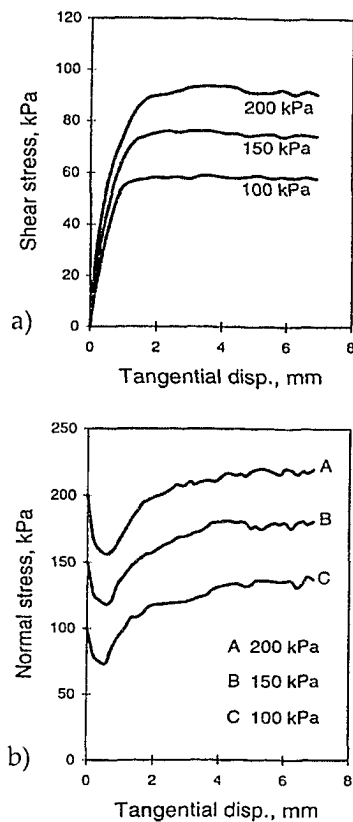


Figure 2.21 Constant Volume Tests on Clean Medium Dense Sand
a) variation of shear stress
b) variation of normal stress with tangential displacement

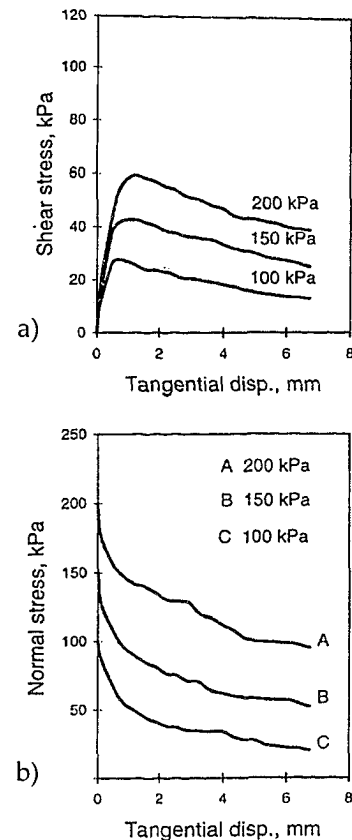


Figure 2.22 Constant Volume Tests on Oil Contaminated Medium Dense Sand
a) variation of shear stress
b) variation of normal stress with tangential displacement

The main conclusions reached from this experimental study are that:

- oil contamination reduces the coefficient of friction at the interface by about 10-15%;
- oil contamination at the interface in medium dense sand alters its behavioural characteristics such as strain softening and dilation; interface behaviour in oil contaminated medium dense sand behaves like an interface in clean loose sand; and
- constant volume test data show that the undrained behaviour of the interface would be significantly affected by oil contamination.

3. TESTING PROGRAM

3.1 Introduction

The main objective of this research is to assess the influence of oil contamination on the stress-strain-strength and interface properties of an analog sand representing sand layer IV found within the Cantarell Field. The analog sand was reconstituted to have the same grain size distribution as Sand Layer IV. The following section describes the three distinct test programs conducted in this research:

1. consolidated-undrained compression tests, to study variations in deformation properties (E_i), strength parameters (c' , ϕ') and undrained stress path;
2. direct shear tests, to study variations in strength parameters (c , ϕ) of the sand due to oil contamination; and
3. interface shear tests, to examine the influence of oil contamination on the sand-steel interface strength parameters (c , δ).

3.2 Materials used in Laboratory Program

3.2.1 Analog Sand

Sand specimens from sand layer IV were not available for this research study. In fact, due to the offshore location, the availability of any in situ sample from the Cantarell field was extremely limited. Consequently, an analog sand

was reconstituted to the specifications of Sand Layer IV in order to provide sufficient material to complete the test program. The analog sand is a silty sand reconstituted using sieve analyses of locally available Saskatchewan sand and the addition of 19.32 % (dry weight basis) of commercial silica sand identified as “Sil 325”. This sand has no plastic properties and is composed primarily of silt size grains with a d_{50} of 75 μm . Table 3.1 shows the generalized stratigraphy of the soil layer of interest based on two boreholes located nearest the platform AKAL-H, which was identified as the platform exposed to the largest risk from strength loss imposed by the oil seepage.

Table 3.1 Description of Soil Layer IV

Borehole	Soil Layer	Penetration (m)		Thickness (m)	Relative Density D_r (%)	Description
		from	to			
AKAL-H2	IV	22.3	37.5	15.2	10-50	Dense to very loose calcareous silty fine to fine sand
AKAL-H (Gas 1)		23.2	38.1	14.9	65-100	Dense calcareous silty fine to fine sand

Figure 3.1 shows the grain size distribution curves of a series of samples taken from the boreholes AKAL-H2 and AKAL-H (Gas 1) at different depths into the layer IV (FUGRO, 2002), including the grain size distribution of the analog sand.

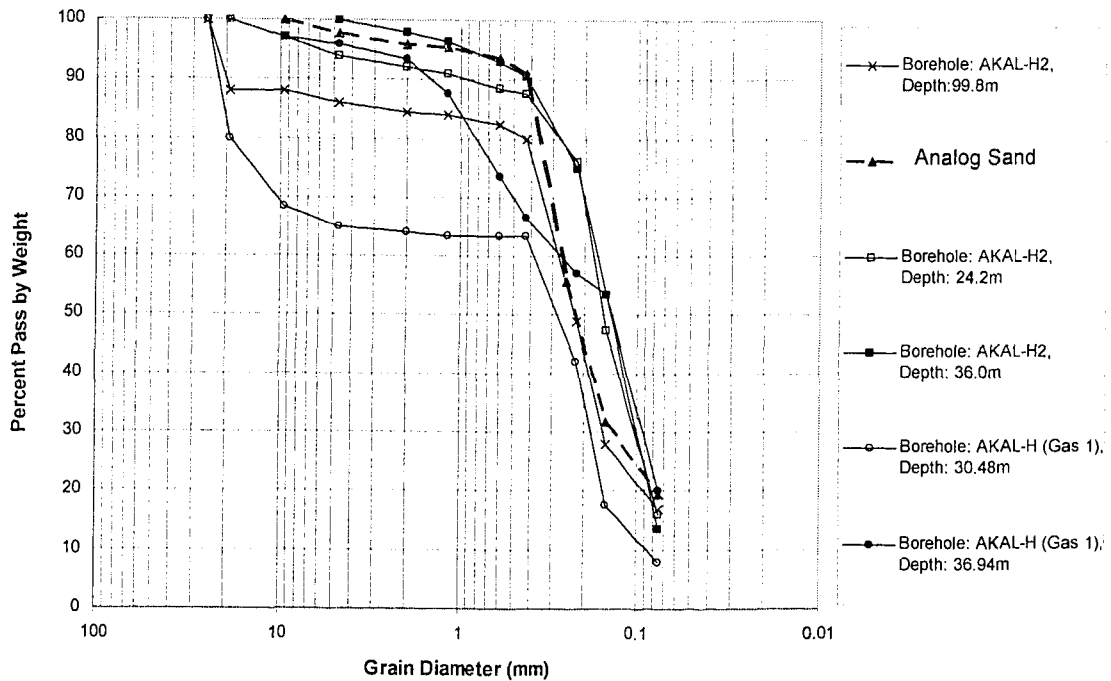


Figure 3.1 Grain Size Distribution Curves

Saskatchewan silica sand has highly rounded grains and contains up to 98.5 per cent silica (SiO_2). (Industry and Resources, 2004). The specific gravity of the analog sand, G_s , was 2.65 since both the Saskatchewan sand and the silica flour both had a $G_s = 2.65$.

The maximum and minimum densities for the analog sand were determined using ASTM D 4253-00 dry method and ASTM D 4254 -00 A method respectively. Table 3.2 summarizes the properties of the analog sand.

Table 3.2 Soil Properties for Analog Sand

Soil Type	Dry Density ρ (g/cm ³)			Void Ratio (e)			Relative Density (D _r)
	ρ_{dmax}	ρ_{dmin}	ρ_{target}	e_{min}	e_{max}	e_{target}	Target for Test Specimens
Analog Sand	1.994	1.500	1.760	0.332	0.767	0.506	60 %

The analog sand is classified as SM (silty sand) according to the Unified Soil Classification System (USCS).

3.2.2 Oil

It was also necessary to select an analog for the heavy crude oil which had seeped into the sand layer IV. The oil selected for this research was a commercial engine oil, which closely matches the kinematic viscosity of the Maya Mexican heavy crude oil at 25° Celsius. The viscosity of the Maya Mexican crude oil at 25° Celsius is equal to 696.0 Seconds Saybolt Universal (SSU) number (Sandoval, 1998). The SSU number is a unit of measure for viscosity and is determined using ASTM Method D88. The SSU is a measure of the efflux time, in seconds, required for 60 mL of a petroleum product to flow through the calibrated orifice of a Saybolt Universal viscometer, under carefully controlled temperature. To convert SSU to the more common units of kinematic viscosity, Centistokes, the following conversion factor is applicable:

$$\text{Centistokes Units} = \frac{SSU}{4.55} \quad (3.1)$$

This equation is applicable for centistokes units greater than 50. Consequently, the viscosity for the analog oil should be near a kinematic viscosity of 153 Centistokes.

In the AKAL-H (Gas 1) borehole, the in situ temperatures ranged between 25° and 28° Celsius over the depths between 20 and 80 meters. The in situ temperatures were taken during the field investigations in July and August 2002 using a temperature transducer in the Piezoprobe as well as in the Deepwater Gas Probe (DGP) supplied by the NGI (FUGRO, 2002).

The characteristics of sand layer IV were chosen from a depth of 30 m, approximately mid-depth in this sand layer. At this depth, the temperature is approximately 25° C. A match of the analog (engine) oil and Maya crude oil viscosity at a temperature of 25° Celsius was used in selected the analog oil. It should be noted that although the viscosity of the engine oil and the Maya crude oil were similar at 25° Celsius, the viscosity measurements performed on several oil samples, as shown below, was measured at a temperature equal to 20° ± 1° Celsius which corresponded to the average temperature in the laboratory. In this way, the analog oil viscosity at 20° C would match the Maya crude oil viscosity at the in situ temperature of 25° C.

The oil used in this study was chosen from a range of commercial engine oils, whose viscosities were measured in the laboratory by means of a Brookfield viscometer. Figure 3.2 shows all the engine oils tested at different shear rates. From this figure it is possible to observe that the engine oil with the commercial name “Pennzoil 5W-30” matches best the kinematic viscosity of the Maya crude oil. The measured kinematic viscosity of the chosen oil at $20^{\circ} \pm 1^{\circ}$ Celsius is equal to 147.63 centistokes (just 5 units below the Maya crude oil) with a measured density equal to 0.8467 g/cm^3 .

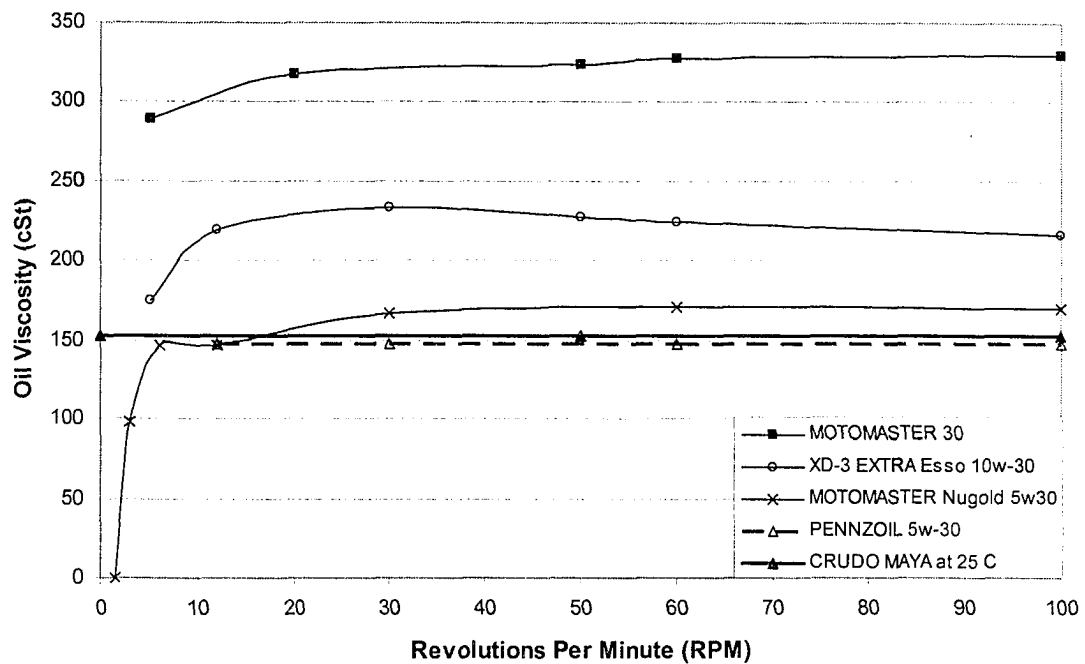


Figure 3.2 Oils Tested at Different Rates using the Brookfield Viscometer

3.2.3 Steel

The offshore platforms within the Bay of Campeche are constructed of steel with structural steel specifications conforming American Petroleum Institute (API) standards (API-RP2A-WSD, 1993). For the interface strength tests, it was important to represent as closely as possible the interfacial conditions between the steel piles of the platforms and the surrounding sand localized in the layer IV. To achieve this, a mild steel plate with dimensions of 60 mm x 60 mm x 11.48 mm and a measured average roughness of $Ra = 3.25 \mu\text{m}$, which is considered smooth, was used in this research to measure the interface friction strength between sand and steel using the direct shear apparatus.

Surface roughness was measured by special precision instruments that measure the vertical deviation when traversing the metal surface. Ra is the most commonly used parameter to describe the average surface roughness and is defined as an integral of the absolute value of the roughness profile measured over an evaluation length:

$$Ra = \frac{1}{l} \int_0^l |z(x)| dx \quad (3.2)$$

The average roughness is the total area of the peaks and valleys divided by the evaluation length and are expressed in unit of length, typically μm . The

total area of the peaks above the mean line should be equal to the total area of the valleys below the mean line.

The surface roughness characteristics of the mild steel plate were achieved using a milling process performed in the laboratories of the Mechanical Department at the University of Alberta. The average surface roughness (R_a) was obtained by means of a portable surface roughness gage, called "Pocket Surf", where the gage was set up to use an evaluation length of 4 mm. In total 4 readings were taken at different locations in the shearing direction on the surface of the mild steel plate, with the following results R_a : 3.4, 3.2, 3.1 and 3.3 μm , with an average R_a value of 3.25 μm .

3.2.4 Water

The water used in these experiments was de-aired water.

3.3 Triaxial Tests

The triaxial test program undertaken for this investigation used a loading frame model ELE Tritest 50 and a conventional triaxial cell. Figure 3.3 shows the complete configuration of the triaxial testing system used for this research.

In total 7 triaxial tests were carried out, 4 using water and 3 using oil as the permeating liquid.

3.3.1 Sample Preparation

A variety of methods have been developed for reconstituting granular specimens in the laboratory. These methods can be categorized according to the moisture condition of the soil (e.g., dry, moist, or wet), the method of soil placement (e.g., pluviation, spooning, or flowing), and the medium through which the soil is placed (e.g., air or water). Specimens prepared using a combination of the above factors can be densified to any desired condition by various mechanical procedures including tamping, tapping, rodding, and vibrating (Frost and Park, 2003).

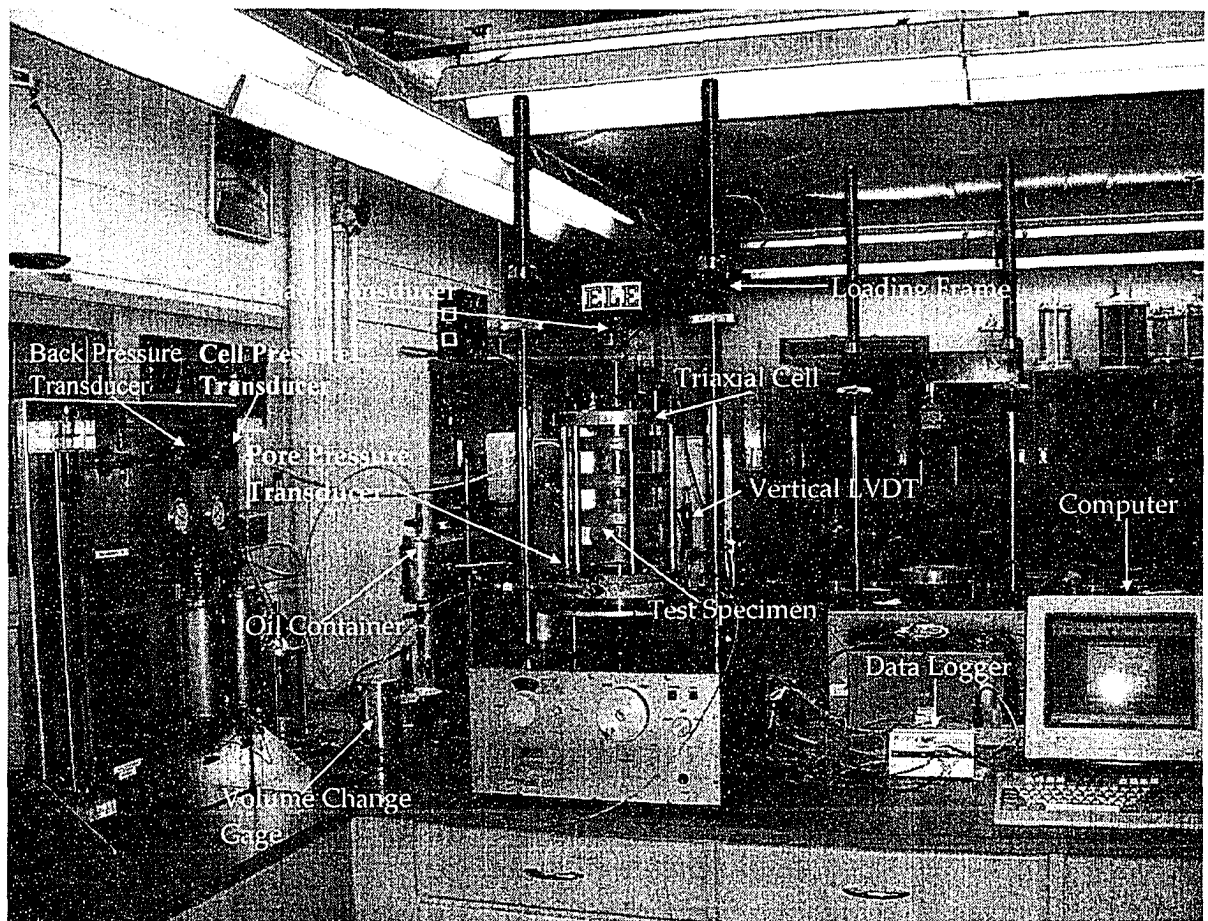


Figure 3.3 Triaxial Test Equipment Configuration

It is well known that the mechanical properties of the sand changes depending on the chosen method to reconstitute the specimens (Vaid et al., (1995), Vaid and Sivathayalan, (2000)). It has also been noted that the laboratory stress strain results obtained from reconstituted silt and silty sands cannot be used to predict the in situ behaviour, unless special efforts are made to reproduce the soil fabric (Høeg et al., 2000). Moreover, other studies have pointed out that even for identical initial fabric (and density), the response is profoundly influenced by other factors such as confining and static shear stress levels, direction of principal stresses, and undrained stress path, in addition to density (Vaid and Sivathayalan, 2001). Clearly, reproducing in situ conditions in the laboratory is extremely difficult.

The main objective in this research was to examine the influence of oil contamination on the behaviour of sand analogous to offshore platform foundation sands found in the Bay of Campeche. Since in situ sand samples were not available, attempts to strictly recreate the in situ conditions would have been extremely difficult if not impossible. Consequently, it was decided to focus on developing a systematic procedure for the preparation and testing of the sand specimens, using an analog sand that closely matches the in situ characteristics and to study the relative changes in its behaviour as a result of the oil contamination. To achieve this goal, all sand samples were prepared under dry

conditions using a hand-held tamper to reach the target relative density of D_r 60%. The density of the sand samples was computed by sensitive measurement of the weight and volume of the sand.

All the samples were reconstituted into an aluminium split mold. The dimensions of the sand specimens were 63.13 mm diameter and approximately 118.80 mm height, providing a height-diameter ratio equal to 1.88. During the preparation, each sand specimen was divided into 4 layers, each layer being formed by means of applying a quasi-static load, which was used to control the density, after pouring 5 small quasi-full spoons into the split mold. Special care was required to ensure no damage occurred to the rubber membrane. The mold was dismantled, and the vacuum was raised to 25 kPa while ensuring that the specimen was able to deform freely both in the axial and lateral directions, then initial specimen height and diameter were measured, and the results were recorded. The partial vacuum was replaced with a seating cell pressure of 25 kPa.

3.3.1.1 Samples with Water as Permeating Liquid

In the triaxial cell the vacuum line was removed and the pore pressure in the specimen was restored to atmospheric pressure. De-aired water was then admitted through the base pedestal, and allowed to percolate upwards through the sample, displacing most of the air to atmosphere through the top drainage line. This stage was maintained until a water volume equal to 2 times the void

volume of the specimen (around 250 ml) was collected. The pumping rate was 25 ml/hr using a pumping pressure around 7.00 kPa, which was considered slow enough to avoid any grain segregation and fabric disturbance.

3.3.1.2 Samples with Oil-Water mix as Permeating Liquid

For the preparation of the oil contaminated samples, the first stages were the same as described above, except that for these specimens, two membranes separated by a thin film of silicon grease, which provided protection of the outer membrane from the oil, was used for the test program. After water was flushed from the specimen, oil was introduced from the top drainage line to the base pedestal line until an oil-water mix volume equal to 3 times the void volume of the specimen (around 375 ml) was collected. The pumping rate was about 20 ml/hr using a pumping pressure around 30 kPa which is considered slow enough to avoid any grain segregation and fabric disturbance.

3.3.2 Testing Procedure

3.3.2.1 Saturation Phase

A series of back saturation B tests were undertaken to ensure that adequate sample saturation was achieved. For all samples a back pressure of 400 kPa was applied by alternative increments in the cell and back pressure. The increments in the cell pressure were 25, 50, 100 and 210 kPa, always keeping the back pressure 10 kPa below the cell pressure trying to avoid any specimen

disturbance. In order to accomplish specimen saturation, the 400 kPa back pressure was applied for a period of 24 hrs. After the application of the back pressure for the 24 hrs period, the cell pressure was increased to the desired effective stress and on final B test was performed. The B value for the clean sand ranged from 0.73 to 0.82, conversely, for the oil contaminated sands the B value was always 1.00.

The chosen effective stresses were 250, 500 and 750 kPa with a back pressure of 400 kPa, therefore applying cell pressures of 650, 900 and 1,150 kPa respectively.

3.3.2.2 Consolidation Phase

During the consolidation phase all the specimens were consolidated isotropically and the volume change and time was recorded every 10 seconds. The consolidation phase was assumed to be completed no incremental volume change was occurring and the pore pressure transducer had reached a constant value. Even though all the samples reached a constant volume and pore pressure before 15 minutes, this phase was considered finished after 1 hr.

3.3.2.3 Compression Phase

All samples were tested undrained under constant strain rate controlled conditions. A constant strain rate of 0.15 mm/min was used through the test program. The compression testing was continued until a steady state or

maximum deviator stress was reached. All samples were strained to greater than 20 percent. The pore pressure, cell pressure, back pressure, vertical displacement, and vertical load on the sample were monitored at intervals of 1 minute using electronic transducer devices. All data was recorded in a computer by means of a Dolphin data logger.

3.3.3 Problems Observed during the Test Program

Several problems were encountered during the test program. The main problems that were encountered are listed below:

- Lack of suction in the inner membranes during the preparation of 2 specimens selected for oil contamination. The use of two membranes instead of one during the sample preparation decreased the effectiveness of the pump to create the suction in the inner membrane.
- Loss of control board pressure for the 2 specimens confined to 750 kPa effective stress. Although the pressure system shows a maximum capacity of 1,200 kPa, the real capacity (maintaining a constant maximum pressure) is about 900 kPa, therefore it was not possible to maintain a constant cell pressure of 1,150 kPa to perform the maximum chosen confining pressures properly.
- A pore pressure transducer cable was damaged and had to be replaced.

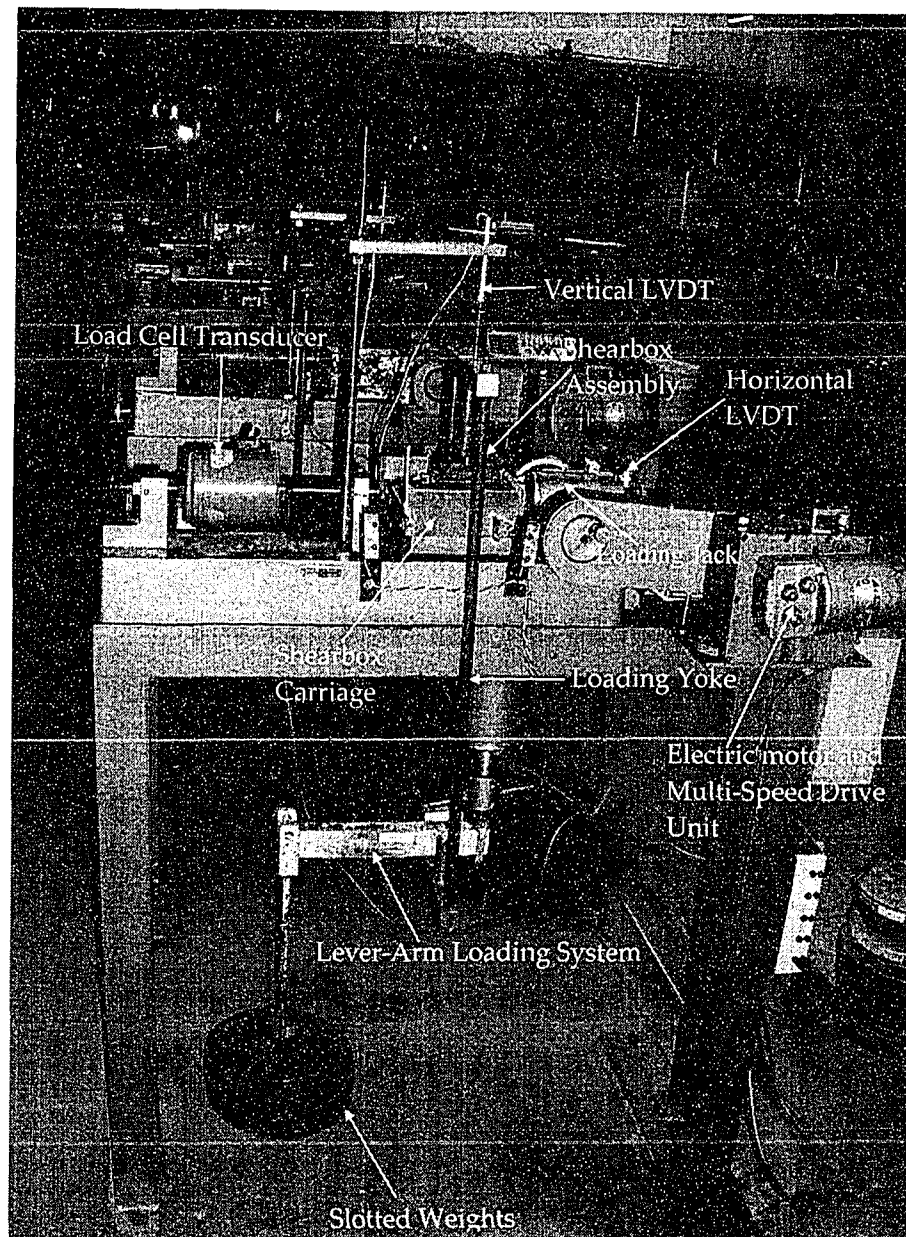


Figure 3.4 Direct Shear Test Equipment Configuration

3.4.1 Sample Preparation

The density of the sand was determined by sensitive measurement of the weight and volume of the sand. The target initial relative density for the samples was $D_d = 60\%$. To facilitate drainage during shear, perforated grid plates were

- The membranes used for the oil contaminated specimens were partially damaged (showed plastic deformation).
- It was observed that in the oil flushing stage, during the preparation of the oil contaminated samples, the collected fluid showed a milky color. It is inferred that this phenomena was caused for four possible situations: 1) water was dissolved into oil 2) a chemical reaction between the oil, water and sand, 3) a washing of fines during this stage, 4) a combination of the previous three situations simultaneously.

3.4 Direct Shear Test

The direct shear test program undertaken for this investigation used a Wykeman Farrance direct shear apparatus with a shearbox size of 60 mm.

Figure 3.4 shows the whole configuration of the direct shear test equipment.

In total six direct shear tests were carried out; 3 using water and 3 using oil as permeating liquid.

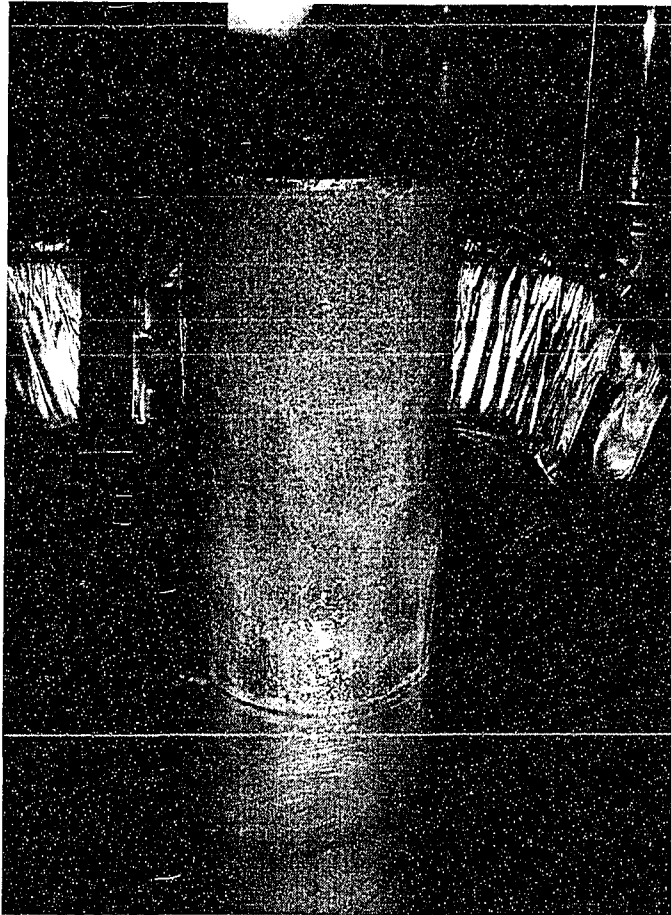


Figure 3.5 Oil Contaminated Sand Specimen Prepared in the Triaxial Cell

After the oil contaminated sand sample was prepared in the triaxial cell, it was split into three sections and each section was disaggregated, as shown in Figure 3.6, to allow for the preparation of the three direct shear specimens. Special care was taken to ensure moisture contents did not change in the disaggregated sand material. The oil contaminated sand was placed in a damp state in the shearbox and compacted (tamped) as necessary to produce the desired density, as shown in Figure 3.7.

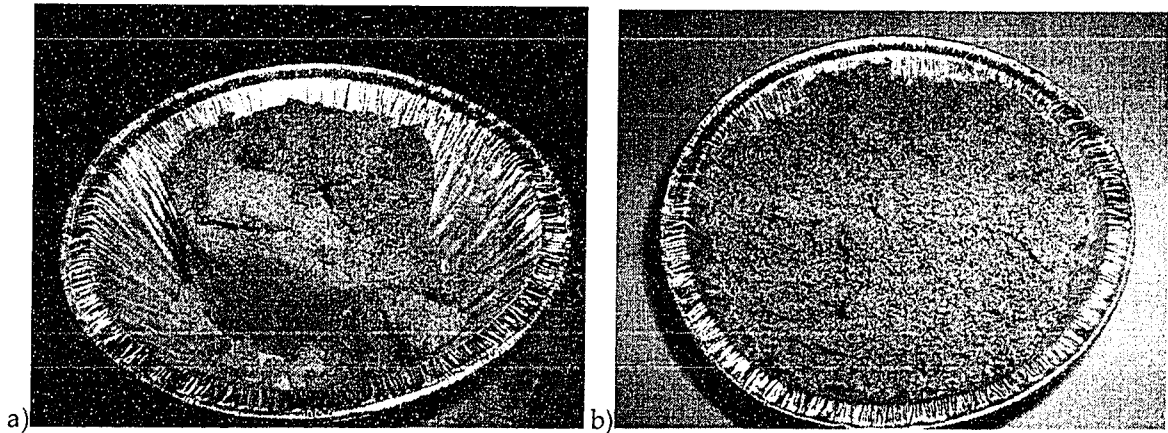


Figure 3.6 Oil Contaminated Specimen Preparation: a) Trimmed Soil from Triaxial Specimen and b) Disaggregated Sand Sample

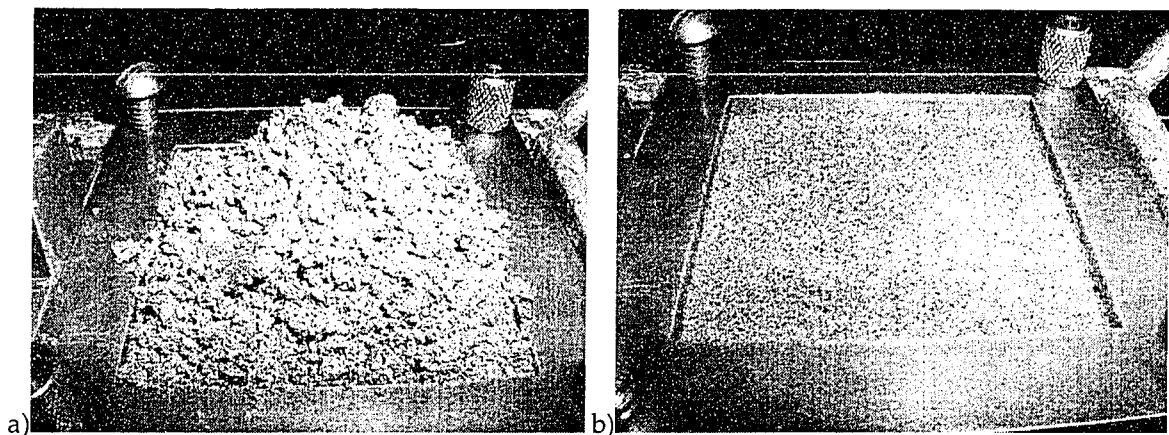


Figure 3.7 Oil Contaminated Specimen Preparation in the Shearbox: a) Soil in Damp State in the Shearbox and b) Soil in Compacted State into the Shearbox

3.4.2 Testing Procedure

3.4.2.1 Saturation

As described previously, specimens prepared with water as the permeating liquid, water was poured steadily into the space between the carriage and the shearbox, so that water could penetrate upwards through the

used instead of the solid plates, together with a porous plate behind each grid plate.

3.4.1.1 Samples with Water as Permeating Liquid

To avoid segregation, because of the appreciable quantity of silt, the dry sand was placed in a damp state and compacted (tamped) as necessary, then water was poured carefully into the carriage so that it percolates slowly upwards through the specimen (Head, 1981).

3.4.1.2 Samples with Oil-Water mix as Permeating Liquid

To prepare oil contaminated specimens for direct shear testing, the triaxial cell was used to ensure the same proportion of water and oil in the samples as the oil contaminated specimens selected for the triaxial tests. Utilizing the same procedure discussed in Section 3.3.1.2, one specimen was prepared, as shown in Figure 3.5, which provided sufficient material for three oil contaminated direct shear specimens.

specimen, thereby displacing as much air as possible present in the voids. After adding water, the specimens were left for 1 hour and any vertical movement resulting from inundation was recorded.

For specimens prepared with oil-water mix as the permeating liquid, oil was poured steadily into the space between the carriage and the shearbox. After adding oil, the specimens were left for 1 hour and any vertical movement resulting from inundation was recorded.

3.4.2.2 Consolidation

After the application of the specified effective normal stress σ_v (62.5, 125 and 250 kPa respectively) the specimens were allowed to consolidate for 1 hour and vertical movement was recorded. FUGRO (2002) had estimated that K_o at 30 m depth was approximately 0.5. Given the in situ effective vertical stresses 250 kPa, this corresponds to an in situ effective horizontal stress of 125 kPa. The stress range 62.5 kPa to 250 kPa brackets this stress level and provides a reasonable range of anticipated stresses applied to the steel piles at a depth of 30 m.

3.4.2.3 Shearing

All samples were tested drained under constant strain rate controlled conditions. A constant strain rate of 0.123 mm/min was used through the test program, which was sufficiently slow to avoid any excess pore pressure induced

by shearing. The shear testing was continued until a horizontal displacement around 8 mm was reached. The horizontal shear force, vertical movement, and horizontal displacement were monitored at intervals of 30 seconds using electronic transducer devices. All data were recorded in a computer by means of a Hewlett Packard data logger.

3.4.3 Problems Observed during the Test Program

The problems presented in this testing program, as any laboratory test carried out on sand, were in the reconstitution of the specimens specifically to reach the same initial relative density ($D_r = 60\%$) in all the specimens.

3.5 Interface Direct Shear Test

Many studies have been investigated experimentally the interface angle of friction between soil and construction materials under a wide range of boundary conditions (Potyondy, 1961; Brumund and Leonards, 1973; Desai, 1981; Boulon and Foray, 1986; Kishida and Uesugi, 1987; Boulon, 1989; Al-Douri and Poulos, 1992; Tabucanon et al., 1995; Subba Rao et al., 1998; Reddy et al., 2000; and Hu and Pu, 2004). Very few studies, however, have been conducted to investigate the interface behaviour between oil contaminated soils and construction materials or between soils and lubricated surfaces and these were primarily the studies discussed in Chapter 2 (Amor, 1990; Evgin et al., 1995; Evgin et al., 1996; and Hasan and Mostafa, 1996).

The interface shear test program undertaken for this investigation used a Wykeman Farrance direct shear apparatus with a shearbox size of 60 mm, which basically keeps the same test configuration used in the direct shear test as shown in Figure 3.4. The main difference in setup was the insertion of a metal plate at the base of the shearbox assembly, as schematically shown in Figure 3.8. In total, 9 interface shear tests were conducted; 5 using water and 4 using oil as permeating liquid.

3.5.1 Sample Preparation

The target relative density remained 60% for this test series. The mild steel plate was placed in the lower half of the shear box where the upper surface of the plate was levelled with the top edges of the lower half, as shown in Figure 3.9. To achieve the relative density, a specified weight of sand is placed and compacted in the upper half of the shear box.

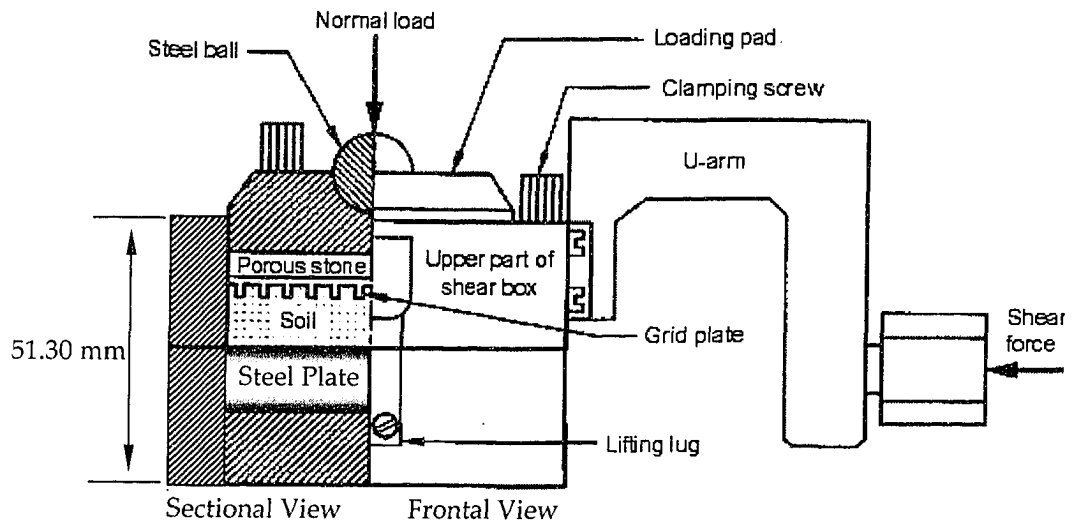


Figure 3.8 Shearbox Assembly for Interface Shear Test
(modified from Subba Rao et al., 2000)

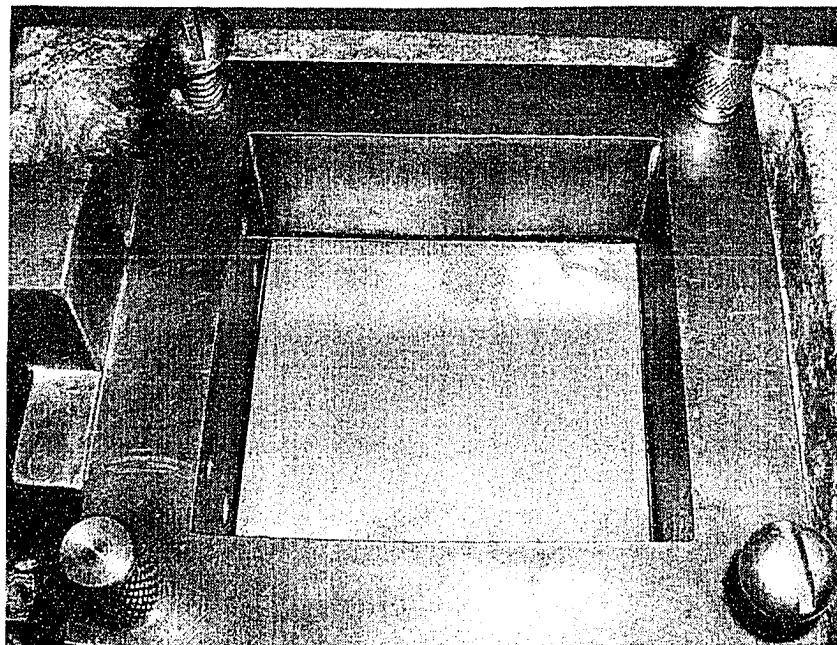


Figure 3.9 Steel Plate Placed into the Lower Half of the Shearbox

3.5.1.1 Samples with Water as Permeating Liquid

The same procedure used for the preparation of the direct shear specimens, as discussed in Section 3.4.1.1, was followed for the preparation of the water-sand interface test specimens.

3.5.1.2 Samples with Oil-Water mix as Permeating Liquid

The same procedure used for the preparation of the direct shear specimens, as discussed in Section 3.4.1.2, was followed for the preparation of the oil-water-sand interface test specimens. Another triaxial cell specimen was prepared for this test series.

3.5.2 Testing Procedure

The saturation, consolidation and shearing phases followed the same procedures explained in Sections 3.4.2.1, 3.4.2.2 and 3.4.2.3 respectively.

3.5.3 Problems Observed during the Test Program

Achieving consistent results for the specimen preparation in the interface test program was difficult. Two additional water-sand specimens and one additional oil-water-sand specimen were required due to three tests which did not show satisfactory results.

4. TEST RESULTS AND DISCUSSION

4.1. Triaxial Tests

Two sets of triaxial tests were conducted on medium dense sand (relative density equal to 60%). One set had water as the permeant or pore fluid and the second set had an oil-water mix as the pore fluid. Table 4.1 shows the test conditions for the specimens prepared with water as permeating liquid, called “water samples” and Table 4.2 shows the test conditions for specimens prepared with an oil-water mix as the permeating liquid, called “oil samples”.

As shown in these tables, lower moisture contents, 5% for the oil samples as compared to 17% for the water samples, were obtained following consolidation of the test specimens. The 5% moisture content for the oil samples corresponds to the residual water remaining on the water-wet sand grains following oil saturation.

Table 4.1 Test Conditions for Water Samples

SPECIMEN		Water#1	Water#2	Water#3
INITIAL	Density (g/cm ³)	2.098	2.095	2.096
	Moisture (%)	----	----	----
	Dry Density (g/cm ³)	1.764	1.759	1.760
	Void Ratio	0.502	0.507	0.506
AFTER CONSOLIDATION	Density (g/cm ³)	2.110	2.116	2.119
	Moisture (%)	17.91	16.48	18.31
	Dry Density (g/cm ³)	1.783	1.792	1.798
	Void Ratio	0.486	0.479	0.474
SATURATION STAGE	Initial pwp (kPa)	5	5	5
	Saturated pwp (kPa)	400	400	400
	Final Cell Pressure (kPa)	410	410	410
	B value	0.73	0.85	0.82
CONSOLIDATION STAGE	Cell Pressure (kPa)	650	900	1070
	Back Pressure (kPa)	400	400	400
	Initial pwp (kPa)	575	817	941
	Final pwp (kPa)	400	400	400
COMPRESSION STAGE	Cell Pressure (kPa)	650	900	1070
	Initial pwp (kPa)	400	400	400
	Initial σ_3' (kPa)	250	500	670
	Rate of Strain (% per hour)	7.35	7.35	7.35
FAILURE CONDITIONS	Strain %	23.820	20.160	21.840
	$(\sigma_1 - \sigma_3)_f$ (kPa)	544	977	1016
	u_f (kPa)	435	529	646
	σ_3' (kPa)	215	371	424
	σ_1' (kPa)	759	1348	1441

Table 4.2 Test Conditions for Oil Samples

SPECIMEN		Oil#1	Oil#2	Oil#3
INITIAL	Density (g/cm ³)	2.045	2.076	2.116
	Moisture (%)	----	----	----
	Dry Density (g/cm ³)	1.771	1.822	1.889
	Void Ratio	0.496	0.454	0.403
AFTER CONSOLIDATION	Density (g/cm ³)	2.056	2.098	2.143
	Moisture water (%)	5.22	6.69	4.95
	Dry Density (g/cm ³)	1.790	1.858	1.933
	Void Ratio	0.434	0.387	0.333
SATURATION STAGE	Initial pmp (kPa)	10	10	10
	Saturated pmp (kPa)	400	400	400
	Final Cell Pressure (kPa)	410	410	410
	B value	1	1	1
CONSOLIDATION STAGE	Cell Pressure (kPa)	650	900	1055
	Back Pressure (kPa)	400	400	400
	Initial pmp (kPa)	640	890	1045
	Final pmp (kPa)	400	400	400
COMPRESSION STAGE	Cell Pressure (kPa)	650	900	1055
	Initial pmp (kPa)	400	400	400
	Initial σ_3' (kPa)	250	500	655
	Rate of strain (% per hour)	7.35	7.35	7.35
FAILURE CONDITIONS	Strain %	13.700	13.970	16.590
	$(\sigma_1 - \sigma_3)_f$ (kPa)	1516	2953	2941
	u_f (kPa)	144	94	64
	σ_{3f}' (kPa)	506	806	991
	σ_{1f}' (kPa)	2022	3758	3931

4.1.1. Isotropic Consolidation – Pore Pressure Dissipation

All samples were isotropically consolidated. Figures 4.1 and 4.2 provide comparative results on the rate of excess pore pressure dissipation during consolidation for oil contaminated and clean specimens at effective confining stresses of 250 kPa and 500 kPa, respectively. These results clearly show that oil contaminated samples take longer to fully consolidate than clean samples. The primary reason is the higher viscosity of the oil prevents the rapid dissipation of excess pore pressures. This behaviour was also evident in the experimental results from Evgin and Das (1992), Cook et al. (1993), Hasan et al. (1995), Wissam and Evgin (1998) and Vijay (2000).

4.1.2. Undrained Behaviour during Triaxial Compression

Figures 4.3, 4.4, and 4.5 provide the stress-strain and pore pressure response curves for water and oil samples #1, #2 and #3, respectively. Both sands display similar low strain response; contractant behaviour manifested with increasing pore pressures during undrained shear. At the initiation of a dilatant response in the samples, however, the behaviour between the water and oil samples begins to differ. The water sample displays mild strain hardening response with an eventual decrease in pore pressure at large (> 10%) axial strains. The oil sample, however, displays a highly dilatant, strain hardening response with the concomitant rapid decrease in pore pressures. Because of the highly

dilatant response for the oil samples, they tend to reach a maximum deviator stress at lower axial strain ($\epsilon_a \sim 14\%$) than the clean samples ($\epsilon_a \sim 25\%$). The strain hardening response of the oil samples results in a larger maximum deviator stress than the water specimens. The implication of this type of behaviour is that oil contamination may positively influence the undrained strength of silty sand, given that the sand shows a dense behaviour in the stress-strain curves, with a peak deviator stress and strain softening after the peak. On the other hand, the clean sand behaves more like loose sand, showing the maximum deviator stress at high axial strain (around 22 %) without any peak.

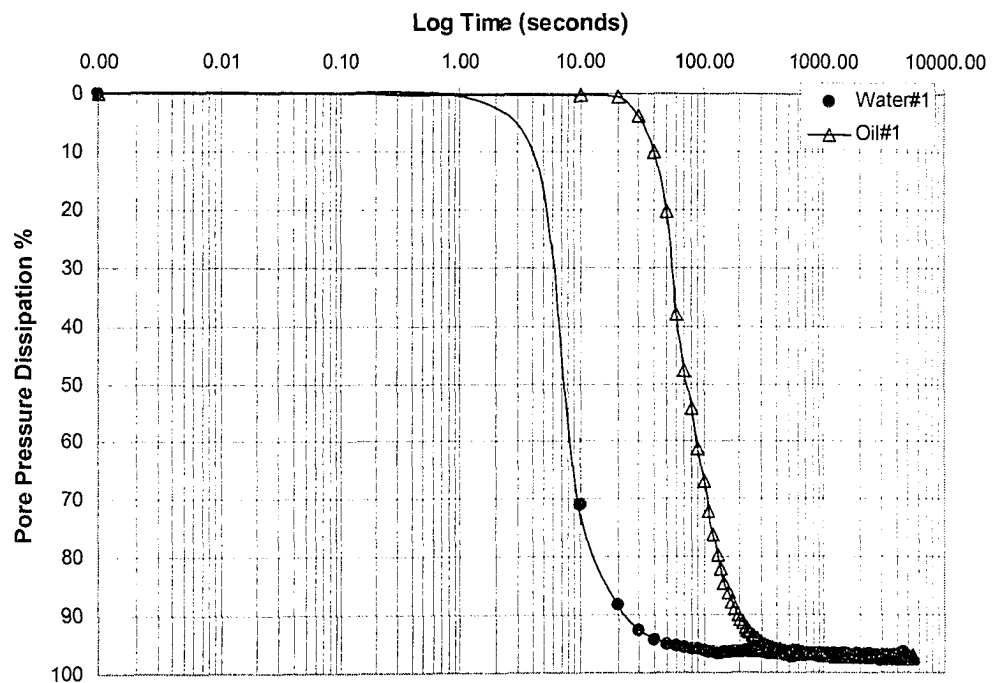


Figure 4.1 Pore Pressure Dissipation for Water and Oil Samples #1 ($\sigma'_3=250$ kPa)

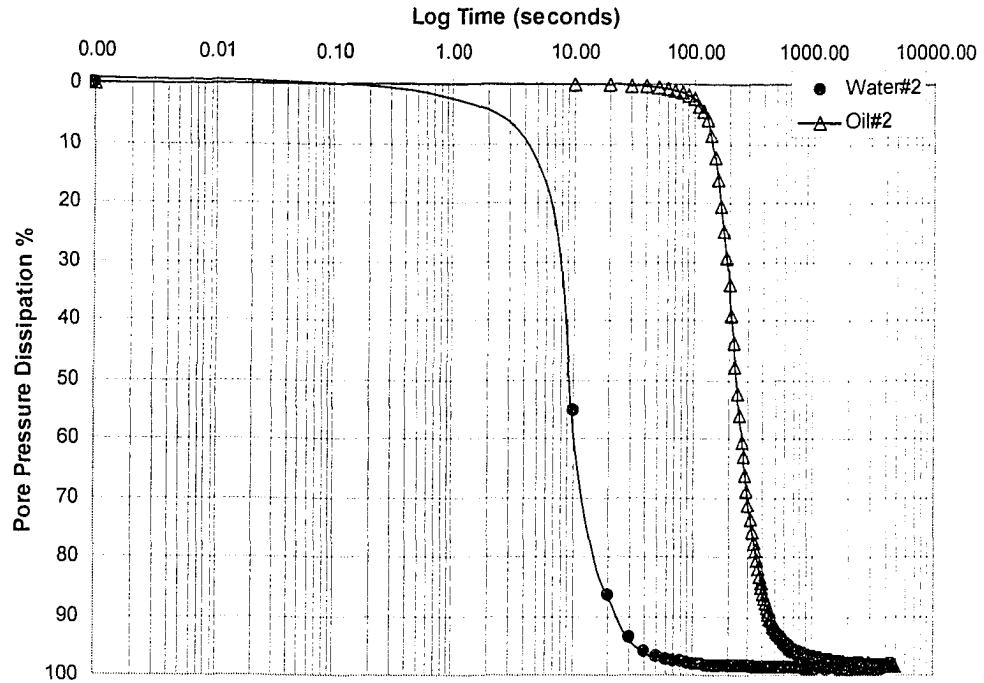


Figure 4.2 Pore Pressure Dissipation for Water and Oil Samples #2
($\sigma'_3=500$ kPa)

The cyclic pressure response that occurred in the tests for Sample #3 (Figure 4.5) occurred because of pressure loss in the control board of the testing system. This intermittent pressure loss caused the cell pressure to increase and decrease in a cyclic manner without any control when it was intended to apply the maximum capacity of the pressure system.

Also shown in Figures 4.3, 4.4 and 4.5 are undrained pore pressure responses that developed in the samples during shear. The same trend is apparent in all tests; the water samples develop higher pore pressures than the oil samples during shearing, causing a reduction in mean effective confining

stress and therefore a lower maximum deviator stress or failure stress is reached in the clean sand than in the oil contaminated sand.

Table 4.3 summarizes the soil strength and deformation parameters determined from the triaxial tests data. For frictional strength, the normalized stress or stress ratio curves shown in Figure 4.6 are utilized. Based on the q/p' values at failure noted in this figure, the effective friction angle for the water samples is 35.4° and the effective friction angle for the oil samples is 39.4° . Note that sample #3 for both the water and the oil samples was excluded from this analysis. While the mechanisms are unclear, these results show that the – presence of the oil improves the strength parameters of the sand since the effective friction angle is almost 4° higher than the water saturated sand. Furthermore, the initial tangent modulus (E_i) and secant elastic modulus (E_s) show higher values for the oil contaminated specimens than for the clean specimens. The values of the secant elastic modulus (E_s) were computed as the ratio of maximum deviator stress to the axial strain at this stress level.

4.1.3. Undrained Stress Paths

Figures 4.7 4.8 and 4.9 compare the stress paths between the oil contaminated samples and the clean samples. These plots show how the effective normal pressure, in the plane of the maximum shear stress of the specimens, changes during the shearing. From these plots can it be seen that the oil

contaminated samples clearly exhibit strain hardening behaviour and can develop significantly higher shear stresses at failure than the water samples. The primary mechanism for this is the development of higher effective normal pressures in the shear plane for the oil contaminated samples compared with the clean samples.

4.2. Direct Shear Tests

Tables 4.4 and 4.5 show the initial and after consolidation conditions of the sand specimens. Although the original idea was to prepare the sand specimens with a relative density around $D_r = 60\%$, it was experienced the challenge to prepare the sand specimens with the same densities under different sample preparation conditions. Like the one for oil contaminated sand (sand already saturated) and clean sand (dry sand).

The result was in general sand specimens prepared with a density slightly lower than the proposed, especially the oil contaminated specimens which showed lower calculated dry densities in all cases.

Appendix A provides additional information about a couple of sand samples tested during the triaxial test program.

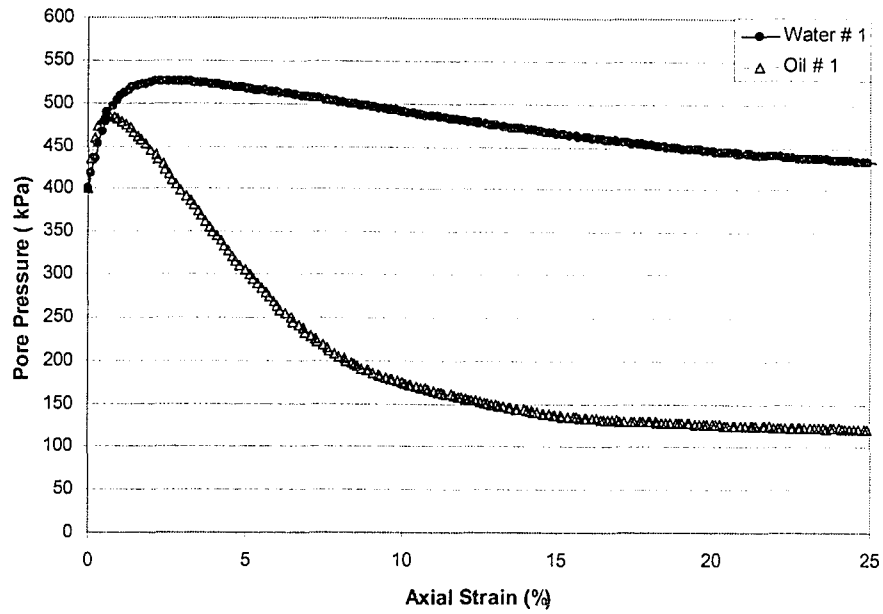
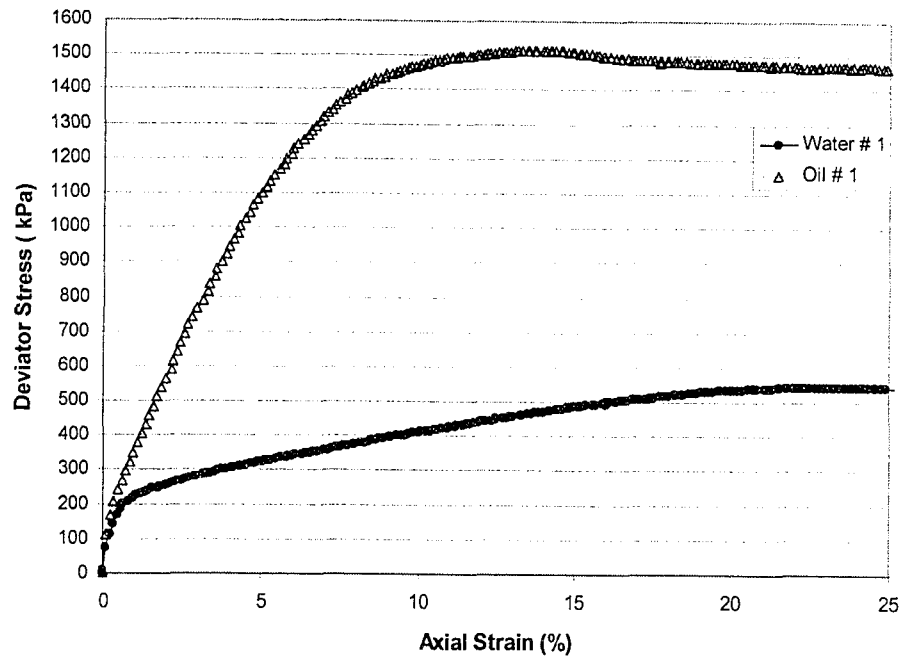


Figure 4.3 Undrained Stress-Strain Behaviour for Water and Oil Specimens #1 ($\sigma'_3 = 250$ kPa)

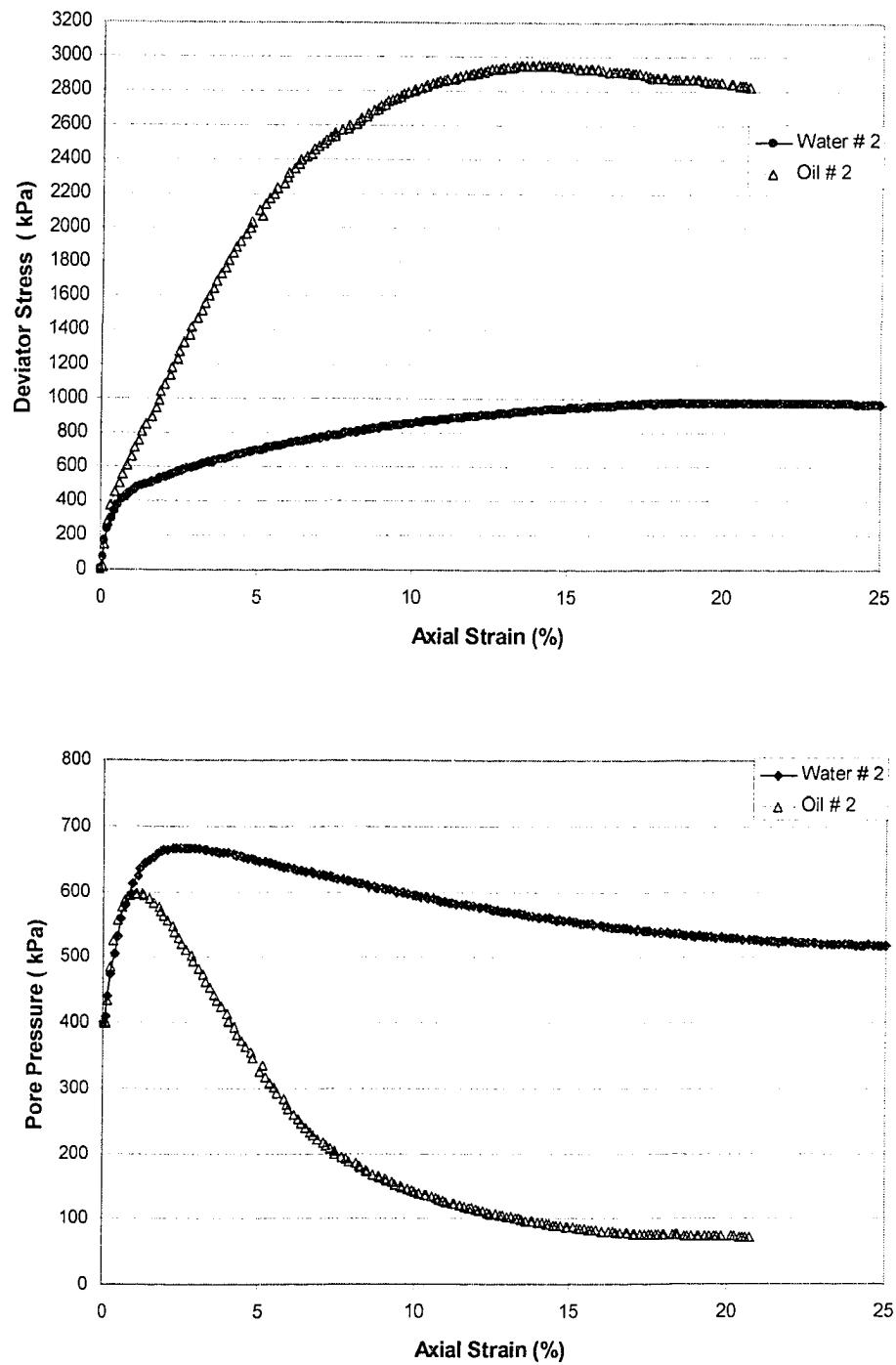


Figure 4.4 Undrained Stress-Strain Behaviour for Water and Oil Specimens #2
($\sigma'_3 = 500$ kPa)

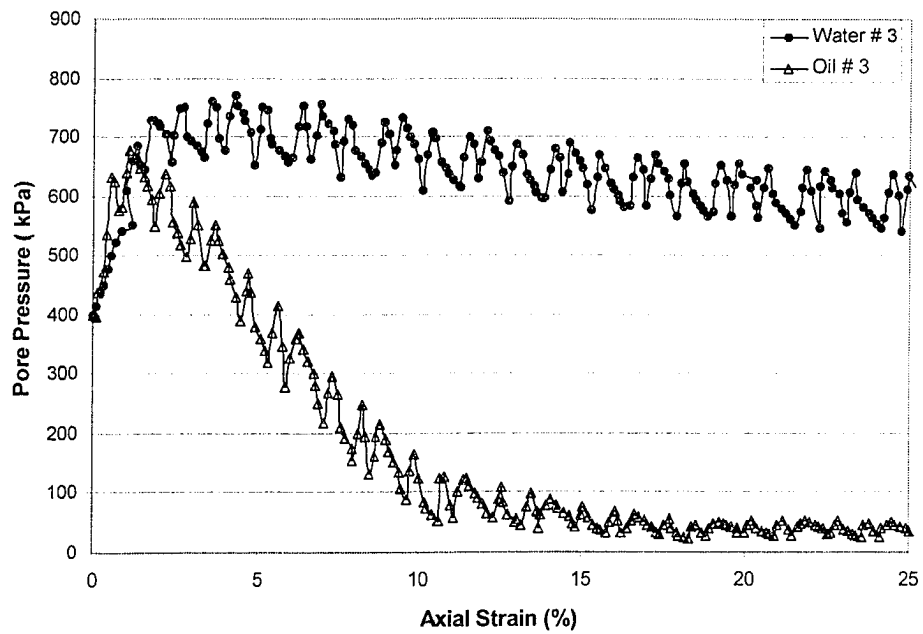
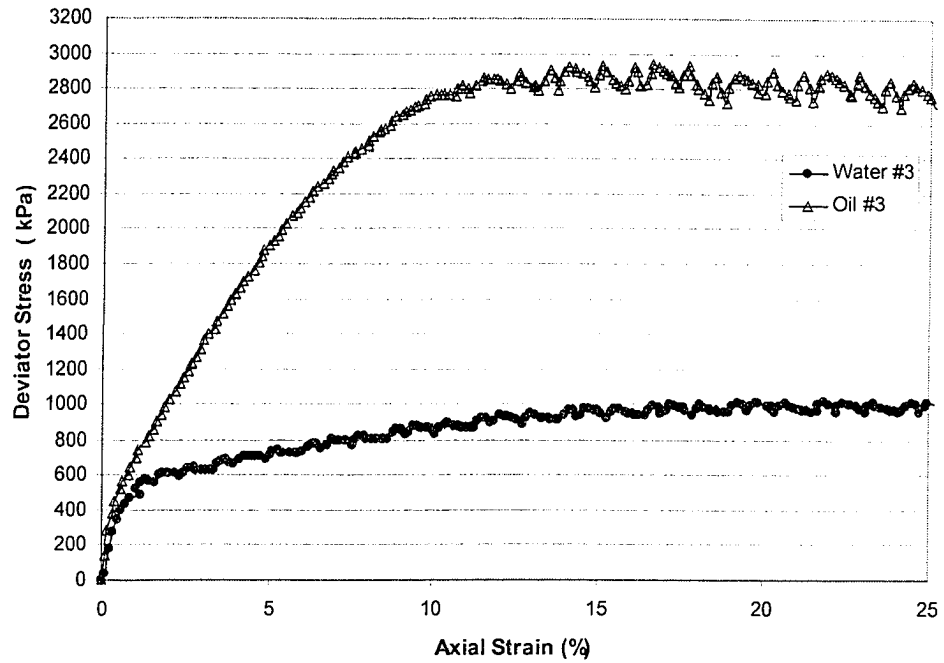


Figure 4.5 Undrained Stress-Strain Behaviour for Water and Oil Specimens #3 ($\sigma'_3 = 670$ kPa)

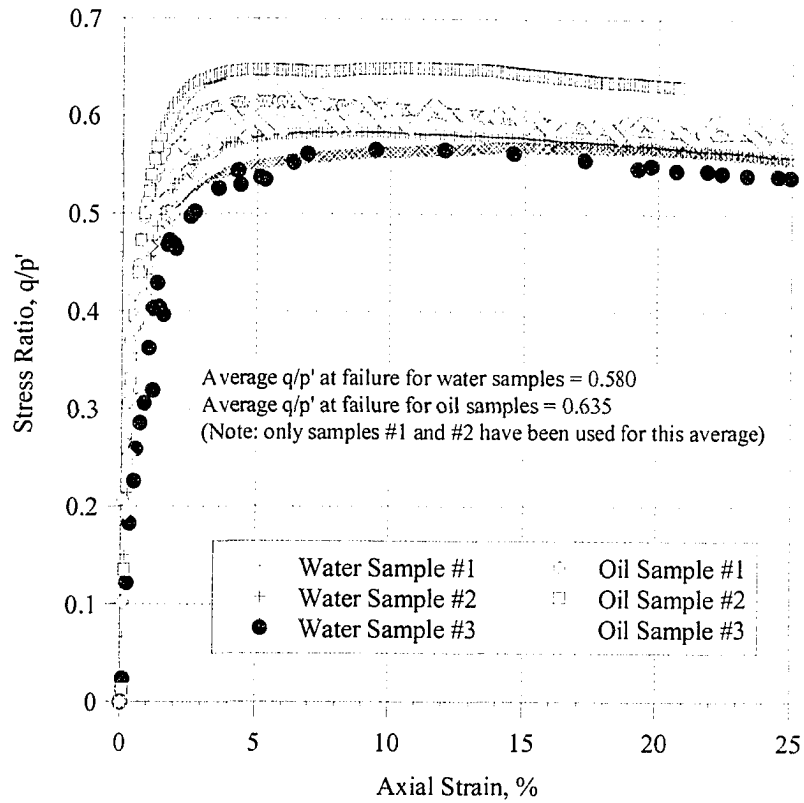


Figure 4.6 Stress Ratio Plot for All Triaxial Tests

Table 4.3 Summary of Soil Parameters - Triaxial Test -

		Clean Sand	Oil Sand
Effective Internal Friction Angle ϕ' (degrees)		35.4	39.4
A_f ($\Delta u_f / \Delta q_f$)	Specimen #1	+0.07	-0.17
	Specimen #2	+0.13	-0.10
	Specimen #3	+0.20	-0.12
Initial Tangent Modulus E_i (MPa)	Specimen #1	23	28
	Specimen #2	101	120
	Specimen #3	128	157 (for $\sigma_3 = 1,055$ kPa)
Secant Elastic Modulus E_s (MPa)	Specimen #1	2.3	11
	Specimen #2	4.9	21
	Specimen #3	4.7	20 (for $\sigma_3 = 1,055$ kPa)

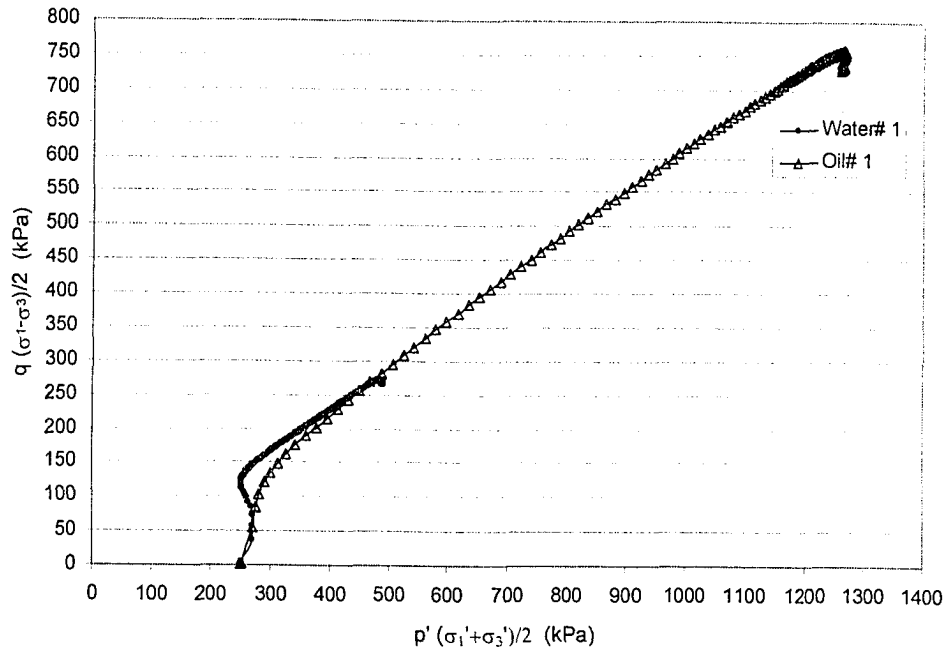


Figure 4.7 p'-q Diagram ($\sigma_3=650$ kPa, $\sigma_3'=250$ kPa)

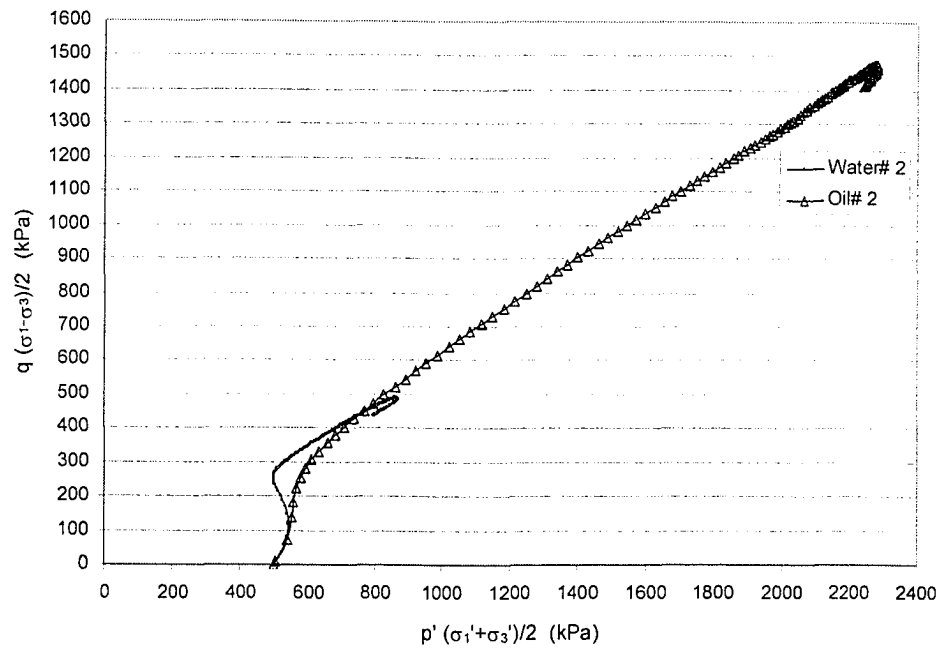


Figure 4.8 p'-q Diagram ($\sigma_3=900$ kPa, $\sigma_3'=500$ kPa)

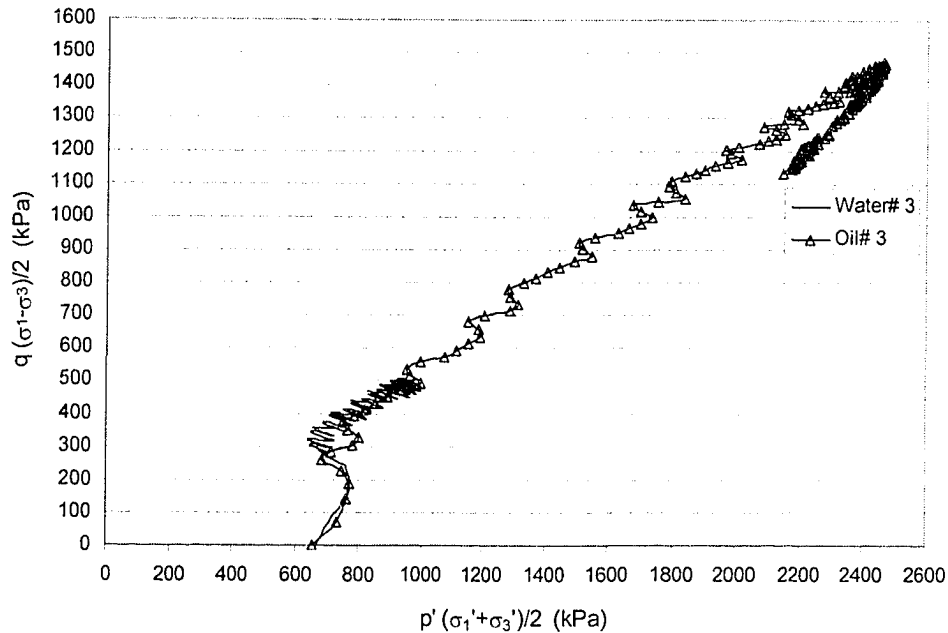


Figure 4.9 p' - q Diagram for Water ($\sigma_3=1,070$ kPa, $\sigma_3'=670$ kPa);
for Oil ($\sigma_3=1,055$ kPa and $\sigma_3'=655$ kPa)

Table 4.6 shows the failure conditions for the sand specimens. The failure condition was taken at the maximum shear stress developed during shearing in all cases. It can be seen that for all specimens tested under the same normal stress, the oil samples show better strength/deformation properties than the water samples. It appears that the oil saturation is causing the sand to behave in a dense manner, even though the density is below the dense state for this silty sand. These results agree with the triaxial tests results presented in the previous section.

Table 4.7 shows the water content of the specimens after shearing. The water content of the specimens after shearing agrees with the triaxial test

samples for both clean and oil contaminated soil conditions. This implies a consistent sample preparation between the triaxial and direct shear tests.

4.2.1. Shear Stress and Vertical Movement versus Horizontal Displacement

Figures 4.10, 4.11 and 4.12 compare the shear stress/vertical displacement v.s. horizontal displacement behaviour of the oil and water sand specimens. These plots clearly illustrate the oil samples behaving like dense sands as evidenced by the strain softening behaviour after the peak shear stress has been reached. The water sand samples behaviour very much like loose sand. The dense, dilatant response for the oil samples is also reflected in the vertical displacement behaviour during shear. Oil samples show an increase in volume or increasing vertical displacement while the water sands samples decrease in volume during shear.

Appendix A provides additional information about an oil contaminated sand sample tested during the direct shear test program.

Table 4.4 Initial Soil Conditions - Direct Shear Test -

Sample	Void Ratio e_0	Dry Density ρ_0 (g/cm ³)	Δ Dry Density ρ_0 Water vs Oil (%)	Δ Dry Density from target ρ_{target} 1.760 g/cm ³ (%)
Soil-Soil Water #1	0.573	1.683		-4.3
Soil-Soil Oil #1	0.697	1.520	-9.7	-13.6
Soil-Soil Water #2	0.547	1.712		-2.7
Soil-Soil Oil #2	0.637	1.576	-7.9	-10.4
Soil-Soil Water #3	0.565	1.693		-3.8
Soil-Soil Oil #3	0.597	1.615	-4.6	-8.2

Table 4.5 Soil Conditions after Inundation and Consolidation - Direct Shear Test -

Sample	Void Ratio e_1	Dry Density ρ_1 (g/cm ³)	Δ Dry Density ρ_1 Water vs Oil (%)	Δ Dry Density from target ρ_{target} 1.760 g/cm ³ (%)
Soil-Soil Water #1	0.515	1.749		-0.6
Soil-Soil Oil #1	0.683	1.533	-12.3	-12.9
Soil-Soil Water #2	0.481	1.788		1.6
Soil-Soil Oil #2	0.617	1.595	-10.8	-9.3
Soil-Soil Water #3	0.489	1.779		1.1
Soil-Soil Oil #3	0.578	1.635	-8.1	-7.1

Table 4.6 Failure Conditions - Direct Shear Test -

Sample	Maximum Shear Stress (kPa)	Normal Stress (kPa)	Horizontal Displacement (mm)	Vertical Movement (mm)
Soil-Soil Water#1	49.72	62.5	4.261	-0.237
Soil-Soil Oil#1	51.39	62.5	0.876	0.123
Soil-Soil Water#2	89.82	125	4.342	-0.361
Soil-Soil Oil#2	111.55	125	0.898	0.105
Soil-Soil Water#3	162.52	250	4.173	-0.440
Soil-Soil Oil#3	192.60	250	2.059	0.109

Table 4.7 Water Content after Shearing - Direct Shear Test -

Sample	Water Content (w%)
Soil-Soil Water #1	16.99
Soil-Soil Oil #1	4.70
Soil-Soil Water #2	16.60
Soil-Soil Oil #2	5.02
Soil-Soil Water #3	15.58
Soil-Soil Oil #3	4.46

Table 4.8 shows the summary of the soil parameters for each soil condition. The analysis confirms that the shear strength for the oil contaminated sand is higher than the water sand. The internal friction angle for the oil contaminated sand is almost 5° higher than the one of the clean sand, and the cohesion found in the oil contaminated samples is 2 kPa higher than the clean samples. The cohesion found in the direct shear test agrees with the soil parameters found in soils with appreciable amount of silt (Head, 1981).

4.3 Interface Direct Shear Tests

Tables 4.9 and 4.10 show the pre- and post-consolidation state for all the sand specimens. The original concept was to prepare the sand specimens with a relative density around $D_r = 60\%$ but unfortunately, significant challenges were experienced during the preparation of sand specimens that had the same densities as the oil contaminated sand (sand already saturated) and clean sand (dry sand).

As a result, interface shear tests specimens were prepared with a density slightly lower than the target density, especially the oil contaminated specimens which had lower dry densities in all cases.

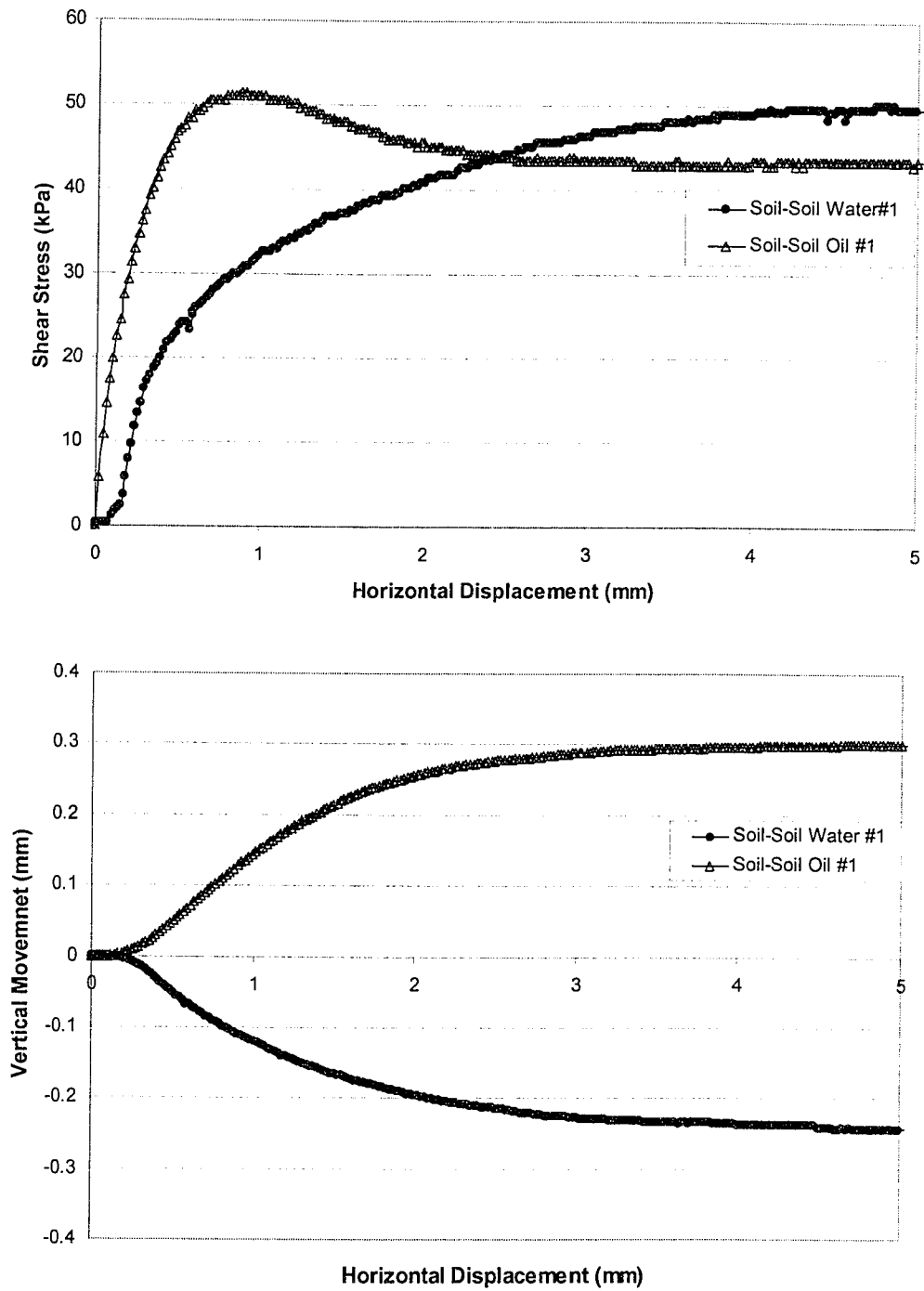


Figure 4.10 Direct Shear Behaviour of Water and Oil Specimen #1
($\sigma_n = 62.5$ kPa)

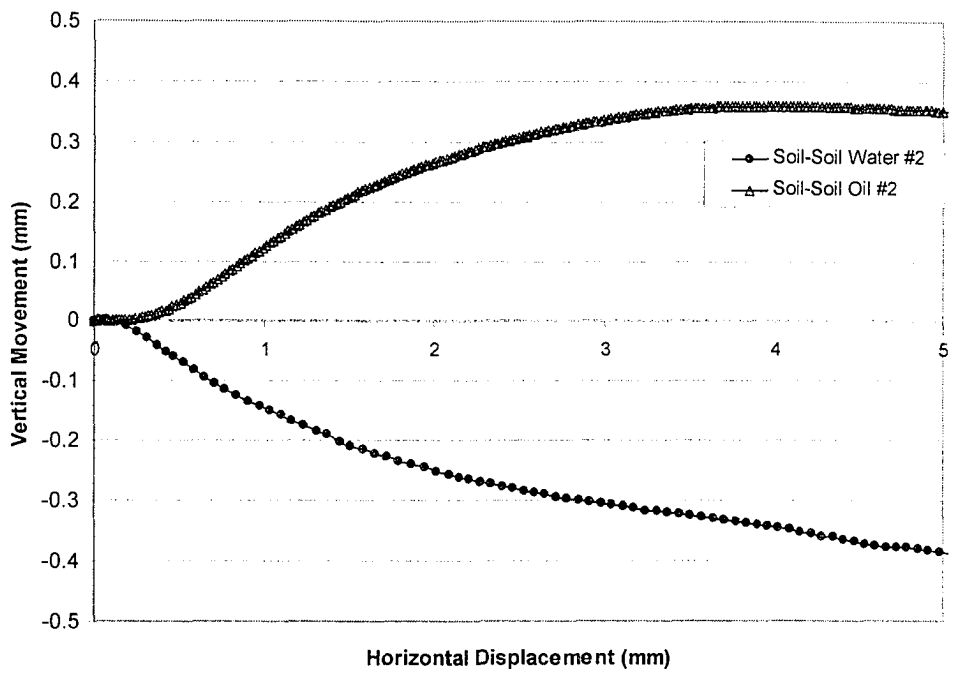
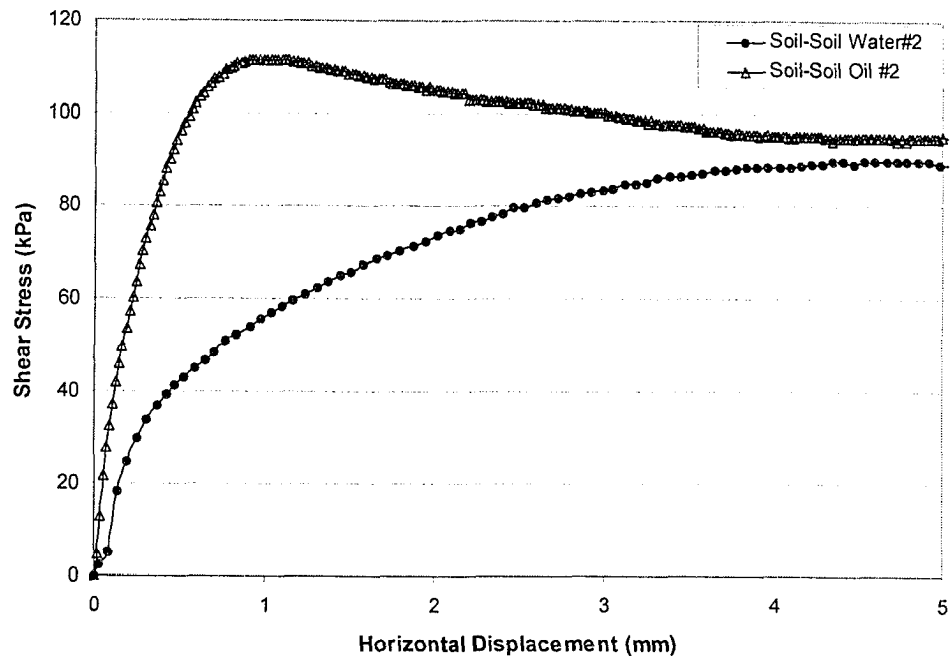


Figure 4.11 Direct Shear Behaviour of Water and Oil Specimen #2 ($\sigma_n = 125$ kPa)

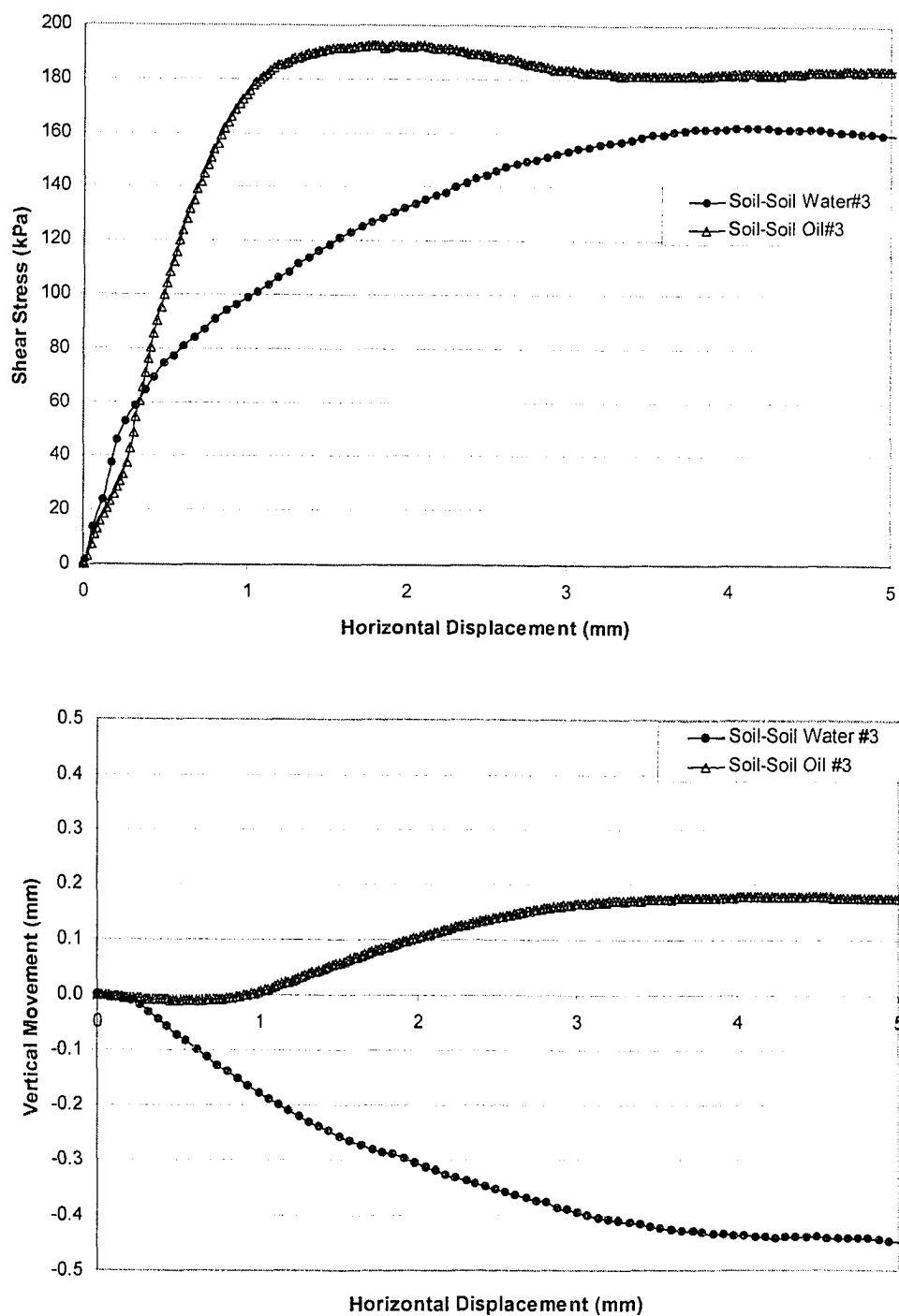


Figure 4.12 Direct Shear Behaviour of Water and Oil specimen #3
 ($\sigma_n = 250$ kPa)

Table 4.8 Summary of Soil Parameters - Direct Shear Test -

	Internal Friction Angle ϕ at Maximum Shear Stress (degrees)	Cohesion c (kPa)
Clean Sand	30.8	13.3
Oil Contaminated Sand	35.3	15.9

Table 4.11 shows the failure conditions for the sand specimens. The failure condition was taken at the maximum shear stress developed during shearing. Table 4.12 shows the water content of the specimens after shearing. The water content in the specimens after shearing is quite similar with the triaxial test and direct shear test samples for both the water and oil contaminated conditions.

4.3.1 Shear Stress and Vertical Movement vs Horizontal Displacement

Figures 4.13, 4.14 and 4.15 compare the shear stress/vertical displacement versus horizontal displacement behaviour for both oil contaminated and water sand specimens. These plots show that the oil contaminated sand behaves like dense sand, displaying a strain softening response following the peak shear stress, even though the density is lower than the water sand, which behaves like loose sand. Although the oil sand specimens behave as if they were prepared in a dense state, their maximum shear stress are almost the same as the clean sand specimens. As well, the steel-sand water #3 sample developed a higher maximum shear stress during shearing than the steel-sand oil #3 sample (Figure 4.15) at the same normal stress.

Table 4.9 Initial Soil Conditions - Interface Direct Shear Test -

Sample	Void Ratio e_0	Dry Density ρ_0 (g/cm ³)	Δ Dry Density ρ_0 Water vs Oil (%)	Δ Dry Density from target $\rho_{\text{target}}=1.760$ g/cm ³ (%)
Steel-Water #1	0.646	1.609		-8.6
Steel-Oil #1	0.737	1.480	-7.99	-15.8
Steel-Water #2 (B)	0.646	1.609		-8.57
Steel-Oil #2	0.706	1.507	-6.29	-14.3
Steel-Water #3 (B)	0.645	1.610		-8.5
Steel-Oil #3	0.659	1.550	-3.70	-11.9

Table 4.10 Soil Conditions after Inundation and Consolidation – Interface Direct Shear Test -

Sample	Void Ratio e_1	Dry Density ρ_1 (g/cm ³)	Δ Dry Density ρ_1 Water vs Oil (%)	Δ Dry Density from target $\rho_{\text{target}}=1.760$ g/cm ³ (%)
Steel-Water #1	0.589	1.667		-5.2
Steel-Oil #1	0.731	1.485	-10.9	-15.6
Steel-Water #2 (B)	0.578	1.678		-4.6
Steel-Oil #2	0.687	1.524	-9.2	-13.4
Steel-Water #3 (B)	0.582	1.674		-4.9
Steel-Oil #3	0.635	1.572	-6.0	-10.6

Table 4.11 Failure Conditions – Interface Direct Shear Test -

Sample	Maximum Shear Stress (kPa)	Normal Stress (kPa)	Horizontal Displacement (mm)	Vertical Movement (mm)
Steel-Soil Water#1	39.3	62.5	4.75	-0.38
Steel-Soil Oil #1	44.3	62.5	0.86	0.02
Steel-Soil Water#2 (B)	72.7	125	4.21	-0.21
Steel-Soil Oil #2	76.5	125	0.50	0.02
Steel-Soil Water#3 (B)	141.2	250	4.98	-0.31
Steel-Soil Oil #3	138.7	250	1.12	0.01

Table 4.12 Water Content after Shearing – Interface Direct Shear Test -

Sample	Water Content (w%)
Steel-Water #1	15.6
Steel-Oil #1	2.9
Steel-Water #2 (B)	15.4
Steel-Oil #2	3.4
Steel-Water #3 (B)	15.2
Steel-Oil #3	3.6

With respect to vertical displacements during shear, the oil contaminated specimens showed a modest increase in the vertical displacement supporting the dilatant response seen in the shear stress results. In comparison, the oil contaminated samples used for the interface steel-sand direct shear tests showed less dilation (less than 0.1 mm of vertical movement) than the oil contaminated samples used for the direct shear test (around 0.3 mm of vertical movement).

Table 4.13 shows the summary of the soil parameters for each test condition. These parameters confirm that the shear strength for the water sand is higher than the oil contaminated sand. This is contrary to the result obtained from the direct shear and triaxial testing results. The interface steel-sand friction angle for the water sand is almost 3° higher than the interfacial friction angle for oil contaminated sand. It is noted that the oil contaminated sand shows a higher cohesion value than the clean sand.

Table 4.14 shows the summary of the soil parameters for each soil condition at 5 mm of horizontal displacement. This displacement was chosen to determine soil parameters at a point which is closer to a critical state for these silty sands. This will help minimize the influence of differences in the initial relative density of the test samples. These results show that for water sand specimens, the interface steel-sand friction angle remains 1° higher than the oil contaminated sand. As well, the cohesion decreases, for both soil conditions,

compared with the analysis carried out using the maximum shear strength. This reduction was found higher for the oil contaminated samples.

Clearly, these interfacial test results indicate that the oil contamination has a negative impact on the interface steel-sand shear strength for the tested sand.

Appendix A provides additional information about an oil contaminated sand sample tested during the interface direct shear test program.

4.4 Discussion of Test Results

The soil parameters used to assess the impact of oil contamination on the selected sand were: initial tangent modulus (E_i); friction angle (ϕ' and ϕ) and cohesion (c) in direct shear tests. Each of these parameters showed an increase in their magnitude for oil sand samples, as presented in Table 4.15 and 4.16. As discussed previously, this leads to the conclusion that the oil contamination improves the mechanical properties of the analog sand. By inference, this would suggest that contamination of sand layer IV near the offshore structures in the Cantarell Field by Maya crude oil will not significantly affect the mechanical properties of the sand.

At conditions of failure, important observations can be made concerning the difference in behaviour between oil and water sand samples. The axial strain and pore water pressure at failure were lower for the oil samples than for the

water samples. In addition, the deviator stress was observed to be higher for the oil samples than for the water samples in all the specimens tested.

In contrast, interfacial test results indicate that the oil contamination has a negative impact on the interface steel-sand shear strength for the tested sand.

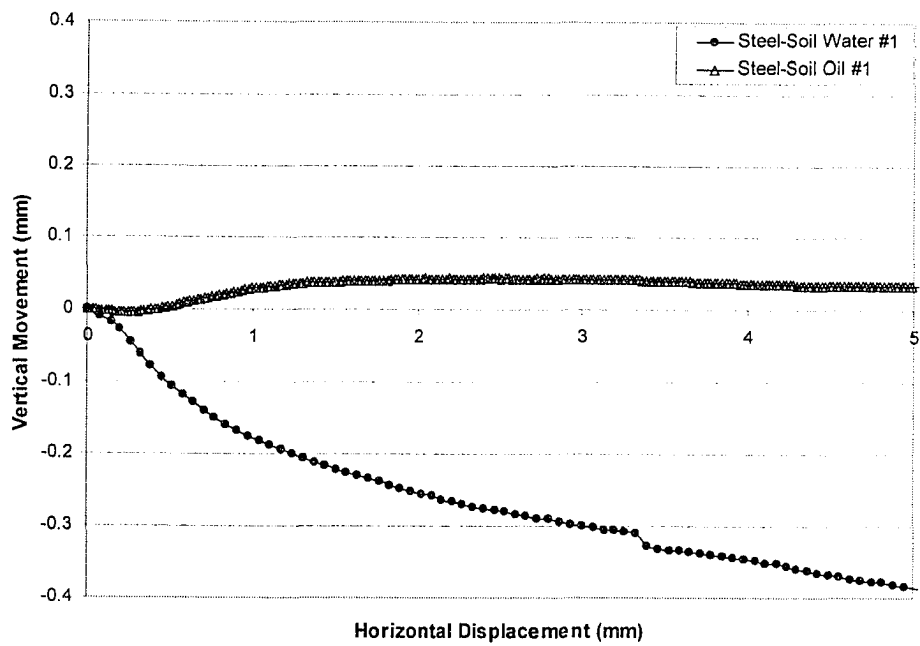
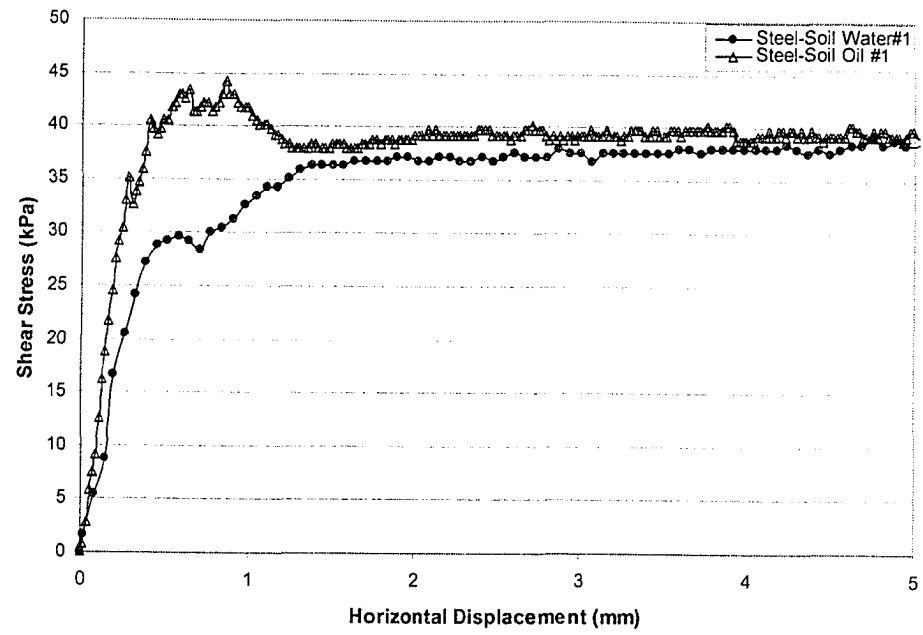


Figure 4.13 Shear Stress vs Horizontal Displacement ($\sigma_n = 62.5$ kPa)
Interface Direct Shear Test

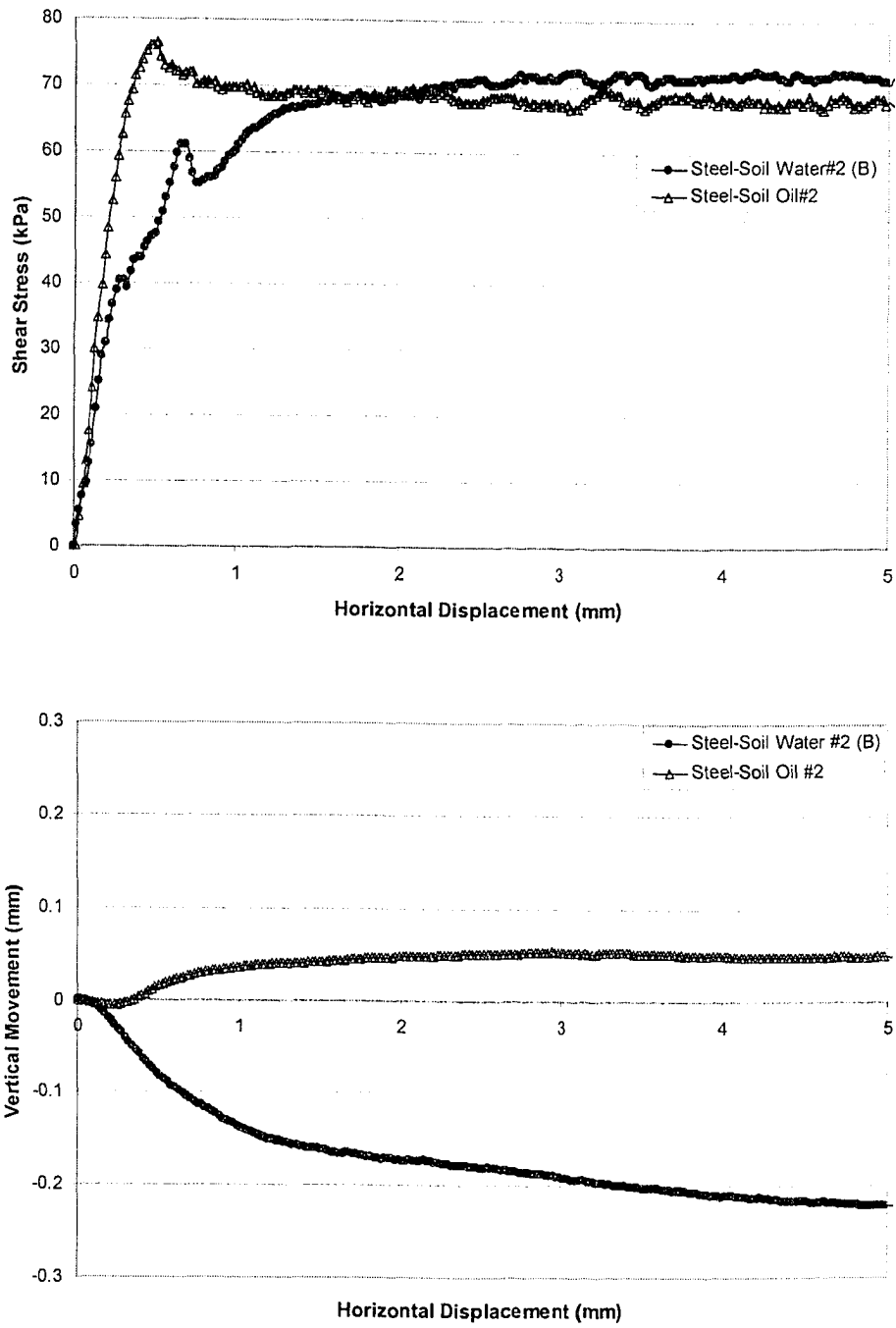


Figure 4.14 Shear Stress vs Horizontal Displacement ($\sigma_n = 125 \text{ kPa}$)
Interface Direct Shear Test

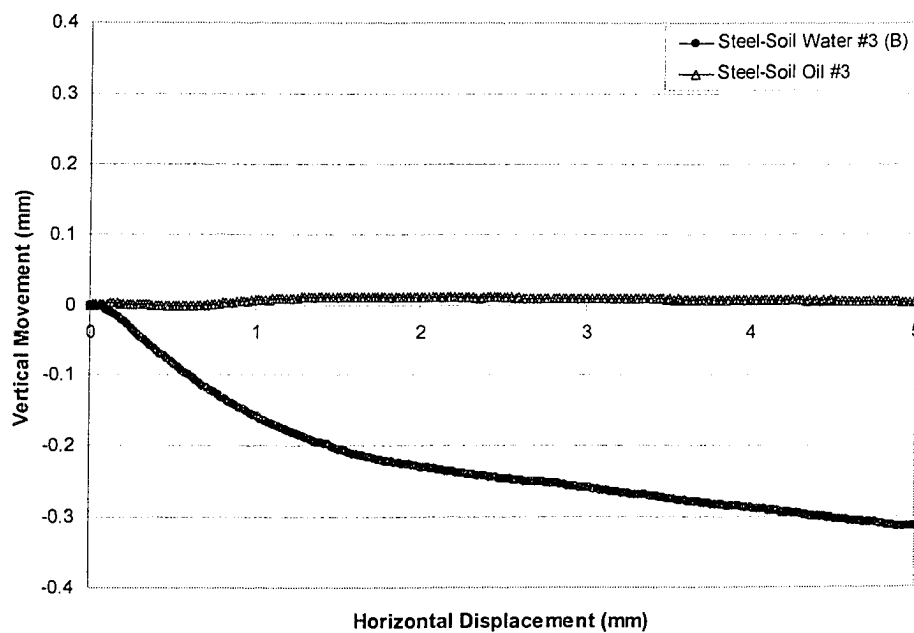
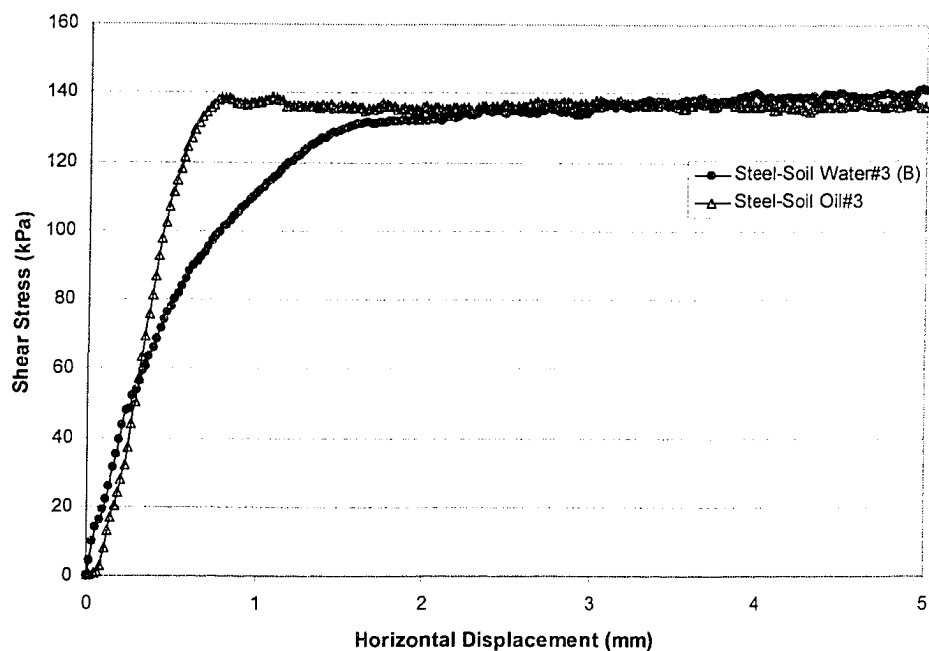


Figure 4.15 Shear Stress vs Horizontal Displacement ($\sigma_n = 250$ kPa)
Interface Direct Shear Test

Table 4.13 Summary of Soil Parameters – Interface Direct Shear Test -

Soil Condition	Interface Friction Angle δ at Maximum Shear Stress (degrees)	Cohesion c (kPa)
Clean Sand	28.6	5.0
Oil Contaminated Sand	26.0	13.2

Table 4.14 Summary of Soil Parameters close to Critical State
– Interface Direct Shear Test -

Soil Condition	Interface Friction Angle δ at 5 mm Horizontal Displacement (degrees)	Cohesion c (kPa)
Clean Sand	28.7	2.9
Oil Contaminated Sand	27.3	5.4

Table 4.15 Initial Tangent Modulus – Based on Triaxial Test -

		Clean Sand	Oil Contaminated Sand
Initial Tangent Modulus E_i (MPa)	$\sigma_3 = 650$ kPa	22.7	28.4
	$\sigma_3 = 900$ kPa	101.3	119.6
	$\sigma_3 = 1,070$ kPa	127.9	156.5 (for $\sigma_3 = 1,055$ kPa)

Table 4.16 Summary of Soil Parameters

Type of test	Friction Angle (degrees)		Cohesion (kPa)	
	Clean Sand	Oil Contaminated Sand	Clean Sand	Oil Contaminated Sand
Undrained Compression Triaxial Test (ϕ')	35.4	39.4	0	0
Direct Shear Box Test (ϕ)	30.8	35.3	13.3	15.9

Although dilation behaviour was observed during the shearing stage of the interface direct shear test between steel and soil, the effect of oil contamination on the sand within the range of factors studied caused a decrease in the interface friction angle (δ) between the smooth steel plate and the sand. This suggests a possible decrease in the frictional resistance of the steel piles, which constitute the foundation of the offshore platforms, because of oil contamination. Table 4.17 compares the parameters obtained between clean and oil contaminated sand obtained from the interface direct shear test.

Table 4.17 Interface Steel-Soil Direct Shear Test Results

Condition	Interface Friction Angle δ (degrees)		Cohesion c (kPa)	
	Clean Sand	Oil Contaminated Sand	Clean Sand	Oil Contaminated Sand
at Maximum Shear Stress	28.6	26.0	5.0	13.2
at 5 mm Horizontal Displacement	28.7	27.3	3.0	5.4

5. CONCLUSIONS AND RECOMMENDATIONS FOR FUTURE RESEARCH

5.1 Conclusions

- The effect of oil contamination, within the range of parameters studied in this research, was to convert the mildly dilatant/contractant behaviour of water saturated silty sand samples to a strongly dilatant behaviour. This behaviour was found in all three different geotechnical tests used for this investigation; undrained triaxial compression, direct shear and interface direct shear tests.
- The soil parameters (initial tangent modulus, E_i ; friction angle, ϕ' , ϕ ; and cohesion, c) all increased in magnitude as a result of the oil saturation. This implies that the oil contamination may improve the mechanical properties of the analog sand and by inference, the mechanical properties of the in situ sand in the Bay of Campeche.
- Oil contamination within the sand, for the range of factors studied in this research, caused a decrease in the interface friction angle (δ) between the smooth steel plate and the sand. This suggests a possible decrease in the frictional resistance of the steel piles, which constitute the foundation of the offshore platforms, because of oil contamination.

- The positive influence of oil contamination on the mechanical properties of the analog sand is contrary to the results of previous researchers who have concluded that oil contamination leads to a decrease in strength. The methodology for producing oil saturated sand specimens differed substantially between the current research and the previous research studies. Care was taken in this study to preserve the water wet characteristics of the oil contaminated sand specimens. Previous researchers simply saturated their specimens with oil. As well, a silty sand was used in this study whereas previous investigators utilized clean sand with little to no fines content. It is postulated that these two reasons are the primary basis for the differences found for the influence of oil contamination on silty sand behaviour.
- From the geotechnical investigations carried out by FUGRO either in the field or in the laboratory, it was concluded that where the soil was permeated with liquid hydrocarbons, no direct effects could be discerned; however, where the hydrocarbon content is high, it was almost certain that there will be free gas in the pore spaces which could affect the soil response. The results of this research agree with FUGRO's conclusions to

discard the assumption of a negative impact in the mechanical properties of sand because of oil contamination.

- Previous researchers studied the interface steel-sand phenomena using different apparatus under several variables such as: test conditions (constant volume test, constant vertical load test), initial density, percent of oil contamination, dry or saturated sand, techniques to lubricate the smooth steel surface. In general, these previous studies agree that oil modifies the behaviour of the interface between sand and the smooth steel surface, when either there is an oil contaminated sand or a lubricated steel surface. Further, oil reduces the coefficient of friction and causes changes in the behaviour similar to the effect of reduction in density. Because this research did not conduct interfacial shear tests over a range of densities, it is difficult to compare the results of the present research with previous research studies. This research did, however, generate similar results with regard to the conclusion that oil contamination will negatively influence interfacial strength properties. This suggests that the major issue about oil contamination may be the decrease in the frictional resistance of the steel piles in an oil contaminated sand zone which may lead to a structural risk for offshore platforms in the Bay of Campeche.

5.2 Recommendations for Further Research

1. The implication of using higher vertical stresses, in the interface direct shear test, to simulate the frictional resistance of the steel piles with the oil contaminated sand on deeper sand layers in the Bay of Campeche must be addressed.
2. The effect of using calcareous or carbonate sands instead of silica sand needs to be investigated. This includes any chemical reaction between calcium carbonate, sea water and in situ hydrocarbons.
3. The effect of using Maya crude oil instead of engine motor oil needs to be addressed.
4. The effect of using sea water (brine) instead of fresh water in the soil mass needs to be investigated.
5. The temperature factor needs to be investigated, given that the in situ temperature is higher than the average temperature in the laboratory. However, it is expected that the temperature has no effect in the shear resistance of the sand but may cause an increase in its compressibility.
6. A complete assessment of any fine migration, during the oil flushing stage in the triaxial cell, for the sample preparation must be addressed.

7. Pile foundation system design assumptions (for pile capacity) should be reviewed in light of modified soil parameters, especially the reduced interfacial steel-soil friction angle (δ). Lateral and axial load capacity for piles in the Bay of Campeche oil contaminated soils subjected to hurricane wave loadings using any analytical available model as: SPASM, DRAIN3D or ULSLEA.

BIBLIOGRAPHY

- American Petroleum Institute – API (1993) *Recommended Practice for Planning, Designing and Constructing Fixed Offshore Platforms-Working Stress Design*, API Recommended Practice 2A-WSD (RP 2-A-WSD), 20th edition, Washington: API.
- American Society for Testing and Materials -ASTM (2003) “Standard Test Method for Direct Shear Test of Soils Under Consolidated Drained Conditions”, designation D3080-98, *Annual Book of Standards*, Section four, Construction, volume 04.08, Soil and Rock (I): D420-D5611, pp. 347-352.
- American Society for Testing and Materials -ASTM (2003) “Standard Specification for Welded and Seamless Steel Pipe Pile”, designation A252-98 (reapproved 2002), *Annual Book of Standards*, Section One, Iron and Steel Products, volume 04.01, Steel-Piping, Tubing, Fittings, pp. 147-153.
- American Society for Testing and Materials -ASTM (2003) “Standard Test Method for Consolidated Undrained Triaxial Compression Test for Cohesive Soils”, designation D4767-95, *Annual Book of Standards*, Section four, Construction, volume 04.08, Soil and Rock (I): D420-D5611, pp. 924-933.
- American Society for Testing and Materials -ASTM (2003) “Standard Test Method for Particle-Size Analysis of Soils”, designation D422-63, *Annual Book of Standards*, Section four, Construction, volume 04.08, Soil and Rock (I): D420-D5611, pp. 10-17.
- American Society for Testing and Materials -ASTM (2003) “Standard Test Methods for Minimum Index Density and Unit Weight of Soils and Calculation of Relative Density”, designation D4254-00, *Annual Book of Standards*, Section four, Construction, volume 04.08, Soil and Rock (I): D420-D5611, pp. 571-579.
- American Society for Testing and Materials -ASTM (2003) “Standard Test Methods for Maximum Index Density and Unit Weight of Soils Using a Vibratory Table”, designation D4243-00, *Annual Book of Standards*, Section four, Construction, volume 04.08, Soil and Rock (I): D420-D5611, pp. 556-570.
- Amor, B. F. (1990) "Effect of Oil Contamination on the Properties of Sands", unpublished M.A.Sc. Thesis, University of Ottawa.

- Anonymous (2001a) El Reto de las plataformas petroleras, [Electronic version], *Investigación y Desarrollo: Periodismo de Ciencia y Tecnología*, March, <http://www.invdes.com.mx/anteriores/Marzo2001/index2.html>
- Anonymous (2001b) Las Plataformas Marinas de PEMEX, [Electronic version], *Investigación y Desarrollo: Periodismo de Ciencia y Tecnología*, November, <http://www.invdes.com.mx/anteriores/Noviembre2001/index2.html>
- Al-Douri, R.H., and H.G. Poulos (1992) "Static and Cyclic Direct Shear Tests on Carbonate Sands", *Geotechnical Testing Journal*, Vol. 15, No.1, March, pp. 138-157.
- Bea, R.G., et al. (1999) "Evaluation of Reliability of Platform Pile Foundations", *Journal of Geotechnical and Geoenvironmental Engineering*, August, pp. 696-704
- Boulon, M. (1989) "Basic Features of Soil Structure Interface Behaviour", *Computers and Geotechnics*, Vol. 7, pp. 115-131.
- Boulon, M. and P. Foray (1986) "Physical and Numerical Simulation of Lateral Shaft Friction along Offshore Piles in Sand", *Numerical Methods in Offshore Piling*, Editions Technip: Paris, pp. 127-147.
- Brumund, W.F., and G.A. Leonards (1973) "Experimental Study of Static and Dynamic Friction Between Sand and Typical Construction Materials", *Journal of Testing and Evaluation*, Vol. 1, No. 1, pp. 162-165.
- Budhu, M. (2000) "Soil Mechanics and Foundations", John Wiley & Sons, Inc.: New York, pp. 586.
- Cook, E.E., B.C. Devkota and B. Yeo (1993) "Permeability of Oil-Contaminated Sands", *Proceedings of the Third International Offshore and Polar Engineering Conference*, Vol. 1, June, pp. 491-495.
- Cook, E.E., V.K. Puri and E.C. Shin (1992) "Geotechnical Characteristics of Crude Oil-Contaminated Sands", *Proceedings of the Second International Offshore and Polar Engineering Conference*, Vol. 1, June, pp.384-387.
- Desai, C.S. (1981) "Behavior of interfaces Between Structural and Geologic Media", *International Conference on Recent Advances in Geotechnical Earthquake Engineering and Soil Dynamics*, Vol. II, pp. 619-638.
- Drawe III, W. J, and M.D. Reifel (1986) " Platform Function and Types", in B. McClelland and M.D. Reifel (eds.), *Planning and Design of Fixed Offshore Platforms*, New York: Van Nostrand Reinhold Company, pp. 11-23.

- Eving, E., B.F. Amor, and A. Altaee (1989) "Effect of an Oil Spill on Soil Properties, *Proceedings of the Eighth International Conference on Offshore Mechanics and Arctic Engineering*, Vol. 1, pp. 715-720.
- Evgin, E., M. Boulon, and G. Armand (1996) "Effect of Oil Contamination on the Behaviour of an Interface", *49th Canadian Geotechnical Conference of the Canadian Geotechnical Society*, September, pp.377-384.
- Evgin, E., M. Boulon, and B.M. Das (1995) "Finite Element Analysis of a Model Scale Footing on Clean and Oil Contaminated Sand", *Proceedings of the Fifth International Offshore and Polar Engineering Conference*, The Hague, The Netherlands, June 11-16.
- Eving, E. and B.M. Das (1992) "Mechanical Behavior of an Oil Contaminated Sand", in Mumtaz. A. Usmen and Y. B. Acar (eds.) *Environmental Geotechnology*, Balkema: Rotterdam, pp. 101-108.
- Eving, E. and A. Altaee (1992) "Effect of Oil Contamination on the Behavior of an Arctic Offshore Structure", *Proceedings of the Second International Offshore and Polar Engineering Conference*, June, pp. 376-383.
- Frost, J.D. and J.Y. Park (2003) "A critical Assessment of the Moist Tamping Technique", *Journal of Geotechnical Testing*, March, Vol. 26, No. 1, pp. 1-14.
- FUGRO (2002) *Final Report Geotechnical and Geochemical site investigation, Boring: AKAL-H (Gas 1), Cantarell Field, Bay of Campeche, Mexico*, Report No. 0201-4642-3.
- FUGRO (1998) *Final Report Geotechnical site investigation, Platform: AKAL-H, Bay of Campeche, Mexico*, Report No. 0201-3576.
- Hasan, A.A.. and A. A. K. Mostafa (1996) "The Interface Angle of Friction Between Dry Sand and Lubricated Surfaces", *Kuwait Journal of Science and Engineering*, No. 23, Vol.2, pp. 249-265.
- Hasan A. A. and F. I. Nabil (1997) "Aging Effects on Oil-Contaminated Kuwaiti Sand", *Journal of Geotechnical and Geoenvironmental Engineering*, vol. 123, No. 3, March, pp. 290-293.
- Hasan A. A., K. E. Walid., and F.I. Nabil (1995) "Geotechnical Properties of Oil-Contaminated Kuwaiti Sand", *Journal of Geotechnical Engineering*, Vol. 121, No. 5, May, pp. 407-788.
- Head, K.H. (1992) *Manual of Soil Laboratory Testing: Volume I, Soil Classification and Compaction Tests*, 2nd ed., London: Pentech Press Limited.

- Head, K.H. (1981) *Manual of Soil Laboratory Testing: Volume II, Permeability, Shear Strength and Compressibility Tests*, 1st ed., London: Pentech Press Limited.
- Hu, L. and J. Pu (2004) "Testing and Modeling of Soil-Structure Interface", *Journal of Geotechnical and Geoenvironmental Engineering*, August, pp. 851-860.
- Høeg, K., R. Dyvik, and G. Sandbækken (2000) "Strength of Undisturbed versus Reconstituted Silt and Silty Sand Specimens", *Journal of Geotechnical and Geoenvironmental Engineering*, July, pp. 606-617.
- Industry and Resources, Mineral Resources of Saskatchewan (accessed October 10, 2004)
<http://www.ir.gov.sk.ca/Default.aspx?DN=3561,3541,3538,3385,2936,Document>
- Instituto Mexicano del Petroleo - IMP (2000) "Especialistas del IMP investigan "bolsas de gas" que se forman en el lecho marino de Campeche y provocan problemas en plataformas", Press Release 21, June 21, [WWW document]
<http://www.imp.mx/publicaciones/comunicados/2000/txt21.htm>
- Kishida, H. and M. Uesugi (1987) "Test of the Interface Between Sand and Steel in the Simple Shear Apparatus", *Géotechnique*, Vol. XXXVII, pp. 45-52.
- Lambe, T.W. and R.V. Whitman (1979) "Soil Mechanics, SI Version", John Wiley & Sons, Inc.: New York, pp.553.
- Meegoda, N.J. and P. Ratnaweera (1994) "Compressibility of Contaminated Fine-Grained Soils", *Geotechnical Testing Journal*, Vol. 17, March-December, pp. 101-112.
- Petroleos Mexicanos -PEMEX (2004) "Pemex mejora índice de pozos perforados en la Sonda de Campeche", Press Release 173, July 25, [WWW document]
<http://www.pemex.com/index.cfm/action/content/sectionID/8/catID/40/subcatID/2112/index.cfm?action=content§ionID=8&catID=40&subcatID=2112>
- Potyondy, J.G. (1961) "Skin Friction Between Various Soils and Construction Materials", *Géotechnique*, Vol. XI, pp. 339-353.
- Reddy, E.S., D.N. Champman, and V.V.R.N. Sastry (2000) "Direct Shear Interface Test for Shaft Capacity of Piles and Sand", *Geotechnical Testing Journal*, Vol. 23, No. 2, June, pp. 199-205.

- Saad A. A. (1998) "The Effect of Temperature on the Engineering Properties of Oil-Contaminated Sands", *Environment international*, Vol. 24, No. 1/2, pp. 153-161.
- Scott, J.D., R.J. Chalaturnyk, D. Chan and G.Y.K. Wong (2001) *Manual of Artificial Oil Sand Sample Preparation*, Geotechnical Group, Department of Civil & Environmental Engineering, University of Alberta.
- Subba Rao, K.S., M.M. Allam and R.G. Robinson (1998) "Interfacial Friction Between Sands and Solid Surfaces", *Proceedings Of The Institution Of Civil Engineers-Geotechnical Engineering*, No. 131, April, pp. 75-82.
- Subba Rao, K.S., M.M. Allam and R.G. Robinson (2000) "Drained Shear strength of fine-grained soil-solid surface interfaces", *Proceedings Of The Institution Of Civil Engineers-Geotechnical Engineering*, No. 143, April, pp. 75-81.
- Sandoval, A.A. (1998) "Los crudos Mexicanos, sus características", *Boletín del Instituto de Investigaciones Eléctricas (IIE)*, may-june, [WWW document] <http://www.iie.org.mx/publica/bolmj98/secmj98.htm>
- Secretaría de Energía, (2004), Official web site of the Mexican Ministry of Energy, [WWW Document] (accessed October 10, 2004) <http://www.energia.gob.mx/wb/distribuidor.jsp?seccion=1495>
- Tabucanon, J.T., D.W. Airey, and H.G. Poulos (1995) "Pile Skin Friction in Sands from Constant Normal Stiffness Tests", *Geotechnical Testing Journal*, Vol. 18, March-December, pp. 350-364.
- Terzagui, K., R.B. Peck and G. Mesri (1996) "Soil Mechanics in Engineering Practice", John Wiley & Sons, Inc.: New York, pp. 549.
- The American Society of Mechanical Engineers (1995) *Surface Texture (Surface Roughness, Waviness, and Lay)*, An American National Standard, ASME B46.1-1995 (Revision of ANSI/ASME B46.1-1985), pp. 1-83.
- The American Society of Mechanical Engineers (1996) *Welded and Seamless wrought Steel Pipe*, An American National Standard, ASME B36.10-10M-1996 (Revision of ASME B36.10M-1995), pp. 1-18.
- Tuncan, A. (1989) "Influence of Fuel-Oil Sludge on geotechnical Properties of Marine Sediments", in Hsai-Yang Fang and Sibel Pamukcu (eds.) *Environmental Geotechnology*, Vol. 1, Envo Publishing Co., pp.135-152.
- Tuncan, A. and S. Pamakcu (1992) "Predicted Mechanism of Crude Oil and Marine Clay Interactions in Salt Water", in Mumtaz. A. Usmen and Y. B. Acar (eds.) *Environmental Geotechnology*, Balkema: Rotterdam, pp. 109-121.

- Vaid, Y.P. and S. Sivathayalan (2001) Discussion of the paper -Strength of Undisturbed versus Reconstituted Silt and Silty Sand Specimens by Høeg, K., Dyvik, R. and Sandbækken, G. (2000)- *Journal of Geotechnical and Geoenvironmental Engineering*, November, pp. 993-994.
- Vaid, Y.P. and S. Sivathayalan (2000) "Fundamental factors affecting liquefaction susceptibility of sands", *Canadian Geotechnical Journal*, 37, pp. 592-606.
- Vaid, Y.P., M. Uthayakumar, S. Sivathayalan, P.K. Robertson, and B. Hoffman (1995) "Laboratory testing of Syncrude sand", Proc., 48th Canadian Geotechnical Conference, Vancouver, 1, pp. 223-232.
- Vijay, K. Puri (2000) "Geotechnical Aspects of Oil-Contaminated Sands, *Soil and Sediment Contamination*, No. 9, Vol. 4, pp. 359-374.
- Wissam G.G. F. and E. Evgin (1998) "A Model Scale Footing on Oil Contaminated Sand", Conference Preprints Vol. 1, 51st Canadian Geotechnical Conference, Edmonton, AB, pp. 351-357.

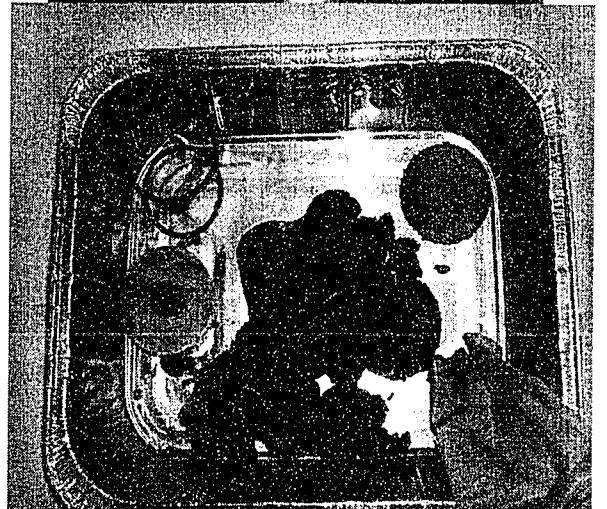
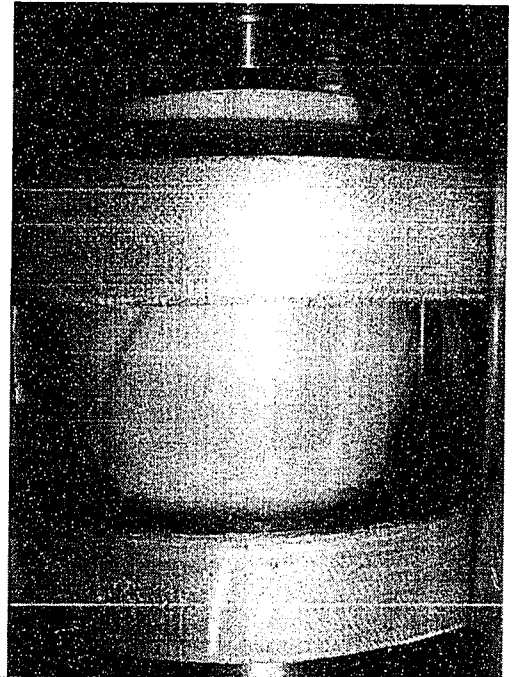
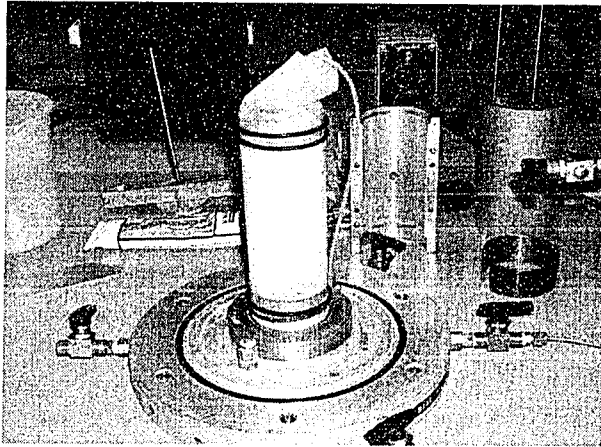


Figure A.1 Sand Sample (Water #3) used in the Triaxial Test Program having Water as Permeating Liquid

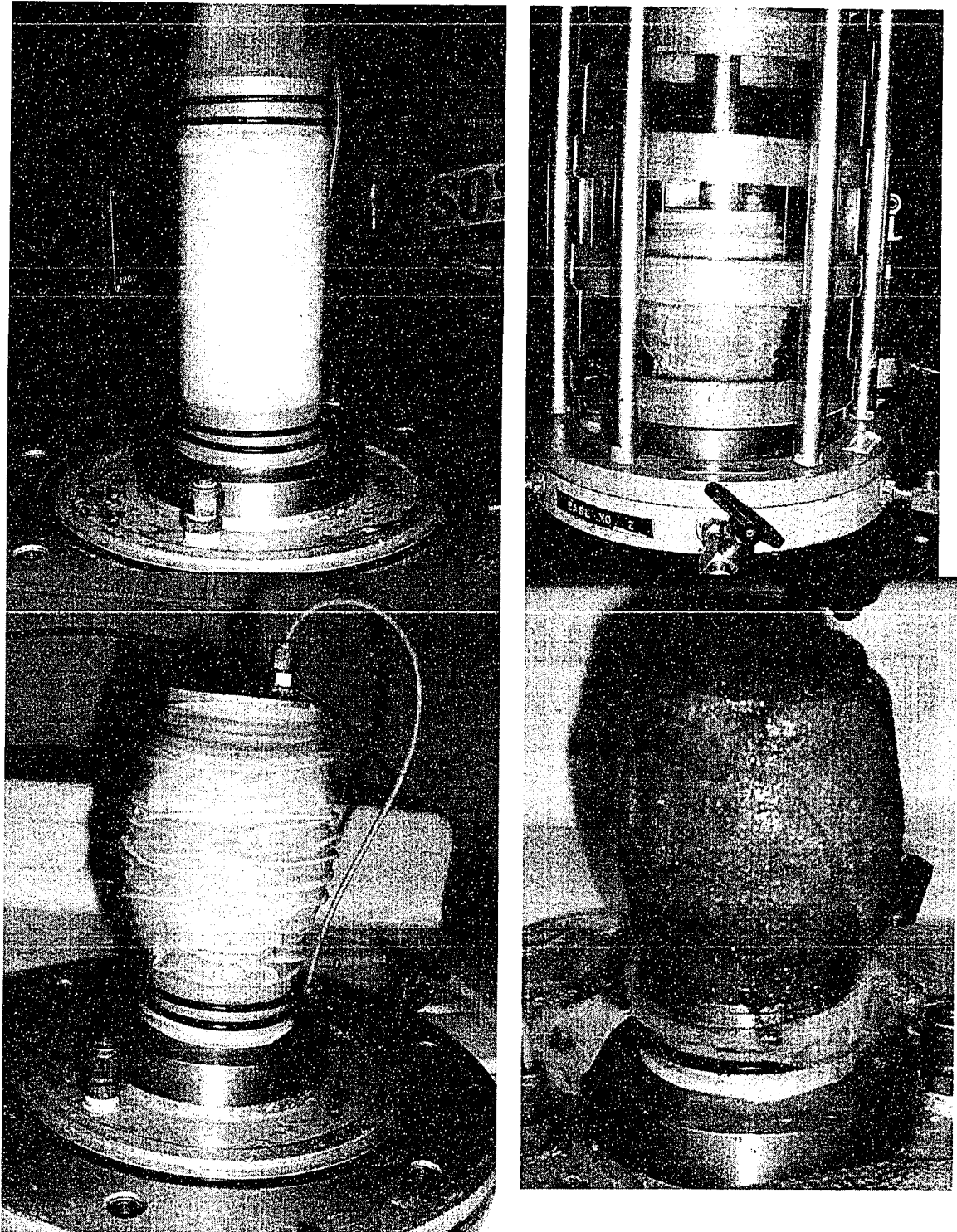


Figure A.2 Sand Sample (Oil #3) used in the Triaxial Test Program having Oil-Water Mix as Permeating Liquid

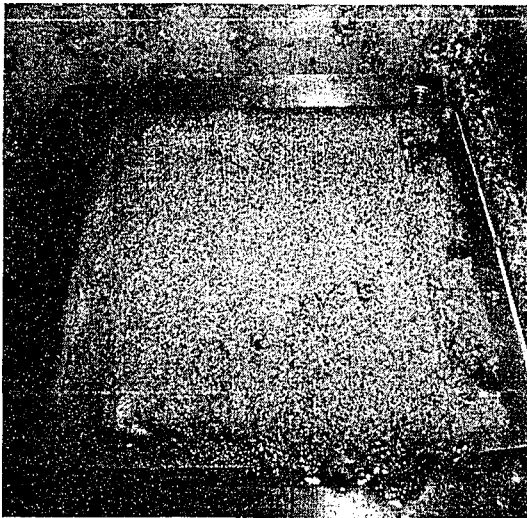
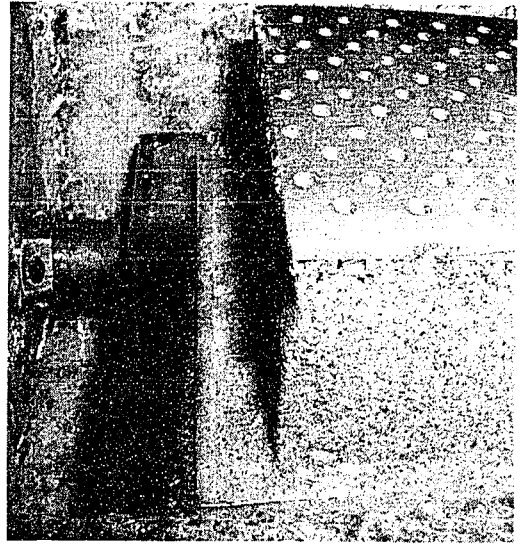
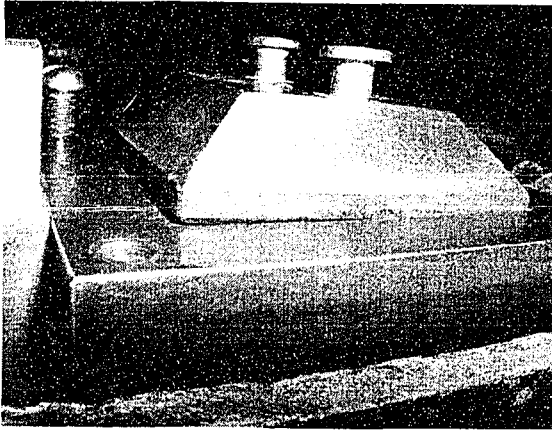


Figure A.3 Sand Sample (Soil-Soil Oil # 3) used in the Direct Shear Test Program, having Oil-Water Mix as Permeating Liquid

APPENDIX A SAND SAMPLES

This Appendix contains pictures of sand samples showing the main steps in each test program, including Triaxial, Direct Shear and Interface Direct Shear Testing.

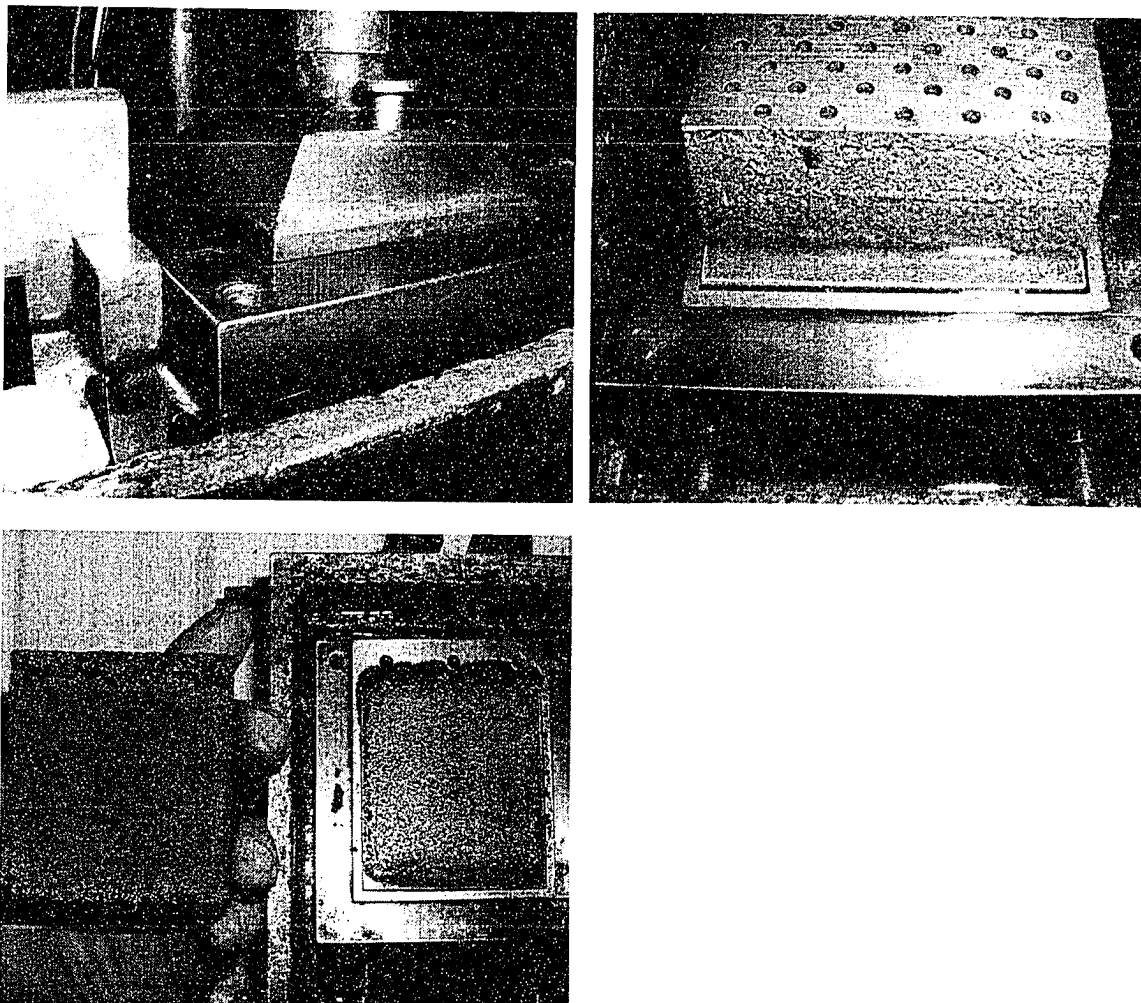


Figure A.4 Sand Sample (Steel-Soil Oil # 2) used in the Interface Direct Shear Test Program, having Oil-Water Mix as the Permeating Liquid